

NMDAR-PSD95-NNOS AXIS-MEDIATED MOLECULAR MECHANISMS IN THE  
BASOLATERAL AMYGDALA UNDERLYING FEAR CONSOLIDATION

Jheel Patel

Submitted to the faculty of the University Graduate School  
in partial fulfillment of the requirements  
for the degree  
Doctor of Philosophy  
in the Program of Medical Neuroscience,  
Indiana University

May 2021

Accepted by the Graduate Faculty of Indiana University, in partial fulfillment of the requirements for the degree of Doctor of Philosophy.

Doctoral Committee

---

Patrick Sheets, Ph.D., Chair

---

Anantha Shekhar, M.D., Ph.D.

April 5, 2021

---

David McKinzie, Ph.D.

---

Bryan Yamamoto, Ph.D.

---

Yunlong Liu, Ph.D.

© 2021

Jheel Patel

## DEDICATION

To my loving family and all the women who paved the path for me.

## ACKNOWLEDGEMENT

I would like to thank my mentor, Dr. Anantha Shekhar, for the opportunity to do my dissertation work in his lab. I appreciate the time he took out of his busy schedule to mentor and guide me, share ideas, and train me to be a better scientist. I am grateful for the opportunity to learn from him.

I also want to thank my committee members, Dr. Patrick Sheets, Dr. David McKinzie, Dr. Bryan Yamamoto, and Dr. Yunlong Liu. I always came out of committee meetings with a swarm of ideas and next steps, and that is thanks to my committee. They provided invaluable insights into my projects, gave useful feedback, and pushed me to be a greater scientist.

I want to thank the many lab members who supported and encouraged me. To Dr. Andrei Molosh, for offering his mentorship and expertise towards my project. To Dr. Jodi Lukkes for her mentorship, constant support, and encouragement when the going got tough. To my lab members, present and past, for making lab an enjoyable and exciting place to be – Ping Li, Melissa Haulcomb, Erik Dustrude, Cris Bernabe, Izabela Caliman, Aline Abreu, Hayley Drozd, Sotirios Karathanasis, Stephanie Fitz, Janet Eng, Sreeparna Majumdar, Katie Andrews, Betsy Lungwitz, Amy Dietrich, and Andrew Burke. Every single one has contributed significantly to my journey in grad school. Specifically, thank you to Ping for laying the groundwork for my dissertation work, and for being a very smart, very funny, always positive person to talk to. A tremendous thank you to Melissa and Erik for not only training me and helping collect data for this project, but also teaching me how to be a fun, empathetic, and effective mentor.

I want to thank the Stark Neurosciences Research Institute Administrative team, Building Operations team, and leadership for their support and assistance. Without them, my job would be a lot harder and more stressful, and I am grateful for their hard work that made SNRI a great place for my graduate research.

I am also grateful for Dr. Stephanie Florio and Dr. Yvonne Lai, who are both amazing mentors and experts in their fields. I consider both of them my role models, and I am very excited to be working with them in this next year.

I would like to thank Mark Kesling and the DaVinci Pursuit, for granting me an opportunity to bring together the two things that I love most: art and science. I am in awe of the work that dVP does in the community. I have been enriched by my experiences thus far, and I am excited to contribute and create much more in the future.

I want to thank my friends who were my loudest cheerleaders in this journey and who made my heart full every single day. To the very best IBMG cohort, I doubt I would have made it past the first year of grad school had it not been for the funniest, most easy-going, and supportive group of people I was lucky enough to enter grad school with. I am thankful for my friends within the Medical Neuroscience program, specifically David Haggerty and Andy Tsai, for their support and friendship. To my best friends, Karol Santiago and Kaitlynn McShea. Words cannot describe how lucky I am to have Karol and Kaitlynn by me in this journey; they have brought me joy, laughter, and fun travel stories, and for that, I am grateful.

I would like to thank Dr. Stephanie Cunningham, my therapist, for being a big part of the reason why I have been able to achieve as much as I have in grad school.

Finally, I want to thank my family. To Mansi, Krishna, and Ranen – the most supportive and loving siblings I could have asked for, who know just the right things to say, the right gifts to give, and the right food to cook for me. To my mother, Daina, my hero. I would not be the person I am today without her, her wisdom, the stories she shares with me, and the love she gives me. And finally, to my sweet nephew, Arian, who was born shortly after I began grad school, and so, has grown with me as much as I have grown with him. He has been the best thing about the past 4 years, and I am thankful for him, his laughter, and his love.

Jheel Patel

NMDAR-PSD95-NNOS AXIS-MEDIATED MOLECULAR MECHANISMS IN THE  
BASOLATERAL AMYGDALA UNDERLYING FEAR CONSOLIDATION

Fear is an evolutionarily conserved response that can facilitate avoidance learning and promote survival, but excessive and persistent fear responses lead to development of phobias, generalized fear, and post-traumatic stress disorder. The primary goal of experiments in this dissertation is to determine the molecular mechanisms underlying formation of fear memories. The acquisition and consolidation of fear is dependent upon activation of N-methyl-D-aspartic acid receptors (NMDARs). Stimulation of NMDARs recruits neuronal nitric oxide synthase (nNOS) to the synaptic scaffolding protein, postsynaptic density protein 95 (PSD95), to produce nitric oxide (NO). Our laboratory has previously shown that disruption of the PSD95-nNOS interaction attenuates fear consolidation and impairs long-term potentiation of basolateral amygdala (BLA) neurons in a rodent model of auditory fear conditioning. However, the molecular mechanisms by which disrupting the PSD95-nNOS interaction attenuates fear consolidation are not well understood.

Here, we used pharmacological and genetic approaches to study the effects underlying nNOS activity in the BLA during fear consolidation. During the early stage of fear memory consolidation (4-6 hours after fear acquisition), we observed increased  $\alpha$ -Amino-3-hydroxy-5-methyl-4-isoxazolepropionic acid receptor (AMPA)-mediated current and synaptosomal AMPAR GluR1 subunit trafficking in the BLA; while during the late stage (24h after fear acquisition), we detected a combination of enhanced AMPAR- and NMDAR-mediated currents, increased synaptosomal NMDAR NR2B



subunit expression, and phosphorylation of synaptosomal AMPAR GluR1 and NMDAR NR2B subunits in the BLA. Importantly, we showed that pharmacological and genetic blockade of nNOS activity inhibits all of these glutamatergic synaptic plasticity changes in the BLA. Additionally, we discovered whole transcriptome changes in the BLA following fear consolidation. In the group with pharmacological inhibition of nNOS activity, however, gene expression levels resembled control-like levels. We also observed altered expression of multiple genes and identified the insulin-like growth factor system, D3/D4 dopamine receptor binding, and cGMP effects as key pathways underlying nNOS-mediated consolidation of fear.

Our results reveal nNOS-mediated, sequentially orchestrated synaptic plasticity changes facilitated by AMPA and NMDA receptors in the BLA during early and late stages of fear memory consolidation. We also report novel genetic targets and pathways in the BLA underlying NMDAR-PSD95-nNOS axis-mediated formation of fear memories.

Patrick Sheets, Ph.D., Chair

## TABLE OF CONTENTS

<b>List of Tables</b> .....	xii
<b>List of Figures</b> .....	xiii
<b>List of Abbreviations</b> .....	xiv
<b>CHAPTER 1 Introduction</b> .....	1
1.1 Fear .....	1
1.1.1 Persistent fear as a maladaptive response .....	1
1.1.2 Preclinical models of fear learning .....	2
1.1.3 Fear memory consolidation .....	3
1.2 Neural Substrates of Fear Consolidation .....	3
1.3 Neurobiology of Fear Consolidation .....	8
1.3.1 Glutamate signaling .....	8
1.3.2 NMDAR signaling .....	9
1.3.3 AMPAR signaling .....	11
1.3.4 NMDAR-PSD95-nNOS axis .....	15
1.3.4.1 PSD95 structure & function .....	15
1.3.4.2 nNOS structure & function .....	16
1.3.4.3 NMDAR-PSD95-nNOS dynamics .....	20
1.3.4.4 Downstream implications of NO activity .....	21
1.3.5 Gene transcription .....	25
1.4 nNOS Inhibitors .....	26
1.5 Small-Molecule PSD95-nNOS Binding Inhibitors .....	27
1.6 Aims and Hypothesis .....	28
<b>CHAPTER 2 Transcriptomic Study of Molecular Mechanisms Underlying NMDAR-PSD95-nNOS-NO Axis Mediated Fear Consolidation in the Amygdala: Key Role of IGF2 and IGFBP2</b> .....	30
2.1 Introduction .....	30
2.2 Materials and Methods .....	31
2.3 Results .....	35
2.4 Discussion .....	52
<b>CHAPTER 3 Fear Consolidation Requires nNOS-Dependent, Sequentially Orchestrated Changes in AMPA and NMDA Mediated Glutamatergic Neurotransmission in the Basolateral Amygdala</b> .....	59
3.1 Introduction .....	59
3.2 Materials and Methods .....	61
3.3 Results .....	66
3.4 Discussion .....	81
<b>CHAPTER 4 Intra-Basolateral Amygdala Knockdown of nNOS Weakens Auditory Fear Consolidation and Alters the Synaptosomal Expression and Phosphorylation Levels of GluR1 and NR2B</b> .....	87
4.1 Introduction .....	87
4.2 Materials and Methods .....	88
4.3 Results .....	93
4.4 Discussion .....	98
<b>CHAPTER 5 Conclusion</b> .....	101

5.1 General Summary .....	101
5.2 Significance.....	106
5.3 Limitations & Future Directions.....	107
5.4 Final Remarks .....	110
<b>References .....</b>	<b>111</b>
<b>Curriculum Vitae</b>	

## LIST OF TABLES

Table 1. A summary of ZL006 properties. ....	28
--	----

## LIST OF FIGURES

Figure 1. Afferent and efferent projections of the basal and lateral amygdala .....	5
Figure 2. Amygdalar circuitry in fear responses.....	7
Figure 3. Intracellular signaling cascade downstream of NMDAR activation in an nNOS-expressing cell.....	13
Figure 4. The structure and activation of nNOS.....	18
Figure 5. nNOS-mediated intracellular signaling cascade.....	24
Figure 6. Effects of fear conditioning on the basolateral amygdala transcriptome. ....	37
Figure 7. Fear conditioning and ZL006 treatment schematic and behavioral output. ....	40
Figure 8. Differentially expressed gene patterns associated with fear conditioning and ZL006 treatment.....	43
Figure 9. Heatmaps and gene enrichment analyses of 83 DEGs common between fear conditioning and ZL006-treated groups. ....	46
Figure 10. Key genes, proteins, and transcription factors: putative role of the NMDAR-PSD95-nNOS-NO axis and IGF2/IGFBP2 in cued fear consolidation.....	50
Figure 11. Fear conditioning experimental schematic and behavior. ....	67
Figure 12. AMPAR and NMDAR protein expression and function after fear acquisition.....	69
Figure 13. AMPAR and NMDAR protein expression and function 24h after fear acquisition.....	72
Figure 14. Alterations in phosphorylation of key sites on the synaptosomal GluR1 and NR2B subunits after fear acquisition.....	76
Figure 15. Alterations in phosphorylation of key sites on the synaptosomal GluR1 and NR2B subunits 24h after fear acquisition.....	77
Figure 16. Summary of AMPAR and NMDAR-mediated currents and GluR1 and NR2B total and phosphorylated expression levels immediately after and 24h after fear acquisition.....	78
Figure 17. Graphical summary of molecular changes occurring in the BLA during fear consolidation.....	80
Figure 18. siRNA-mediated knockdown of nNOS in the BLA disrupts cued fear consolidation.....	94
Figure 19. Alterations in phosphorylation of key sites on the synaptosomal GluR1 and NR2B subunits 24h after fear acquisition in nNOS knockdown animals.....	97

## LIST OF ABBREVIATIONS

PTSD	Post-traumatic stress disorder
CS	Conditioned stimulus
US	Unconditioned stimulus
CR	Conditioned response
LTP	Long-term potentiation
mPFC	Medial prefrontal cortex
CeA	Central nucleus of the amygdala
BLA	Basolateral amygdala
LA	Lateral amygdala
BA	Basal amygdala
VTA	Ventral tegmental area
GABA	$\gamma$ -aminobutyric acid
ITC	Intercalated cells
NMDAR	N-methyl-D-aspartate receptor
CNS	Central nervous system
EPSC	Excitatory post-synaptic currents
AMPA	$\alpha$ -amino-3-hydroxy-5-methyl-4-isoxazolepropionic acid receptors
CaMKII	Calcium/calmodulin-dependent protein kinase II
PKC	Protein kinase C
CK2	Casein kinase 2
PKA	Protein kinase A
PKG	cGMP-dependent protein kinase
PSD	Post-synaptic density
PSD95	Post-synaptic density 95
NOS	Nitric oxide synthase
NO	Nitric oxide
nNOS	Neuronal nitric oxide synthase
eNOS	Endothelial nitric oxide synthase
iNOS	Inducible nitric oxide synthase
FMN	Flavin mononucleotide

FAD	Flavin adenine dinucleotide
CaM	Calmodulin
NPY	Neuropeptide Y
SOM	Somatostatin
PV	Parvalbumin
VIP	Vasoactive intestinal peptide
NSF	N-ethylmaleimide sensitive factor
sGC	Soluble guanylate cyclase
GTP	Guanosine-5'-triphosphate
cGMP	Cyclic guanosine monophosphate
CREB	Cyclic adenosine monophosphate response element-binding protein
C/EBP	CCAAT enhancer-binding protein
ERK	Extracellular signal-related kinase
L-NAME	NG-nitro-L-arginine methylester
7-NI	7-nitroindazole
IC87201	2-((1 <i>H</i> -benzotriazol-6-ylamino)methyl)-4,6-dichlorophenol
ZL006	4-(3,5-dichloro-2-hydroxy-benzylamino)-2-hydroxybenzoic acid
MAGUK	Membrane-associated guanylate kinase
i.p.	Intraperitoneal
FC	Fear conditioning
DEGs	Differentially expressed genes
IGF2	Insulin-like growth factor 2
IGFBP2	Insulin-like growth factor binding protein 2
IGF1R	Insulin-like growth factor 1 receptor
PPI	Protein-protein interactions
IGF2R	Insulin-like growth factor 2 receptor
D3R	Dopamine D3 receptor
D4R	Dopamine D4 receptor
MOR	mu-type opioid receptor
cGKII	cGMP-dependent protein kinase II
AAV	Adeno-associated virus

siRNA	Small interfering RNA
CMV	Cytomegalovirus
GFP	Green fluorescent protein
RNAi	RNA interference



# CHAPTER 1

## Introduction

“Nothing in life is to be feared, it is only to be understood. Now is the time to understand more, so that we may fear less.”

– Marie Curie

### 1.1 Fear

#### 1.1.1 Persistent fear as a maladaptive response

“Fear” is a complex, emotional response to a danger or stressor that may cause physical or psychological harm. ‘Fear responses’ serve as an essential survival mechanism for all sentient beings, protecting them from dangers such as predators or environmental catastrophes. In response to such immediate threats, most mammalian species demonstrate characteristic behaviors – autonomic arousal, cognitive vigilance, defensive behaviors, etc. – that ultimately aim to protect themselves and promote survival. Such fear responses are considered innate and conserved across species as an evolutionarily necessary means to survival.

However, fear responses that persist beyond exposure to a threat or traumatic experience can become maladaptive. In fact, sustained and recurrent fear responses can result in further stress and anxiety and lead to the development of neuropsychiatric disorders.

The earliest records of trauma-based psychiatric disorders come from Mesopotamian texts dating back to 609 BC<sup>1</sup>. These ancient texts describe hallucinations, sleep problems, and altered moods in soldiers who returned from battle. Today, these symptoms would be referred to as post-traumatic stress disorder (PTSD), a fear disorder that results from the inappropriate processing of traumatic experiences<sup>2</sup>.

Over the years, the pathology of fear disorders has been studied extensively. Numerous types of triggers, like sexual assault, combat, accidents, or abuse, can lead to PTSD with symptoms such as insomnia, hypervigilance, emotional numbness, self-isolation, anxiety, etc. Due to the complex pathophysiology of PTSD, treatment options remain limited and often target the most severe symptoms, rather than the root causes of the disorder<sup>3</sup>. Thus, there is a dire need to study the mechanisms and neurobiology underlying fear disorders, in order to develop more effective treatments and prevention strategies. Fortunately, as an innate and conserved response, fear has neural substrates that have been characterized in most laboratory animals and can be further studied using preclinical models of fear learning.

### **1.1.2 Preclinical models of fear learning**

A commonly used preclinical model of fear paradigm is Pavlovian fear conditioning. Pavlovian fear conditioning results in associative memory formation using two key stimuli: conditioned and unconditioned stimuli (CS and US, respectively)<sup>4,5</sup>. A CS is a neutral stimulus, such as an auditory tone or light; while a US is an aversive stimulus that elicits a motivational response (e.g., a startle response, vocalizations; also known as the conditioned response (CR)) such as a foot shock<sup>4,5</sup>. In the fear acquisition stage of Pavlovian fear conditioning, the animal is exposed to a CS-US pairing, such as an auditory tone that co-terminates with a mild foot shock. Initially, the tone elicits no response. However, with multiple tone-foot shock presentations, the neural mechanisms associating the tone with the impending foot shock is strengthened, such that when the tone alone is presented at a later time, the animal displays a fear response<sup>6,7</sup>. Thus,

Pavlovian fear conditioning is a convenient and biologically relevant paradigm to study the neural mechanisms underlying learned fear behaviors.

### **1.1.3 Fear memory consolidation**

After fear acquisition, the short-term fear association is labile. It is stabilized over a period of time to generate long-term fear memory in a process known as fear consolidation<sup>8-10</sup>. Fear consolidation occurs within hours after fear acquisition, and multiple molecular and cellular processes promote the strengthening of the memory at the synaptic and behavioral level<sup>9-11</sup>. Specifically, fear consolidation requires gene transcription and protein synthesis for long-term memory stabilization<sup>12,13</sup>. Additionally, a series of synaptic events triggered by initial fear learning results in a persistent strengthening of the synapses at the site of learning (a process known as long-term potentiation, or LTP), which further strengthens the neural network that is involved in fear memory consolidation<sup>14-16</sup>.

## **1.2 Neural Substrates of Fear Consolidation**

The neural substrates mediating fear learning and fear memory formation are well-defined and include, but are not limited to, the amygdala, hippocampus, and medial prefrontal cortex (mPFC). In human and animal models of fear learning, the amygdala is a focal node involved in integration of fear generating sensory stimuli and emotional responses<sup>10,17-22</sup>.

The amygdala is a limbic structure and a vital part of the neural network responsible for emotional learning<sup>23,24</sup>. The amygdala can be divided into multiple sub-structures, such as the central nucleus of the amygdala (CeA) and the basolateral amygdala (BLA), which can be further divided into the lateral amygdala (LA) and the

basal amygdala (BA). The BLA is critical for the integration of threat sensory stimuli and fear responses and has extensive and appropriate afferent and efferent connections. Within the fear neurocircuitry, important afferent projections to the BLA include excitatory projections from the thalamus, mPFC, and hippocampus<sup>25</sup>. The BLA also sends efferent projections to the thalamus, mPFC, and hippocampus, in addition to several other regions, such as the CeA, ventral tegmental area (VTA), dorsal raphe, nucleus accumbens, and locus coeruleus<sup>26</sup>. This information is summarized in Figure 1.

The neuronal population in the BLA is amorphously distributed, and it contains primarily glutamatergic pyramidal neurons (~80%) with a subset (~20%) of GABAergic ( $\gamma$ -aminobutyric acid) interneurons<sup>27,28</sup>.

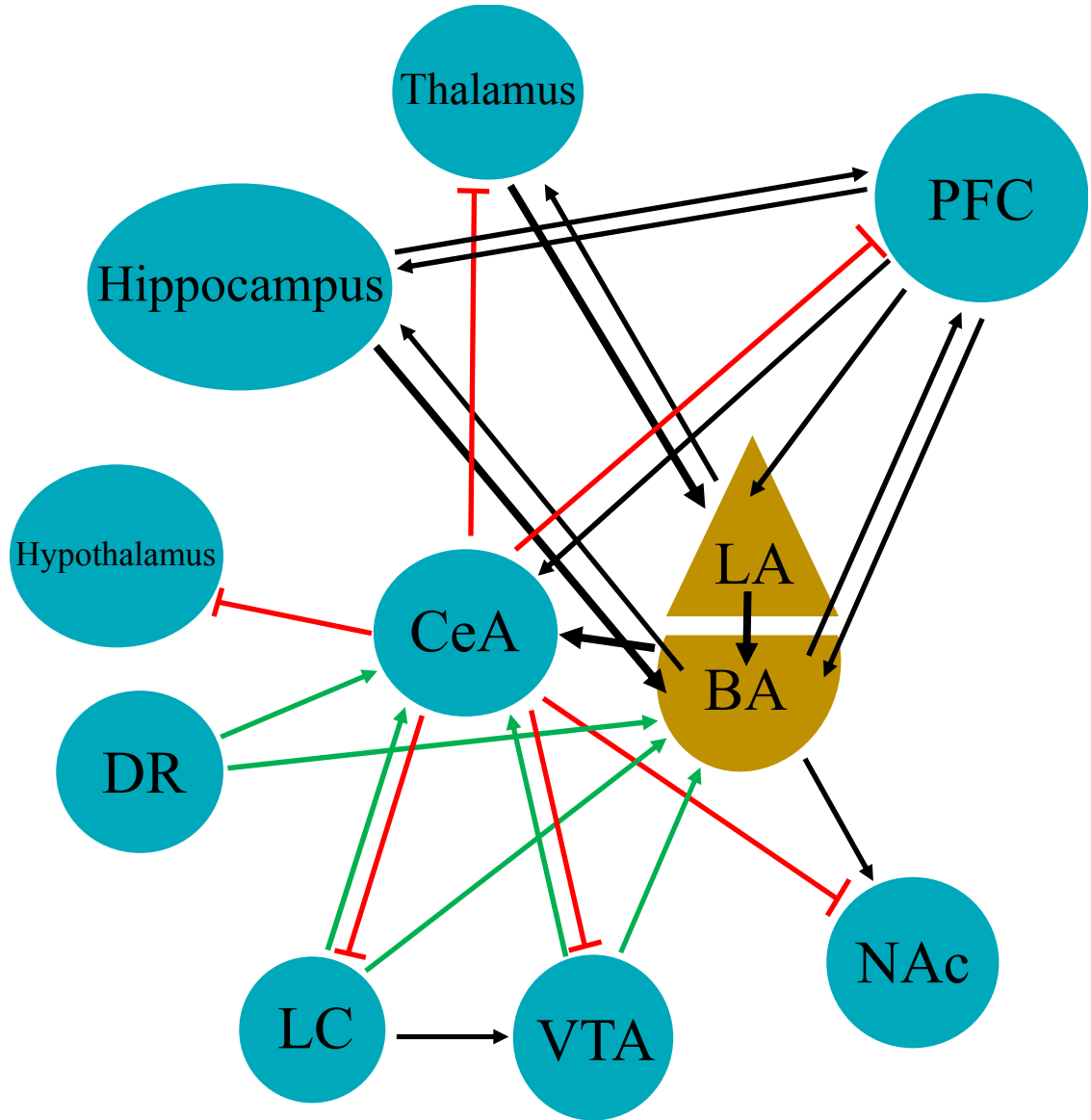


**Figure 1. Afferent and efferent projections of the basal and lateral amygdala.** Black arrows indicate excitatory projections; red arrows with a blunted arrowhead represent inhibitory projections; green lines represent neuromodulatory projections (serotonergic, dopaminergic, etc.). BA = basal amygdala; LA = lateral amygdala; CeA = central nucleus of amygdala; DR = Dorsal Raphe; LC = locus coeruleus; NAc = nucleus accumbens; PFC = prefrontal cortex; VTA = ventral tegmental area.

During a fearful experience, initial sensory inputs, including the CS and US, converge on the BLA via multiple relays including from the LA to BA. Auditory inputs travel through the thalamocortical tract<sup>29</sup>. Contextual information is projected from the hippocampus<sup>7</sup>. Sensory input from the foot shock converges on the BLA through the spinothalamic tract<sup>30</sup>. The BLA then sends excitatory projections to the CeA, which in turn sends inhibitory GABAergic projections to the hypothalamus and brain stem regions, eliciting fearful behaviors, such as flight, freezing, and autonomic responses<sup>10,31,32</sup>. The BLA also sends excitatory projections to the intercalated cells (ITC), which are a mass of GABAergic neurons that act as an inhibitory gating system within the amygdala<sup>33</sup>. Specifically, ITCs send inhibitory projections to the CeA, thereby regulating CeA output<sup>34</sup>. In Figure 2, the amygdalar circuit for fear responses is summarized, in addition to a graphical representation of specific interneurons in the BLA, which is discussed in more detail in Section 1.3.4.2.

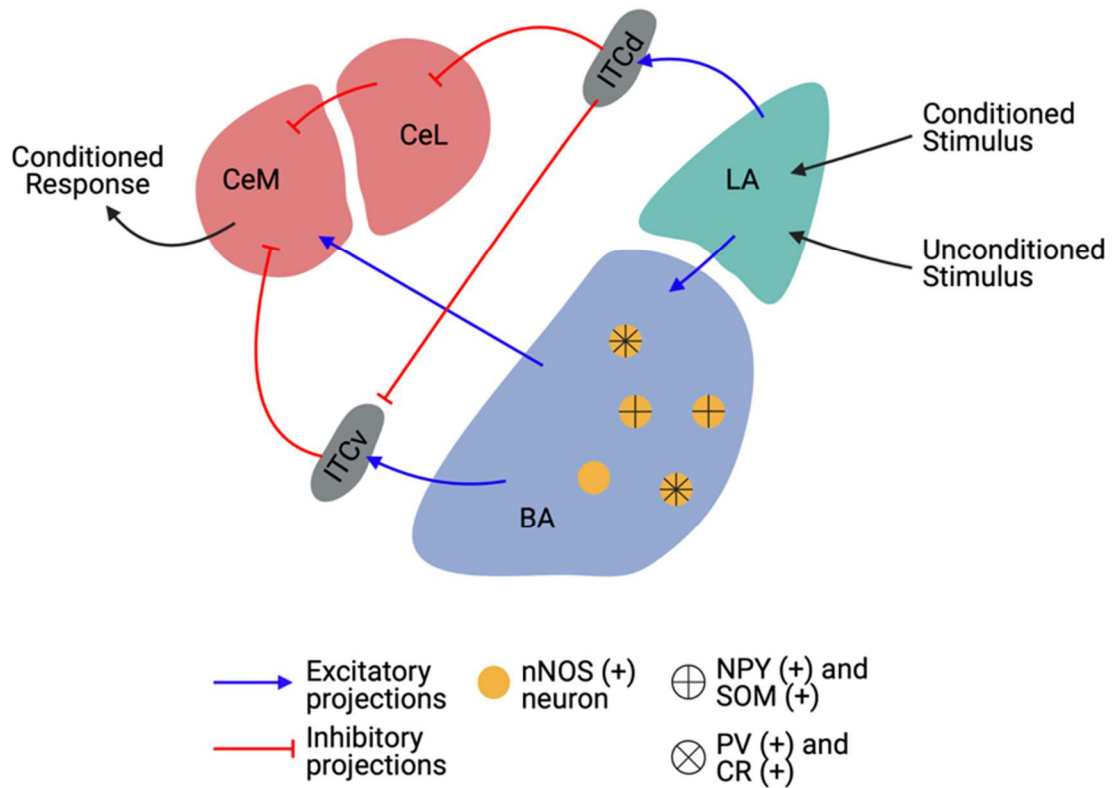


**Figure 2. Amygdalar circuitry in fear responses.** Conditioned, like a musical tone, and unconditioned stimuli, such as a foot shock, converge on the LA, which then projects to the ITCd and BA. The BA sends excitatory projects to the CeM, which projects to other brain regions eventually resulting in a conditioned response, such as freezing. The ITCs send inhibitory projections to the CeL and CeM, thereby serving as an inhibitory gating mechanism in the amygdalar circuitry. LA = lateral amygdala; BA = basal amygdala; ITCd = intercalated cells dorsal; ITCv = intercalated cells ventral; CeL = central nucleus of amygdala, lateral; CeM = central nucleus of amygdala, medial; nNOS = neuronal nitric oxide synthase; NPY = neuropeptide Y; SOM = somatostatin; PV = parvalbumin; CR = calretinin.

In the Pavlovian fear conditioning paradigm, the BLA is believed to encode multiple presentations of the CS-US pairing as an association generator<sup>35-37</sup>. In fact, studies lesioning the BLA show that it is a necessary region for re-expression of conditioned fear responses<sup>38</sup>. Selective inactivation of the BLA immediately after classical fear conditioning resulted in poor fear retention 24 hours after training, implicating the BLA as a critical region for fear memory consolidation<sup>39</sup>. Significant evidence demonstrates, overall, that the BLA is key in fear memory consolidation<sup>18,40-43</sup>. Furthermore, studies confirm that fear consolidation is a coordinated process that is dependent on synchronous *N*-methyl-D-aspartate receptor (NMDAR)-mediated LTP and protein synthesis in the amygdala; blocking either can impair fear consolidation<sup>44-46</sup>. Thus, synaptic plasticity and molecular signaling downstream of NMDAR activation within the BLA play an important role in strengthening the CS-US association, leading to fear memory consolidation. This thesis is focused on the BLA as an important modulator of fear memory consolidation and its role in regulating the mechanisms underlying fear consolidation.

### **1.3 Neurobiology of Fear Consolidation**

#### **1.3.1 Glutamate signaling**

Glutamate is an amino acid and is the primary excitatory neurotransmitter in the central nervous system (CNS). It is stored within vesicles localized to the presynaptic terminals of neurons<sup>47</sup>. Upon glutamatergic afferent signaling, action potential propagation activates glutamatergic terminals, the fusion of glutamate-containing vesicles to the synaptic membrane, and subsequent extracellular glutamate release<sup>48,49</sup>. Glutamate released into the synaptic cleft can then bind to postsynaptic glutamate receptors.



Activation of postsynaptic glutamate receptors generates excitatory postsynaptic currents (EPSCs), which reflect depolarization of the postsynaptic membrane<sup>50,51</sup>. In the BLA during fear conditioning, the activation of postsynaptic glutamate receptors and subsequent synaptic activity leads to the strengthening of synapses (i.e., LTP), which further fortifies the CS-US association<sup>48,52,53</sup>.

There are two major classes of glutamate receptors that glutamate can bind to: metabotropic and ionotropic. Metabotropic glutamate receptors are G-protein coupled receptors that activate intracellular signal transduction<sup>54</sup>. Ionotropic glutamate receptors, on the other hand, are ligand-gated ion channels and conduct fast excitatory neurotransmission<sup>54</sup>.

Of relevance to this project,  $\alpha$ -amino-3-hydroxy-5-methyl-4-isoxazolepropionic acid receptors (AMPA) and NMDARs are tetrameric ionotropic glutamate receptors that conduct excitatory synaptic transmission<sup>55,56</sup>. AMPARs conduct fast synaptic transmission; in contrast, NMDARs generate slower but longer-lasting neurotransmission<sup>57-59</sup>. Both receptors are expressed abundantly in the BLA and play distinct roles in fear memory formation and long-term memory storage within the BLA<sup>60-63</sup>.

### **1.3.2 NMDAR signaling**

NMDARs are ionotropic glutamate receptor that serve as coincidence detectors<sup>64,65</sup>. Unlike AMPARs, which are activated by glutamate binding, NMDARs contain an extracellular  $Mg^{2+}$  block within the channel at basal conditions; in order to remove the  $Mg^{2+}$  ions, there must be presynaptic glutamate release *and* sufficient postsynaptic membrane depolarization, which is mediated by AMPAR activity<sup>64-68</sup>. Once

open, NMDARs are permeable to  $\text{Na}^+$ ,  $\text{K}^+$ , and  $\text{Ca}^{2+}$ <sup>54</sup>. Increased ion flow via NMDARs allows for the activation of intracellular signaling downstream of NMDARs<sup>66,69,70</sup>. Due to their slow activation and deactivation, NMDARs are considered important for the long-lasting strengthening of synapses<sup>68,71,72</sup>. In the BLA, NMDAR-dependent LTP contributes to the formation of fear memories<sup>10,53,73-75</sup>.

NMDARs are tetramers that are composed of three subunits, NR1, NR2, and NR3<sup>76-78</sup>. All NMDARs contain two obligatory NR1 subunits and two NR2 or NR3 subunits, although NR3 is not commonly found within forebrain regions<sup>79-81</sup>. The NR2B subunit of NMDARs is especially important for LTP that contributes to associative learning<sup>82-85</sup>. Additionally, blocking NR2B-containing NMDARs within the BLA can impair cued fear acquisition<sup>86</sup>. However, the role of NR2B and NR2B-mediated intracellular signaling in fear memory consolidation is not clearly elucidated.

Multiple phosphorylation sites on NR2B have been similarly reported to be important for NMDAR function. Phosphorylation at Ser1303 by calcium/calmodulin-dependent protein kinase II (CaMKII) and protein kinase C (PKC) enhances  $\text{Ca}^{2+}$  influx without affecting overall expression levels of NR2B, suggesting that the primary role of p-Ser1303 in modulating NMDAR synaptic activity is to enhance  $\text{Ca}^{2+}$  entry<sup>85,87,88</sup>. Phosphorylation at Tyr1472, which occurs via Fyn kinase activation, increases after LTP and may contribute to normal fear learning by regulating appropriate localization of NMDARs at synapses<sup>89,90</sup>. Finally, the phosphorylation of Ser1480 by casein kinase 2 (CK2) maintains NR2B at extrasynaptic sites. Upon dephosphorylation of Ser1480, NR2B surface expression is increased<sup>91-93</sup>. This suggests that NMDARs phosphorylated

at Ser1480 serve as an extrasynaptic pool of NMDARs that can be recruited to the synapse in an activity-dependent manner<sup>93</sup>.

### 1.3.3 AMPAR signaling

As glutamate is released from presynaptic terminals, it can bind to and open AMPARs<sup>94,95</sup>. Glutamate binding to AMPARs allows for Na<sup>+</sup> influx and K<sup>+</sup> efflux; this contributes to fast and transient synaptic transmission<sup>96</sup>. AMPARs are also selectively permeable to Ca<sup>2+</sup>, depending on the AMPAR subunit composition<sup>96</sup>. AMPARs are composed of four subunits: GluR1, GluR2, GluR3, and GluR4<sup>97,98</sup>. Of these subunits, the presence or absence of GluR2 determines the Ca<sup>2+</sup> permeability of the AMPAR. GluR2-containing AMPARs are Ca<sup>2+</sup>-impermeable, while GluR2-lacking AMPARs are Ca<sup>2+</sup>-permeable<sup>96,99</sup>. As a result, GluR2-lacking AMPARs have higher channel conductance as they allow for intracellular Ca<sup>2+</sup> flow<sup>100</sup>.

In the BLA, specifically, there is evidence for the importance of GluR1 in fear learning. Acquisition of auditory fear conditioning and LTP in the BLA is disrupted in *GluR1*<sup>-/-</sup> knockout mice<sup>101</sup>. Additionally, fear conditioning results in an increase in GluR1-containing AMPARs in the amygdala, which is reversed with D-cycloserine, a partial NMDAR agonist, suggesting that NMDAR and GluR1-containing AMPAR activity during fear conditioning are linked in the BLA<sup>102</sup>.

Importantly, in addition to increasing membrane trafficking and the expression of GluR1 in the BLA, phosphorylation of GluR1 regulates AMPAR function, similar to NMDARs. There are two essential sites on GluR1 – Ser831 and Ser845 – that are reported to be involved in fear memory-specific AMPAR function. CaMKII and PKC phosphorylate AMPARs at Ser831, and protein kinase A (PKA) and cGMP-dependent

protein kinase (PKG) phosphorylate AMPARs at Ser845<sup>103-105</sup>. The phosphorylation of AMPARs at Ser831 is important for increased AMPAR channel conductance<sup>106</sup>; whereas phosphorylation at Ser845 increases AMPAR open time probability, thereby potentiating AMPAR-mediated current<sup>107</sup>. Phosphorylation of both Ser831 and Ser845 is important for modulating LTP in fear learning<sup>108-110</sup>.

Figure 3 summarizes the information above, focusing on regulation of AMPARs and NMDARs via key intracellular signaling cascades, including signaling downstream of the NMDAR-PSD95-nNOS axis.

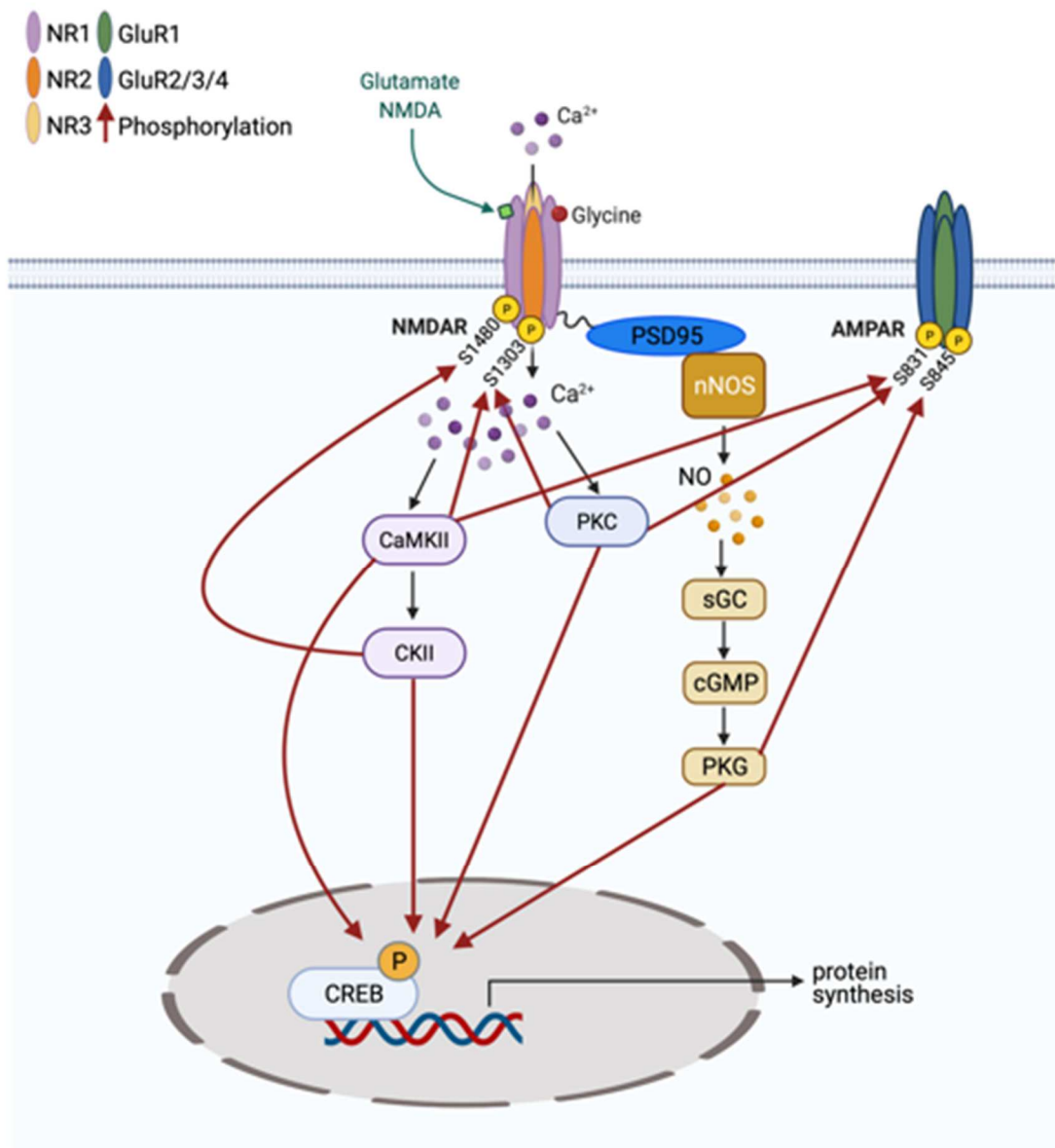


**Figure 3. Intracellular signaling cascade downstream of NMDAR activation in an nNOS-expressing cell.** Intracellular Ca<sup>2+</sup> influx activates PKC and CaMKII, which then activates CKII. The scaffolding of PSD95 and nNOS to the NMDARs, and subsequent Ca<sup>2+</sup> influx also activates production of nNOS, which leads to a cascade resulting in PKG activation. Both CaMKII and PKC phosphorylate AMPARs on Serine 831 and NMDARs on Serine 1303, such that it positively regulates their insertion to the membrane surface. CKII phosphorylates NMDARs on Serine 1480, and PKG phosphorylates AMPARs on Serine 845. Lastly, all signaling pathways lead to transcriptional regulation, gene expression, and protein synthesis. CaMKII = calcium/calmodulin-dependent protein kinase II; PKC = protein kinase C; CKII = casein

kinase II; PSD95 = postsynaptic density protein 95; nNOS = neuronal nitric oxide synthase; sGC = soluble guanylyl cyclase; cGMP = cyclic guanosine monophosphate; PKG = cGMP-dependent protein kinase; CREB = cAMP-response element binding protein.

### **1.3.4 NMDAR-PSD95-nNOS axis**

#### **1.3.4.1 PSD95 structure & function**

The function of AMPARs and NMDARs are linked in part due to intracellular signaling that includes multiple proximal molecules within the synapse where AMPARs and NMDARs are located. These dense regions, referred to as the post-synaptic density (PSD), are compartments localized to the dendritic spines of excitatory synapses and are a central region for signal transduction events<sup>111</sup>. The PSD can contain receptors, scaffolding proteins, and signaling proteins, and these proteins are optimally organized to form complexes that stabilize ion channels and receptors at the synapse and further recruit and activate downstream signaling molecules.

An important scaffolding protein within the PSD is PSD95, a 95 kDa member of the membrane-associated guanylate kinase (MAGUK) family<sup>112</sup>. PSD95 binds, stabilizes, and traffics AMPARs and NMDARs and, upon receptor binding, can also recruit multiple signaling molecules to the surface membrane and close to the channel pores<sup>113-116</sup>. PSD95 is composed of three PDZ domains, a Src homology 3 domain, and a guanylate kinase domain that has no catalytic activity<sup>112,117</sup>. All PSD95 domains promote protein-protein interaction and thus mediate the assembly of protein complexes at the synapse<sup>117-119</sup>.

PSD95 is abundant in the forebrain<sup>120</sup>. The synaptic functions mediating fear memories are dynamically modulated by PSD95. Studies show that PSD95 localizes NMDARs to the synapse and inhibits their internalization<sup>121,122</sup>. Additionally, the loss of PSD95 in synapses leads to diminished synaptic AMPARs, impaired AMPAR-mediated transmission, long-term depression, and decreased dendritic spines<sup>123-128</sup>. Multiple behavioral studies in PSD95-mutant models also demonstrate deficits in spatial memory

tasks, anxiety-like behavior, hypoactivity, and fear learning<sup>129,130</sup>. Thus, by its regulation of synaptic transmission, PSD95 plays an important role in learning and memory.

#### **1.3.4.2 nNOS structure & function**

Nitric oxide synthase (NOS) is an enzyme that catalyzes the production of L-citrulline and nitric oxide (NO) from L-arginine and oxygen<sup>131,132</sup>. There are three distinct NOS isoforms, with 51-60% sequence homology in humans: neuronal NOS (nNOS), endothelial NOS (eNOS), and inducible NOS (iNOS)<sup>133</sup>. All NOS isoforms contain an N-terminal oxygenase domain and a C-terminal reductase domain and are homodimeric<sup>134,135</sup>. The oxygenase domain can bind iron protoporphyrin IX (heme), tetrahydrobiopterin (BH<sub>4</sub>), L-arginine, and oxygen<sup>136</sup>. The reductase domain can bind flavin mononucleotide (FMN), flavin adenine dinucleotide (FAD), and NADPH<sup>132,136</sup>. Separating these two domains is a calmodulin (CaM) binding domain, which serves as a Ca<sup>2+</sup> sensor<sup>137,138</sup>.

While all isoforms are expressed in the CNS, they are not uniformly distributed. nNOS is primarily found in neurons and astrocytes<sup>139,140</sup>. iNOS is expressed in astrocytes and microglia during inflammation<sup>141,142</sup>, and eNOS is found in astrocytes and vascular endothelial cells<sup>143,144</sup>.

The research presented in this thesis focuses on the nNOS isoform, which is a 160 kDa constitutively expressed enzyme<sup>145</sup>. Unlike eNOS and iNOS, nNOS contains a PDZ domain at the N-terminus, which interacts with other PDZ-containing proteins, such as PSD95<sup>146</sup>. Binding to PSD95 via the PDZ-PDZ domain interaction localizes nNOS to the cellular membrane<sup>147</sup>. Moreover, nNOS activity is Ca<sup>2+</sup>-dependent. With elevated intracellular Ca<sup>2+</sup> levels, Ca<sup>2+</sup>/CaM binds to nNOS, which facilitates the production of



NO<sup>148</sup>. Thus, the interaction between PSD95 and nNOS is critical for activation of nNOS, as evident from numerous studies that show that blocking this interaction disrupts the enzymatic activity of nNOS<sup>149-151</sup>.

The production of NO also requires nNOS homodimerization, which is dependent on the binding of BH<sub>4</sub>, heme, and L-arginine at the oxygenase domain<sup>132</sup>. Meanwhile, NADPH in the reductase domain reduces FAD, which shuttles electrons to FMN<sup>132</sup>. Once CaM binds nNOS, a conformational change allows for electron transfer from FMN on one nNOS monomer's reductase domain to the heme on the oxygenase domain of the other nNOS monomer<sup>152,153</sup>. The heme group can then bind oxygen and facilitate catalytic production of L-citrulline and NO, as summarized in Figure 4.

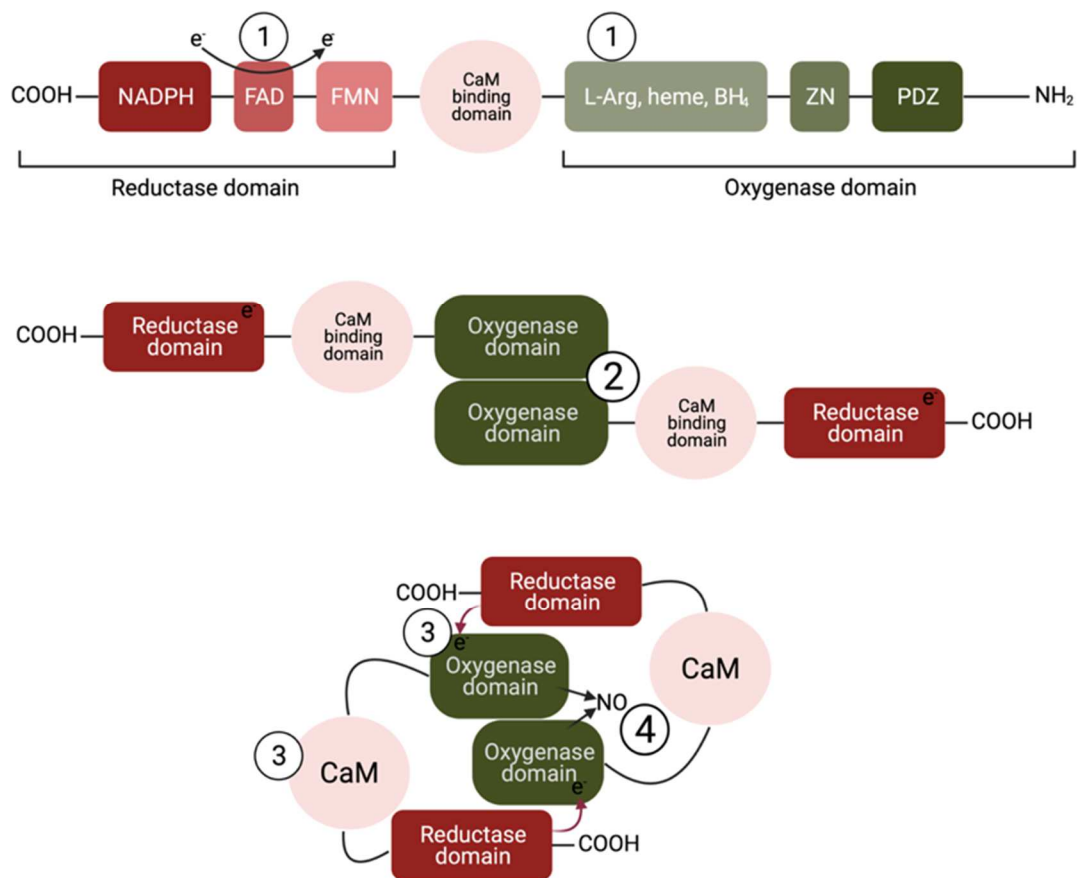


**Figure 4. The structure and activation of nNOS.** (1) NADPH reduces FAD and transfers electrons to FMN. Meanwhile, binding of L-arginine, heme, and BH<sub>4</sub> to the oxygenase domain leads to (2) homodimerization via interaction at the N-terminal oxygenase domains. (3) Upon CaM binding at the CaM-binding site, conformational changes allow for electron transfer from the reductase domain of one nNOS monomer to the oxygenase domain of the other nNOS monomer. (4) With electron transfer to the heme group, heme can now bind oxygen and catalyze production of nitric oxide. FAD = flavin adenine dinucleotide; FMN = flavin adenine mononucleotide; CaM = calmodulin; L-Arg = L-arginine; heme = iron protoporphyrin IX; BH<sub>4</sub> = tetrahydrobiopterin; NO = nitric oxide.

Multiple studies confirm nNOS expression in the BLA and demonstrate that nNOS-expressing cells are largely GABAergic and display high intrinsic excitability<sup>154-156</sup>. A recent study of nNOS-expressing cells in the BLA further revealed that most nNOS-positive cells express neuropeptide Y (NPY) and somatostatin (SOM) and, to a lesser extent, express parvalbumin (PV) and calretinin<sup>156</sup>. In contrast, nNOS-positive cells in the BLA barely express calbindin and vasoactive intestinal peptide (VIP)<sup>156</sup>. Another study found that nNOS-positive neurons project locally within the BLA as well as outside of the BLA, to structures like the piriform cortex and caudate-putamen<sup>154</sup>. In addition to illustrating the heterogeneity of nNOS-positive interneurons in the BLA, these studies indicate that nNOS-positive neurons play diverse roles within the BLA circuit and may have long-range inhibitory projections that regulate other brain regions<sup>154,156</sup>.

The roles of nNOS and NO in neuropsychiatric illnesses are an emerging area of study in neuroscience. While nNOS is known to regulate cardiovascular function, blood clotting, and immune responses<sup>133</sup>, it is also crucial for neurotransmission. In fact, disrupting nNOS function in rodent models results in depressive-like behavior, greater aggression, and impaired social cue processing<sup>157,158</sup>. Mice with a knockdown of the nNOS gene show deficits in both spatial working and reference memory<sup>159</sup>. In addition to cognitive function, nNOS<sup>-/-</sup> mice that undergo fear conditioning exhibit dramatically reduced short-term (1 hour post-fear conditioning) and long-term (24 hours and 7 days post-fear conditioning) memory of cued and contextual fear<sup>160</sup>. nNOS appears to play an important role in cognitive function and behavior, and as such, the neural mechanisms underlying its effects on behaviors are worth investigating.

An initial study of NOS and LTP in the hippocampus suggested that eNOS, not nNOS, was primarily responsible for LTP induction<sup>161</sup>. However, a recent study from our laboratory showed that blocking nNOS activity can disrupt LTP in BLA neurons<sup>162</sup>. Thus, nNOS may have site-specific effects on LTP and thereby modulate the formation of fear memories.

#### **1.3.4.3 NMDAR-PSD95-nNOS dynamics**

While it is established that PSD95 and nNOS are involved in modulating fear behavior, understanding the structure of the NMDAR-PSD95-nNOS complex is key for isolating and therapeutically targeting this interaction. PSD95 contains three PDZ domains<sup>117</sup>. PDZ domains are protein domains that are 80-100 amino acids long and typically contain five or six  $\beta$ -strands and two or three  $\alpha$ -helices<sup>163</sup>. Based on the structure, PDZ domains may bind the C-terminus of other proteins or other PDZ domains<sup>164,165</sup>. Of the three PDZ domains of PSD95, PDZ1 and PDZ2 can bind to the C-terminus of NMDARs, specifically to the NR2 subunit<sup>166</sup>. The PDZ motif of nNOS, which includes a flexible two-stranded  $\beta$ -finger formation, binds to PDZ2 of PSD95; the PDZ dimerization stabilizes the nNOS  $\beta$ -finger into a rigid  $\beta$ -sheet structure<sup>164,167</sup>. This stabilization also requires a salt bridge between Arg121 in the nNOS  $\beta$ -finger and Asp62 in the canonical nNOS PDZ domain<sup>167</sup>. A point mutation at Arg121 changes the  $\beta$ -finger in nNOS to a highly flexible structure and abolishes the PSD95-nNOS dimer formation<sup>167</sup>. This indicates that after binding PSD95, the conformational change in the  $\beta$ -finger in nNOS is necessary to maintain the PSD95-nNOS interaction.

In summary, the typical formation of the NMDAR-PSD95-nNOS complex includes NR2 subunit binding to PDZ1 on PSD95, and the subsequent binding of nNOS

to PDZ2 of PSD95. Upon binding to PSD95, the nNOS PDZ domain shifts conformationally such that it remains tightly anchored to PSD95 and thus maintains proximity to NMDARs. Thus, PDZ interactions via PSD95 mediate the formation of the ternary NMDAR-PSD95-nNOS complex and the subcellular localization of nNOS at the synaptic membrane<sup>118,168</sup>.

Consequently, once NMDARs are activated, intracellular  $\text{Ca}^{2+}$  increases. Intracellular  $\text{Ca}^{2+}$  can bind CaM, a  $\text{Ca}^{2+}$  sensor. CaM binds to a helical region located between the N-terminal oxygenase and C-terminal reductase domains of nNOS. CaM binding to nNOS conformationally alters the catalytic domain of nNOS and thereby catalyzes NO production<sup>169</sup>. The importance of CaM is further supported by a study that showed that CaM-bound nNOS homodimers, unlike CaM-lacking nNOS homodimers or nNOS monomers, are catalytically active<sup>170</sup>. Thus, nNOS enzymatic activity requires a cascade of events, which begins with the formation of the NMDAR-PSD95-nNOS complex. Specifically, the interaction between PSD95 and nNOS is a crucial step in ensuring the proximity between NMDARs and nNOS as well as robust NO production. Downstream of the NMDAR-PSD95-nNOS axis, NO then regulates multiple mechanisms that are important for neurotransmission, specifically in the context of learning and memory.

#### **1.3.4.4 Downstream implications of NO activity**

As NO production is mediated by  $\text{Ca}^{2+}$ /CaM binding, its activity is interconnected to neurotransmission. Downstream of NMDAR activation, NO production has several distinct pathways that affect synaptic activity, as summarized in Figure 5.

First, NO is a free radical that can diffuse through the postsynaptic membrane and retrogradely interact with the presynaptic neuron<sup>171</sup>. In retrograde signaling, NO is shown to modify and potentiate neurotransmitter release and produce LTP<sup>172-175</sup>.

Second, NO reacts with cysteine residues in proteins to produce S-nitrocysteine, in a posttranslational modification known as S-nitrosylation<sup>176,177</sup>. S-nitrosylation sites have been identified in over 1000 proteins<sup>178,179</sup>. In addition to regulating protein function and localization, S-nitrosylation in the CNS also modulates neurotransmission and neurogenesis<sup>180-184</sup>. For example, the NR2B subunit of NMDARs, Src and Fyn kinases (which both phosphorylate NR2B at Tyr 1472), and PSD95 are S-nitrosylated downstream of NO formation, resulting in fine-tuned regulation of NMDAR activity<sup>181,185-187</sup>. Similarly, S-nitrosylation of the GluR1 subunit of AMPARs, stargazin (a transmembrane AMPAR regulatory protein that binds and maintains AMPAR membrane expression), and N-ethylmaleimide sensitive factor (NSF) facilitates enhanced expression and conductance of AMPARs in neurons<sup>188-190</sup>. S-nitrosylation is also involved in the transcriptional regulation of genes<sup>180,191</sup>.

Third, NO binds to the ferrous heme of soluble guanylate cyclase (sGC), which catalyzes the conversion of guanosine-5'-triphosphate (GTP) to cyclic guanosine monophosphate (cGMP), a secondary messenger<sup>137,192</sup>. cGMP activates numerous intracellular signaling cascades and regulates gene transcription<sup>193,194</sup>. Notably, cGMP regulates PKG activity, which has numerous implications for synaptic plasticity<sup>171,195,196</sup>. Studies show that PKG modulates phosphorylation and extrasynaptic expression levels of GluR1 and increases synaptic potentiation by binding to the GluR1 subunit on AMPARs<sup>197-199</sup>. This suggests that NO-mediated PKG can influence the priming of

AMPA receptors at the synapse, clearly affecting synaptic transmission. Additional studies in the visual cortex, spinal neurons, hippocampus, and VTA indicate that NO and cGMP-mediated pathways are crucial for synaptic potentiation<sup>200-203</sup>. There is also evidence that blocking PKG signaling in the LA impairs LTP and fear memory consolidation<sup>204</sup>. In combination with a study published by our laboratory that shows that blocking nNOS activity impairs LTP and fear memory consolidation, this strongly indicates that signaling mechanisms downstream of nNOS modulate synaptic transmission and thereby impact fear memory formation<sup>162</sup>.

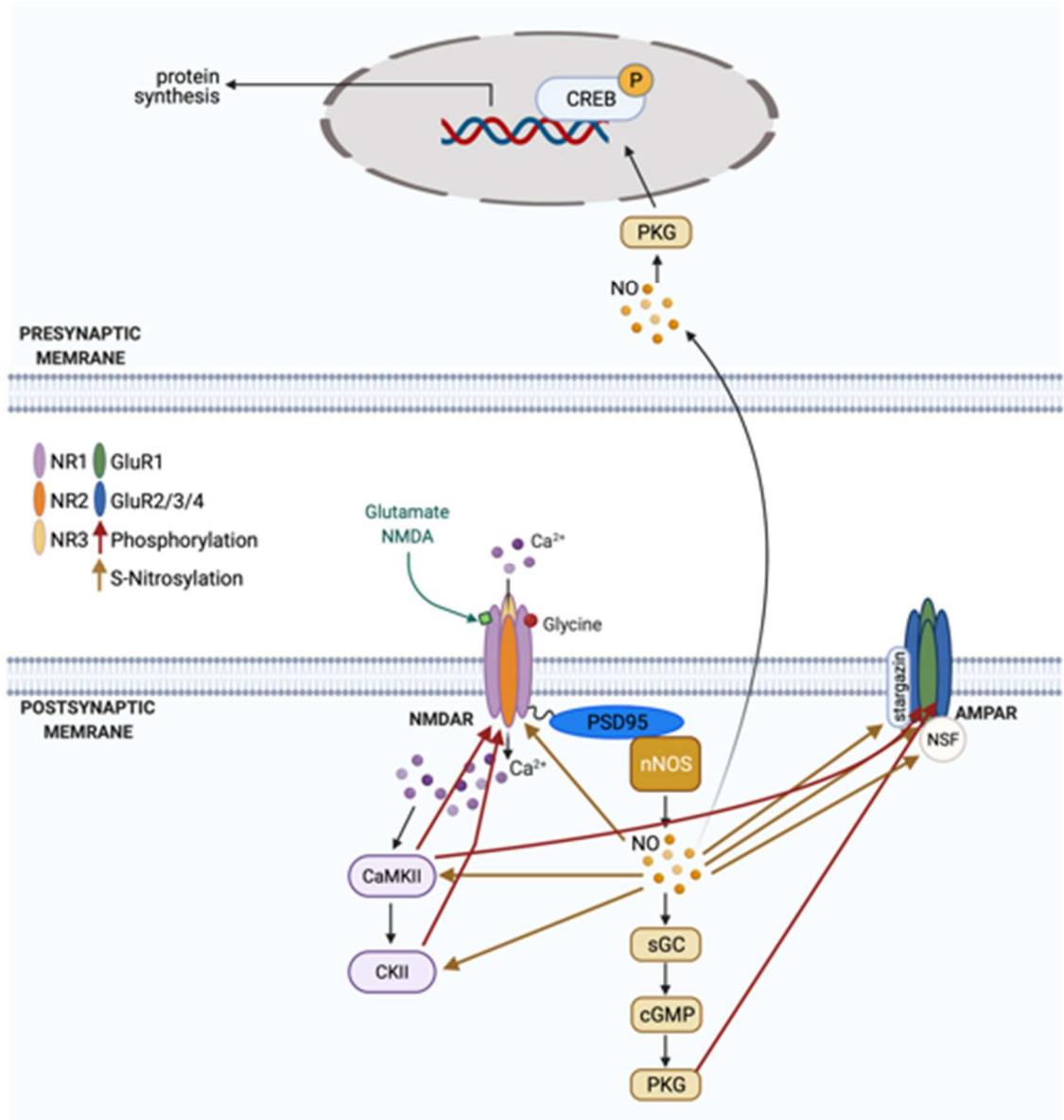


**Figure 5. nNOS-mediated intracellular signaling cascade.** In addition to the cascades shown in figure 2, nNOS activation downstream of NMDAR channel opening results in NO synthesis. NO can activate the sGC-cGMP-PKG pathway, which 1) travels retrogradely and signals to the presynaptic neuron, 2) S-nitrosylates multiple important proteins, and 3) phosphorylates AMPARs at Serine 845. Specifically, NO S-nitrosylates NSF, GluR1, stargazin, PSD95, NR2B, Fyn kinase, and Src kinase, resulting in overall enhancement of AMPAR and NMDAR channel conductance. CaMKII = calcium/calmodulin-dependent protein kinase II; CKII = casein kinase II; PSD95 = postsynaptic density 95; nNOS = neuronal nitric oxide synthase; NO = nitric oxide; sGC = soluble guanylyl cyclase; cGMP = cyclic guanosine monophosphate; PKG = cGMP-dependent protein kinase; NSF = N-ethylmaleimide sensitive fusion protein; CREB = cAMP-response element binding protein.



### 1.3.5 Gene transcription

Transcription is a biological process that copies DNA into RNA during the first step of gene expression and protein synthesis. For long-term memory formation and storage, transcription is necessary and occurs at the time of learning<sup>13,205-207</sup>. More recent studies have also revealed that transcription-dependent consolidation of memory can last more than 24 hours past the initial learning event, indicating that there is a temporal window when initial memory consolidation can be disrupted<sup>208-210</sup>. This is further validated in studies that show that the higher the latency in administering a pharmacological manipulation after a learning event, the less effective it is in regulating long-term memory consolidation<sup>211,212</sup>.

Specifically, in fear consolidation models, disrupting cyclic adenosine monophosphate response element-binding protein (CREB) function in the amygdala can impair fear memory formation<sup>213</sup>. Similarly, CCAAT enhancer-binding protein (C/EBP) can modulate both long-term memory formation and long-term synaptic plasticity<sup>214-216</sup>. CREB is a transcription factor that can activate C/EBP, which is an immediate early gene<sup>217,218</sup>. This reveals the importance of transcriptional elements in the BLA for the long-term storage of fear memories. Studies also show that genes important for fear consolidation and synaptic plasticity are transcriptionally regulated<sup>219,220</sup>. In summary, there is evidence to demonstrate that transcriptional pathway cascades that occur after initial learning within the amygdala activate and maintain long-lasting functional changes.

Interestingly, research in the last 20 years has begun to establish the role of NO signaling in gene transcription. cGMP signaling, downstream of NO production, can

activate transcriptional machinery<sup>221,222</sup>. Specifically, in the BLA during fear conditioning, NO-cGMP-PKG signaling activates extracellular signal-related kinase (ERK) expression and thereby drive gene expression<sup>223</sup>. Furthermore, NO signaling results in increased phosphorylation of CREB, a process required for CREB-driven transcriptional regulation<sup>224</sup>. Therefore, NO signaling plays a well-defined role in regulating gene transcription and may be an important part of the mechanism underlying transcriptional regulation of fear consolidation.

#### **1.4 nNOS Inhibitors**

The inhibition of NMDARs has previously been shown to strongly impair fear consolidation<sup>225-228</sup>. However, blocking the activity of receptors as ubiquitous as NMDARs results in detrimental off-target effects<sup>229,230</sup>. As a result, it has become increasingly necessary to find pathways and therapeutic targets downstream of NMDARs that may selectively improve fear learning deficits. Recent studies of nNOS show that inhibition of nNOS activity, systemically and within the BLA, can specifically impair auditory fear consolidation<sup>162,231</sup>. Thus, nNOS inhibitors are a promising therapeutic target that must be explored further.

Several nNOS inhibitors have been shown to alter fear behaviors. N<sup>G</sup>-nitro-L-arginine methylester (L-NAME) has task-dependent effects on fear extinction in rats<sup>232</sup>. 7-nitroindazole (7-NI) administration in mice resulted in decreased fear expression and greater fear extinction<sup>233</sup>. Amygdala-specific injections of 7-NI and an NO scavenger were both able to inhibit fear renewal<sup>234</sup>. However, these nNOS inhibitors do not have high oral bioavailability nor efficiently cross the blood-brain barrier<sup>235,236</sup>. As a result,

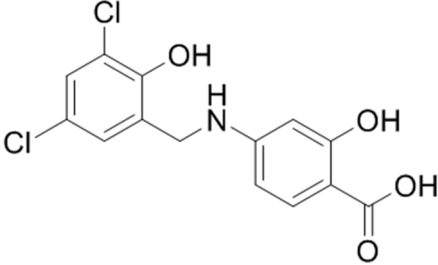
small-molecule protein-protein interaction inhibitors have been increasingly studied as an alternative approach to blocking nNOS signaling.

### **1.5 Small-Molecule PSD95-nNOS Binding Inhibitors**

Small-molecule protein-protein interaction inhibitors are an ideal option for preclinical and clinical studies, because they are not as potent as nNOS inhibitors and have pharmacokinetic properties that are better suited for *in vivo* studies. Significantly, two small-molecule inhibitors have been effective in blocking the PSD95-nNOS interaction. The first is IC87201 (2-((1*H*-benzotriazol-6-ylamino)methyl)-4,6-dichlorophenol), which disrupted the PSD95-nNOS interaction with an IC<sub>50</sub> of 31 μM. While its binding site is unknown, IC87201 inhibited NMDAR-dependent cGMP production, had antinociceptive effects in an NMDA-induced thermal hyperalgesia model and chemotherapy-induced neuropathic pain model, and abolished mechanical allodynia in a nerve injury model<sup>151,237</sup>.

Another PSD95-nNOS inhibitor that is structurally similar to IC87201 but has a lower IC<sub>50</sub> is ZL006 (4-(3,5-dichloro-2-hydroxy-benzylamino)-2-hydroxybenzoic acid)<sup>238</sup>. ZL006 is thought to interact with the Arg121 residue of the β-finger on the PDZ domain of nNOS, resulting in a disrupted salt bridge<sup>238</sup>. This restricts the conformational change in nNOS that is required for binding to PSD95, ultimately inhibiting the PSD95-nNOS interaction and the catalytic activity of nNOS<sup>167,238</sup>. Accordingly, ZL006 inhibited NMDAR-dependent NO synthesis with an IC<sub>50</sub> of 82 nM<sup>238</sup>. ZL006 is also reported to cross the blood-brain barrier and attenuate fear consolidation with systemic and intra-BLA administration<sup>162,238</sup>. Additionally, ZL006 does not affect the NMDAR-PSD95 interaction, but it sufficiently blocks the PSD95-nNOS interaction in the BLA<sup>162,238</sup>. For

these reasons (summarized in Table 1), ZL006 is a useful tool in exclusively analyzing nNOS-dependent signaling within the NMDAR-PSD95-nNOS axis.

<b>ZL006</b>	
<b>Structure</b>	
<b>Molecular weight</b>	328.1 g/mol
<b>Activity site (anticipated)<sup>238</sup></b>	Arg121 of nNOS
<b>IC<sub>50</sub><sup>238</sup></b>	82 nM
<b>ED<sub>50</sub> (suppression of mechanical allodynia, mice)<sup>239</sup></b>	0.93 mg/kg i.p.
<b>[ZL006] serum (1.5 mg/kg intravenous, rat)<sup>238</sup></b>	15 minutes: ~ 2.8 µg/mL 60 minutes: ~ 1.6 µg/mL
<b>[ZL006] brain (1.5 mg/kg intravenous, rat)<sup>238</sup></b>	15 minutes: ~ 0.3 µg/mL 60 minutes: ~ 0.6 µg/mL

**Table 1. A summary of ZL006 properties.**

## 1.6 Aims and Hypothesis

As described in detail above, NMDAR- PSD95-nNOS interaction and thereby generating NO production is a critical step for conditioned fear responses, and corresponding gene transcription, and regulation of glutamate signaling<sup>162,240</sup>. Our laboratory has recently shown that the PSD95-nNOS interaction is especially important in the BLA for fear consolidation, and intra-amygdalar inhibition of the PSD95-nNOS interaction sufficiently impairs auditory fear consolidation<sup>162</sup>. Additionally, disrupting the PSD95-nNOS interaction results in impaired LTP in BLA neurons. Based on these observations, in this dissertation, I focus on the role of the NMDAR-PSD95-nNOS axis

within the BLA in the regulation of the molecular mechanisms underlying cue-induced conditioned fear consolidation.

The central hypothesis of the project is that activation of the NMDAR-PSD95-nNOS axis is required for changes in the glutamatergic signaling, receptor dynamics, and gene transcriptions in the BLA underlying fear consolidation. The specific aims of this project are:

- I. To map the alterations in the BLA transcriptome as a result of auditory fear conditioning with or without pre-treatment with PSD95-nNOS binding inhibitor ZL006.
- II. To determine the role of the NMDAR-PSD95-nNOS axis on time-dependent shifts in glutamatergic signaling and synaptic AMPAR and NMDAR dynamics following auditory fear memory consolidation.
- III. To elucidate the effects of a BLA-specific knockdown of the *nNos* gene on auditory fear consolidation and synaptic AMPAR and NMDAR dynamics.

## CHAPTER 2

### **Transcriptomic Study of Molecular Mechanisms Underlying NMDAR-PSD95-nNOS-NO Axis Mediated Fear Consolidation in the Amygdala: Key Role of IGF2 and IGFBP2**

#### **2.1 Introduction**

Normal fear responses are evolutionarily necessary to promote survival<sup>241</sup>. These responses are often triggered by perceived threats or aversive stimuli such as loud noises or pain. However, persistent fear responses that remain long after cessation of aversive stimuli can lead to anxiety or fear disorders<sup>241,242</sup>. Persistent fear responses have been studied in rodents using Pavlovian cued fear conditioning<sup>242,243</sup>. In this procedure, fear acquisition is induced through the repeated pairing of a neutral conditioned stimulus (CS) such as light or sound with an unconditioned aversive stimulus (US) such as a shock or predator odor<sup>242</sup>. Following acquisition, i.e., fear association with the CS, fear consolidation occurs over the next several hours, during which period the association of the CS and US is further established, and the labile fear memory stabilizes to become a long-term learned response<sup>244-246</sup>. In humans, the consolidation of cue-induced trauma is considered a critical process underlying the pathophysiology of anxiety and fear disorders<sup>247</sup>. As such, identifying potential therapeutic targets for disrupting fear consolidation may lead to novel therapies for anxiety and fear disorders.

During fear acquisition, N-methyl D-aspartate receptors (NMDARs) recruit and assemble postsynaptic density protein 95 (PSD95) and neuronal nitric oxide synthase (nNOS) in a complex at the cell surface<sup>118,248,249</sup>. The assembly of this complex conformationally changes nNOS to actively produce nitric oxide (NO)<sup>250</sup>. We previously

reported that blocking the PSD95-nNOS interaction via systemic and intra-basolateral amygdala (BLA) administration of a small molecule protein-protein inhibitor, ZL006, attenuated fear consolidation, thus establishing the importance of BLA-associated PSD95-nNOS-NO axis in consolidation of cued fear<sup>162</sup>.

Our findings are consistent with other studies highlighting the role of the PSD95-nNOS-NO axis in fear responses; however, little is known about the downstream molecular mechanisms following NO production that regulate fear consolidation<sup>231,251,252</sup>.

In the present study, we explored transcriptome-wide changes in the BLA after cued fear consolidation and demonstrated unique gene expression patterns and corresponding functional enrichment of signaling pathways. Next, we determined which of these gene expression patterns and networks were altered by pre-treatment with ZL006. Our findings demonstrate several novel gene networks critical for NO-induced fear consolidation in the amygdala and identify novel therapeutic targets specific to cued fear consolidation.

## **2.2 Materials and Methods**

Animals: Adult male Sprague-Dawley rats (250-300 g, Harlan, IN, USA) were used for fear conditioning and RNA-sequencing experiments. Rats were housed in a temperature-controlled vivarium (22 °C) on a 12:12h light-dark cycle with food and water provided *ad libitum*. Rats were single-housed and given at least three days to acclimate to the new housing environment before handling and behavioral testing.

Animal care was in accordance with NIH Guidelines for the Care and Use of Laboratory Animals, and all procedures were approved by the IUPUI Institutional Animal Care and Use Committee.

Fear conditioning test: Rats were fear-conditioned and treated as described previously<sup>162</sup>. Briefly, rats were handled for five mins each/day for five days leading up to fear conditioning. On the first day of testing, rats were habituated to the conditioning contexts for 10 min each. Context A was a box with transparent walls, a metal grid floor connected to a shock generator (Stoelting Co., Wood Dale, IL, USA), and was cleaned with 70% ethanol between trials; context B was a box with patterned walls, a solid floor insert, and was cleaned with 1% acetic acid for a novel odor. Both boxes were placed in a larger, soundproof Ugo Basile box.

For fear conditioning, 24 h after habituation, rats were placed in context A for habituation (100s) followed by three tones (20s, 4kHz, 80dB) that co-terminated with a shock (0.5s, 0.8mA). The “tone-only” group experienced the same protocol but without receiving foot-shocks. In the experiments for Figure 7A, all rats received drug or vehicle intraperitoneal injections immediately after fear conditioning. After 24 h, rats were placed in context B with the same protocol, without foot-shocks. Animal movement was tracked using an automated video recording and tracking system (ANYmaze, Stoelting Co.). Fear responses were calculated as percent time spent freezing during tones; freezing was defined as full immobility excluding respiration. A two-way ANOVA was used, with treatment as a between-subjects factor and tones as a within-subjects factor. *Post hoc* Fisher’s LSD test was used when  $p < 0.05$ .

Drugs and chemicals: For intraperitoneal injections, ZL006 (Sigma Aldrich, St. Louis, MO, USA) was dissolved in a vehicle of 10% DMSO (Sigma Aldrich):90% of 100% ethanol (Fisher Scientific, Pittsburgh, PA, USA), emulphor (Alkamuls EL-620,



Solvay, Brussels, Belgium), and sterilized saline (1:1:8). Rats were injected with either the drug formulation (10 mg/kg) or vehicle alone at an injection volume of 1 ml/kg.

Tissue preparation and RNA-sequencing: Fifteen minutes after fear consolidation, rats were deeply anesthetized under isoflurane and decapitated. Brains were removed, snap-frozen in cold iso-pentane (Fisher Scientific) and stored at -80 °C until use. Brains were sectioned on a cryostat (300 µm), and the BLA was punched using a 1 mm diameter micro-punch (Electron Microscopy Sciences, Hatfield, PA, USA). RNA was isolated using the RNeasy Plus Mini Kit (Qiagen, Hilden, Germany). Briefly, after lysis, BLA was homogenized and spun down using gDNA Eliminator spin columns to remove genomic DNA. The flow-through containing total RNA was purified, washed, and eluted using RNeasy Mini spin columns. For library preparation, 300 ng of total RNA was used with TrueSeq Total RNA Sample Prep Kit (Illumina, San Diego, CA, USA). Barcoded libraries were sequenced using the Illumina Hi-Seq 4000.

Volcano plots & heat maps: Differential gene expression analyses were conducted in the statistical environment R (v3.6.0) using package edgeR<sup>253</sup>. In brief, the gene counts were loaded into R and filtered to exclude low expression genes that were not adequate for statistical assessment. Normalization and dispersion factors were estimated following the edgeR default setting. The negative binomial model and likelihood ratio test were used in edgeR to identify differentially expressed genes. The false discovery rate (FDR) was calculated to correct for multiple comparisons, where  $FDR < 0.05$  is considered statistically significant. The volcano plot of differential expression genes was generated using R. Heatmaps for differentially expressed genes were generated using R package gplots with normalized gene expression data of log-transformed count-per-million.

Gene enrichment analyses: Gene ontology enrichment analysis was assessed via The Database for Annotation, Visualization, and Integrated Discovery (DAVID Bioinformatics, v6.8). The enrichment analysis annotated functionally related gene groups with a p-value < 0.05. The most significant canonical signaling pathways downstream of the DEGs were profiled using Kyoto Encyclopedia of Genes and Genomes 2020 (KEGG). The transcription factor pathways activated downstream of DEG expression were analyzed using TRANSFAC and JASPAR databases (p < 0.05).

Protein-protein interaction networks: For protein-protein interaction networks, the STRING application was used in Cytoscape software (v3.7.2) (The Cytoscape Consortium). DEGs and respective fold changes were uploaded for each group and used to find interactions between DEGs and neighboring proteins. Network were mapped using an edge-weighted spring-embedded layout.

Protein expression analysis: Following fear consolidation, rats were deeply anesthetized using isoflurane and decapitated. Brains were removed, rapidly frozen in cold iso-pentane (Thermo Scientific), and stored at -80 °C until ready to process. Brains were sectioned on a cryostat (300 µm), and BLA was punched using a 1 mm diameter micro-punch (Electron Microscopy Sciences). BLA was homogenized in 10% w/v lysis buffer and 1X Halt protease and phosphatase inhibitors cocktail (Thermo Scientific). 15µg protein was loaded and run on NuPage Bis-Tris Protein Gel (Thermo Scientific). The gel was transferred to a nitrocellulose membrane, blocked, and incubated overnight at 4 °C with anti-Igf2 (1:500, Abcam, Cambridge, MA, USA) and anti-Igfbp2 (1:500, Abcam). Blots were incubated for 1 h with IRDye® 800CW goat anti-rabbit secondary antibody (1:10,000, LI-COR Biosciences, Lincoln, NE, USA) and imaged with an

Odyssey<sup>®</sup> CLx Imaging System (LI-COR Biosciences). Densitometry analyses of bands of protein of interest were normalized to loading control,  $\beta$ -actin. A one-way ANOVA was used for multiple group comparisons, followed by a *post hoc* Tukey's HSD test when  $p < 0.05$ .

## 2.3 Results

### Cued fear conditioning uniquely alters the basolateral amygdala transcriptome

We first aimed to validate that cued fear conditioning induces unique transcriptome changes in the BLA. To do this, we presented rats with three 20s tones, each tone co-terminating with a 0.5s foot-shock. A control group received the tones without foot-shocks (Figure 6A). As Figure 6B shows, rats presented with tone-shock pairs displayed high freezing levels by the end of acquisition training ( $70.8 \pm 12.6\%$ ). After 24 h, all rats were placed in a new context and presented with five 20s tones, separated by 60s intervals, to test for cued fear memory consolidation. We observed high freezing levels throughout testing (averaged  $82.55 \pm 3.7\%$ ), thereby demonstrating successful consolidation of cued fear memory.

Following confirmation of fear consolidation 24 h later, rat brains were collected, and the BLA was micro-punched and processed for RNA-sequencing. To study the effects of fear conditioning, we compared gene expression data from the fear-conditioned group with the tone-only group. There were approximately 27 million uniquely mapped reads generated and 11,970 genes sequenced per sample. Figure 6C shows that 24 h after cued fear conditioning, the BLA transcriptome is uniquely altered. Gene ontology and pathway analyses of significantly altered genes ( $p < 0.05$ ) further revealed processes and pathways that are important for normal synaptic function (Figure 6D). Several of these

processes, like response to glucocorticoid ( $p = 0.03$ ), behavioral fear response ( $p = 0.003$ ), and multicellular organismal response to stress ( $p = 2.92 \times 10^{-5}$ ), are expected in our behavioral paradigm, as it activates the body's stress response. Several other processes illustrate the importance of the glutamatergic synapse in fear responses, such as glutamate receptor signaling pathway ( $p = 0.002$ ), NMDA glutamate receptor clustering ( $p = 0.01$ ), and calcium signaling pathway ( $p = 0.01$ ). Finally, we found a subset of molecular functions, biological processes, and canonical pathways from significantly regulated genes that indicate that the PSD95-nNOS pathway, downstream of NMDAR signaling, is important for consolidation of cued fear memory (scaffold protein binding,  $p = 0.01$ ; calmodulin binding,  $p = 2.96 \times 10^{-5}$ ; PDZ domain binding,  $p = 4.40 \times 10^{-5}$ ; cGMP effects,  $p = 0.04$ ; cGMP-PKG signaling pathway,  $p = 9.20 \times 10^{-4}$ ). These results show that, in addition to general stress responses, cued fear consolidation also enriches biological pathways that include NMDAR function and downstream signaling of PSD95 and nNOS.

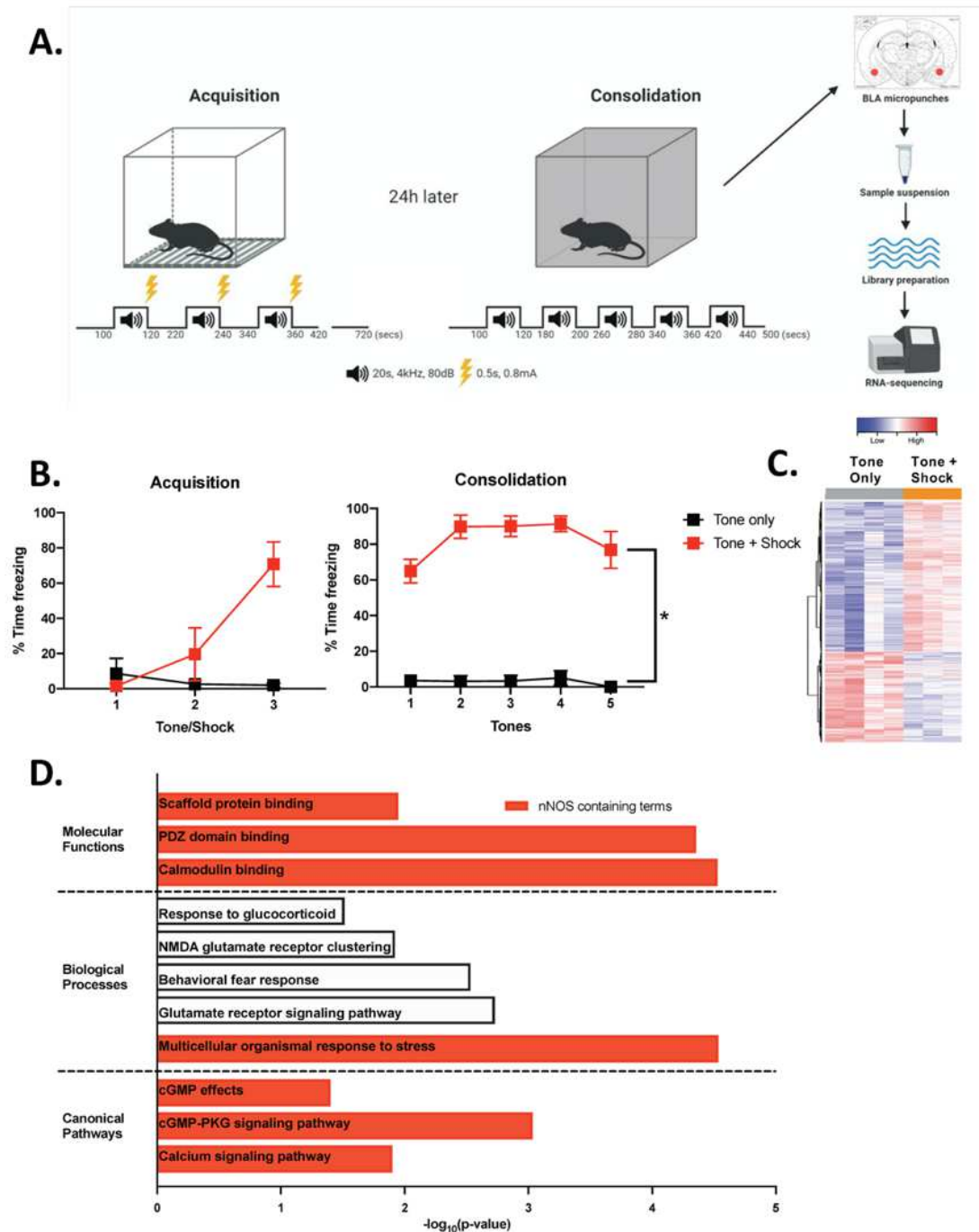


**Figure 6. Effects of fear conditioning on the basolateral amygdala transcriptome.** A) Outline of Experimental Design. Rats were habituated to both experimental contexts 24 h before fear acquisition. For fear acquisition, rats were exposed to 3 tone-shock pairs. Rats were tested for fear expression 24 h later in the second context. Brains from rats were collected, and BLA micro-punches were processed for RNA-sequencing. B) Fear

Conditioning Behavioral Output. Rats exposed to tone-shock pairs showed normal acquisition (Trial:  $F_{2,12} = 10.11$ ,  $p < 0.01$ ). During consolidation testing, rats showed freezing responses similar to end-of-acquisition levels. Rats given tone and shocks ( $n = 4$ ) showed consistently and significantly higher freezing compared to tone only control rats ( $n = 4$ ) (Treatment:  $F_{1,6} = 853.6$ ,  $p < 0.0001$ ). \* $p < 0.0001$  relative to tone only control group. C) Heatmap showing the expression levels of differentially expressed genes from the BLA of fear-conditioned and control rats ( $p < 0.05$ ). D) Gene ontology functional analyses using DAVID and KEGG provided the most significantly enriched biological processes, molecular functions, and canonical pathways. All statistical values were 10-base log-transformed.

Disruption of the PSD95-nNOS protein-protein interaction immediately after cued fear conditioning reduces fear response 24 h later

In light of the results from gene ontology and pathway analyses, we evaluated the specific role of the PSD95-nNOS-NO axis in behavioral and amygdala transcriptomic changes after cued fear conditioning. We used a 2x2 behavioral paradigm with the following groups: 1) rats that received shocks paired with tones during fear conditioning and an intraperitoneal (i.p.) injection of vehicle after fear acquisition (FC + vehicle), 2) rats that received shocks paired with tones during fear conditioning and an i.p. injection of ZL006 after fear acquisition (FC + ZL006), 3) rats that received only tones during fear conditioning and an i.p. injection of vehicle after fear acquisition (tone + vehicle), and 4) rats that received only tones during fear conditioning and an i.p. injection of ZL006 after fear acquisition (tone + ZL006) (Figure 7). Prior to drug treatments, both FC + vehicle and FC + ZL006 groups acquired cue-induced fear to an equal degree, reflected in the gradual increase in freezing during tone presentations (average by the end of acquisition training is  $82.0 \pm 4.5\%$  freezing in FC + vehicle and  $71.3 \pm 11.9\%$  freezing in FC + ZL006 groups) (Figure 7B). When tested for fear consolidation (presented with only tones) 24 h later in a cued fear expression test, the FC + vehicle group displayed freezing levels similar to their previously acquired % freezing ( $76.4 \pm 8.1\%$ , first tone). However, the FC + ZL006 group showed significantly decreased freezing during the cued fear expression test ( $30.6 \pm 8.6\%$ , first tone). The FC + vehicle group had significantly higher freezing levels for the duration of the fear expression test compared to the FC + ZL006 group ( $p < 0.0001$ ). The tone + vehicle and tone + ZL006 groups showed neither fear acquisition nor consolidation. Our results validate previous findings that systemic ZL006

delivery directly after cued fear acquisition can disrupt cued fear memory consolidation in rats (Figure 7B)<sup>162</sup>.

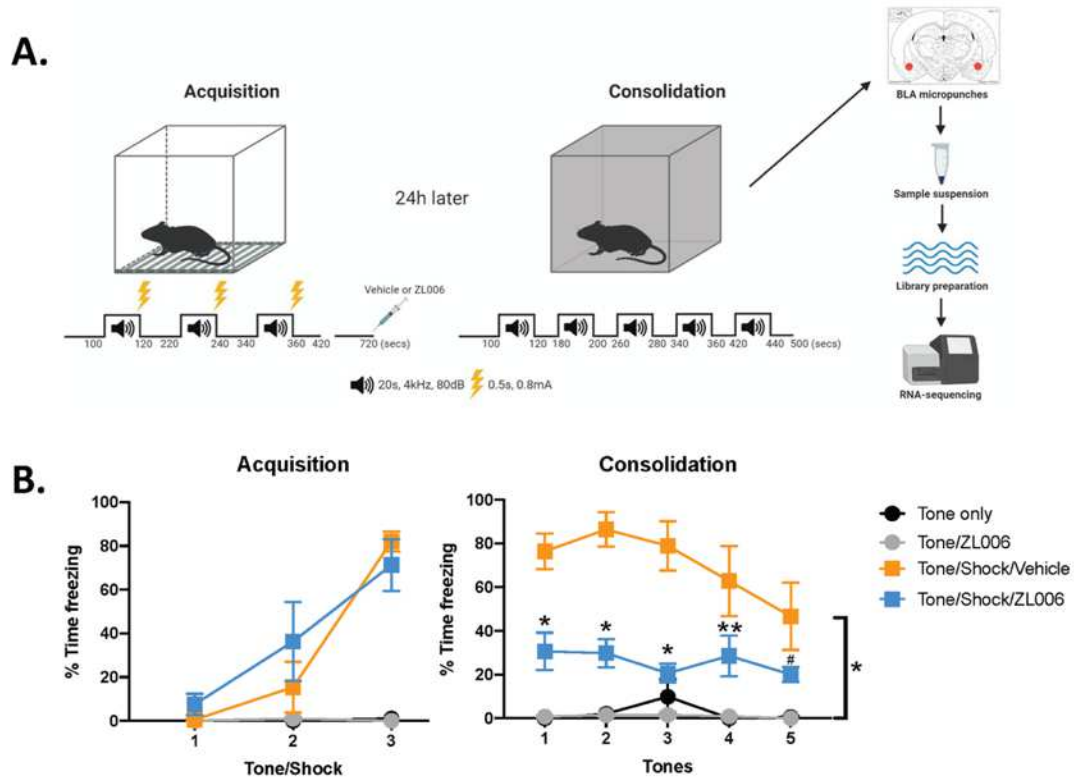


**Figure 7. Fear conditioning and ZL006 treatment schematic and behavioral output.** A) Outline of Experimental Design. Rats were habituated to both experimental contexts 24 h before fear acquisition. For fear acquisition, rats were exposed to 3 tone-shock pairs. Immediately after acquisition, rats were given an i.p. injection of vehicle or ZL006 (10 mg/kg). Rats were tested for fear expression 24 h later in the second context. Brains from rats were collected, and BLA micro-punches were processed for RNA-sequencing. B) Fear Conditioning Behavioral Output. Rats that were exposed to tone-shock pairs showed normal acquisition (Trial:  $F_{2,32} = 31.96$ ,  $p < 0.0001$ ). During consolidation testing, rats from the FC + vehicle group ( $n = 4$ ) displayed freezing responses similar to end-of-acquisition levels. Rats from the FC + ZL006 group ( $n = 4$ ), however, showed consistently and significantly lower freezing compared to FC + vehicle group (Treatment<sub>3,16</sub> = 112.3,  $p < 0.0001$ ). \* $p < 0.0001$ ; \*\* $p < 0.001$ ; # $p < 0.01$  relative to FC + vehicle group.



## Cued fear conditioning with or without ZL006 induces unique gene expression patterns in the basolateral amygdala

Previous transcriptomic studies of the BLA have revealed several molecular pathways underlying BLA-driven fear and stress responses<sup>254-256</sup>. However, little is known about specific molecular mechanisms regulated by the PSD95-nNOS interaction within the BLA during cued fear consolidation. Thus, we used RNA-sequencing in our model to investigate how PSD95-nNOS disruption (via ZL006 treatment) immediately after cued fear conditioning alters the BLA transcriptome. To study the effects of fear conditioning, we first compared gene expression data from the FC + vehicle group with the tone + vehicle group. Next, to understand the mechanisms underlying the attenuating effects of ZL006 on cued fear consolidation, we compared gene expression data from the FC + ZL006 group with the FC + vehicle group. There were approximately 30 million uniquely mapped reads generated and 12,129 genes sequenced per sample. By mapping the fold changes of the 12,129 genes in the FC + ZL006 group against the fold changes in the FC + vehicle group, we discovered a negative correlation ( $R = -0.667$ ) with 65% of genes (7,880 out of 12,129) showing inverted expression in the FC + ZL006 group compared to the FC + vehicle group (Figure 8A). In other words, expression levels of 65% of genes in fear-conditioned rats were reversed with ZL006 treatment, indicating that ZL006 treatment after fear conditioning directionally changed the BLA transcriptome.

To further parse the effects of fear conditioning and ZL006 treatment, we identified differentially expressed genes (DEGs) in all groups using a cutoff of  $FDR < 0.05$ . Summarized in the volcano plots in Figure 8B, which plot  $-\log_{10}FDR$  against

log<sub>2</sub>fold-change, we observed a trend of downregulated DEGs (blue and red dots) in FC + vehicle and upregulated DEGs in FC + ZL006 groups. Specifically, among 516 DEGs in the FC + vehicle group, 88% were downregulated (456 of 516 genes). The FC + ZL006 group revealed 93 DEGs, of which 96% were upregulated (89 out of 93 genes). A comparative analysis of the DEGs showed overlap in 83 DEGs from the FC + vehicle and FC + ZL006 groups. From these 83 DEGs, we observed an interesting pattern of 4 upregulated and 79 downregulated DEGs in the FC + vehicle group and 79 upregulated and 4 downregulated DEGs in the FC + ZL006 group. This information is summarized in Figure 8C. In other words, amongst the overlapping 83 DEGs between the FC + vehicle and FC + ZL006 groups, all were changed in the opposite direction between the two groups. Therefore, these DEGs that overlap may be key in understanding the mechanism via which the ZL006-treated group exhibited decreased consolidation of cued fear.

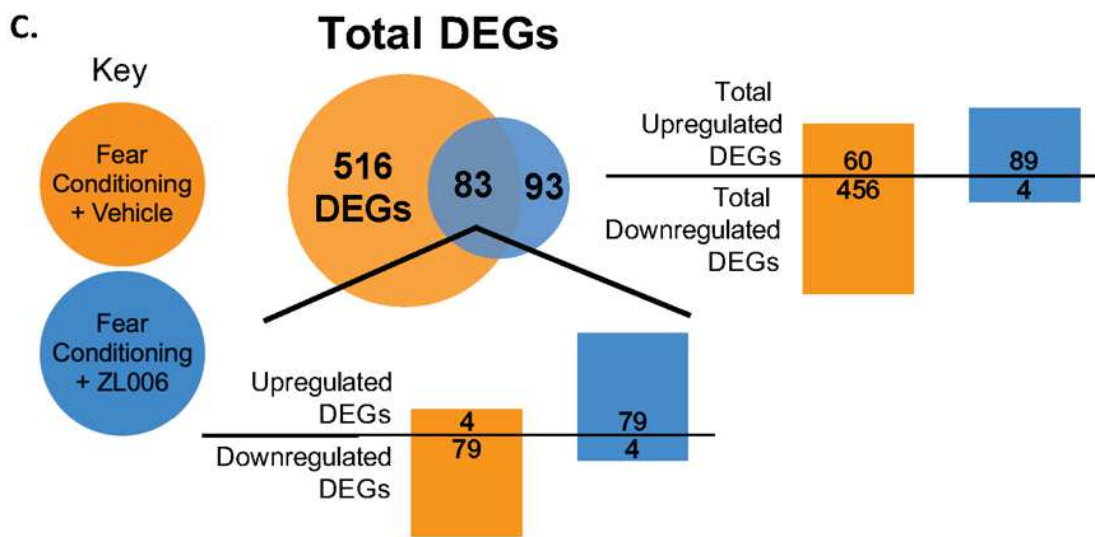
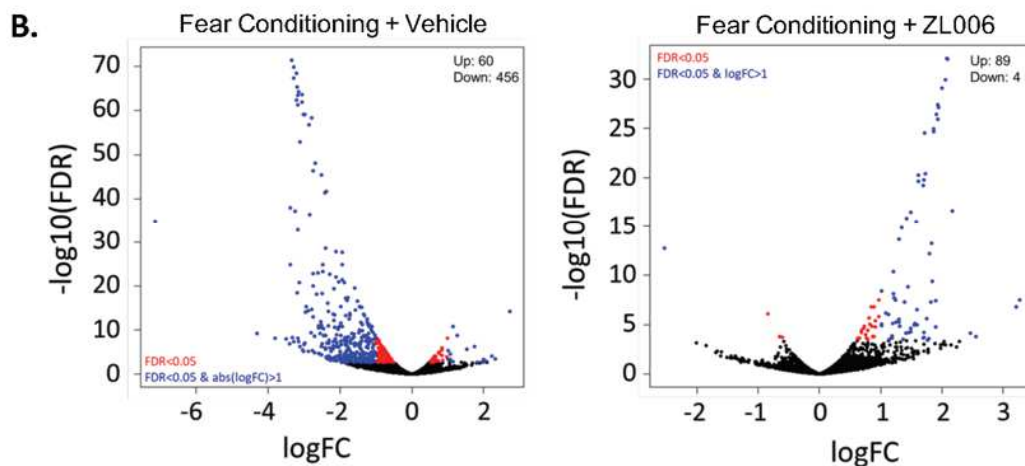
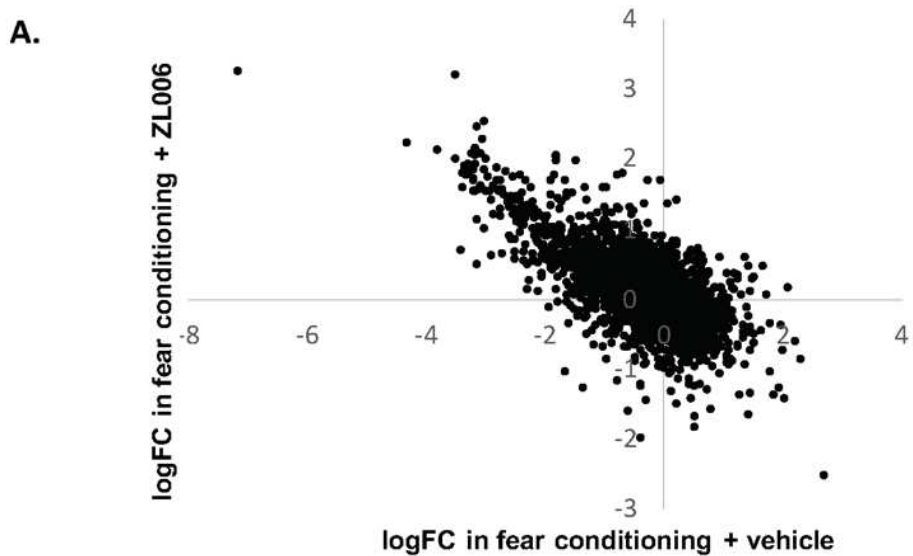


**Figure 8. Differentially expressed gene patterns associated with fear conditioning and ZL006 treatment.** A) Correlation analysis of fold changes of all genes in FC + vehicle and FC + ZL006 groups. B) Volcano plots showing a comparison of significance ( $-\log_{10}\text{FDR}$ ) vs. fold change ( $\log_2\text{FC}$ ). Red dots represent genes with  $\text{FDR} < 0.05$ ; blue dots represent genes with  $\text{FDR} < 0.05$  and an absolute fold change greater than 1. C) Gene patterns observed from volcano plots.

In comparing the expression levels of the 83 overlapping DEGs between the FC + vehicle and FC + ZL006 groups, we discovered that each of the 83 overlapping DEGs is transcriptionally regulated in the opposite direction. These data indicate that each downregulated DEG in the FC + vehicle group is upregulated in the FC + ZL006 group. In contrast, each upregulated DEG in the FC + vehicle group is downregulated in the FC + ZL006 group (Figure 9A-B). Most importantly, we found that gene expression of DEGs in the FC + ZL006 group was closer to the tone + vehicle group's expression levels, suggesting that ZL006 treatment immediately following fear conditioning reverts gene expression within the BLA closer to control levels. This is particularly important as it implies that ZL006 alters transcriptional machinery in the BLA. As such, it may help identify pathways or genes that would serve as effective therapeutic targets for fear disorders.

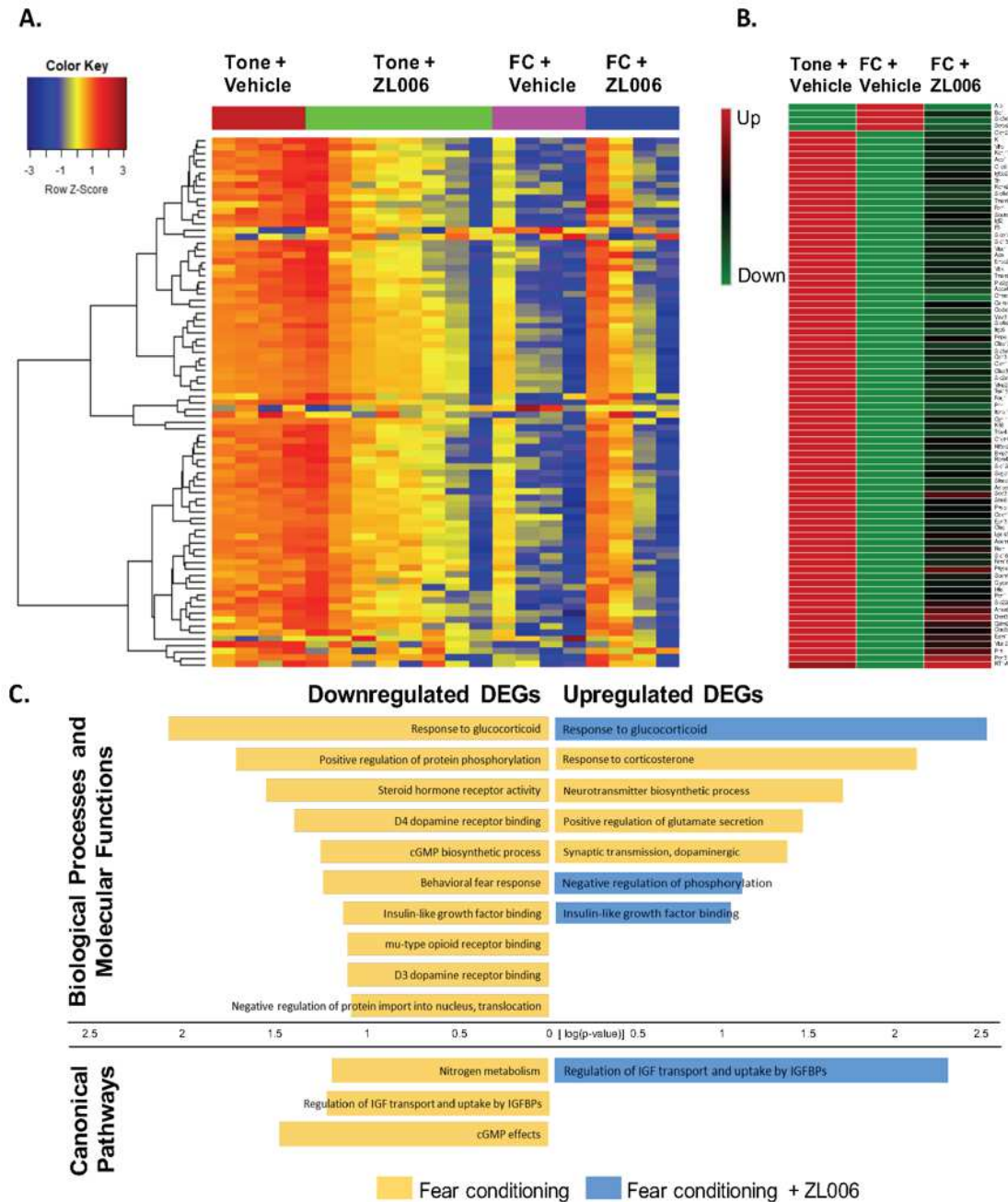


**Figure 9. Heatmaps and gene enrichment analyses of 83 DEGs common between fear conditioning and ZL006-treated groups.** A) Heatmap showing the expression levels of 83 DEGs across all four experimental groups. B) Heatmap of averaged expression levels of the same 83 genes. C) Gene ontology functional analyses using DAVID and KEGG provided the most significantly enriched biological processes, molecular functions, and canonical pathways. All statistical values were 10-base log-transformed.

Gene enrichment analysis indicates key processes that are important for cued fear consolidation

Given that ZL006 treatment appears to alter the BLA transcriptome by restoring gene expression to baseline levels, we next analyzed DEGs from the FC + vehicle and FC + ZL006 groups for enrichment in biological processes, molecular functions, and canonical pathways. We identified numerous significantly enriched processes, many related to memory formation and consolidation, and some related to nNOS function (Figure 9C). Interestingly, downregulated genes in the FC + vehicle group showed enrichment in several processes that were enriched in upregulated genes in the FC + ZL006 group. For example, genes involved in insulin-like growth factor binding protein pathways (*Esm1*, *Igfbp1*, *Igfbp2*) were downregulated in FC + vehicle and upregulated in FC + ZL006 (*Esm1*, *Igfbp2*). These overlapping but contrasting processes may be fundamental to the mechanism of action of ZL006 and the downstream mechanism of NO-mediated fear consolidation. Next, we looked at enrichment specific only to the FC + vehicle or FC + ZL006 groups to distinguish processes and canonical pathways altered with fear conditioning and ZL006 treatment (Figure 9C). We observed enrichment in the FC + vehicle group of the behavioral fear response, which validates our behavioral model. We also found enrichment of the cyclic guanosine monophosphate (cGMP) biosynthetic process, nitrogen metabolism pathway, and cGMP effects pathway (Figure 9C) in the FC + vehicle group. Additionally, gene ontology and pathway analyses of the FC + vehicle group revealed enrichment of D3 and D4 dopamine receptor binding, dopaminergic synaptic transmission, and mu-type opioid receptor binding. Finally, we found enrichment of positive regulation of protein phosphorylation in the FC + vehicle

group but negative regulation of phosphorylation in the FC + ZL006 group, indicating that the direction of phosphorylation may be key in cued fear consolidation and the mechanism via which ZL006 attenuates it.

#### Novel target genes and potential mechanisms for cued fear consolidation

With a better understanding of functional processes and pathways in the FC + vehicle and FC + ZL006 groups, we next focused on the 83 overlapping DEGs to identify and investigate candidate genes for further study. After performing a thorough literature search of the 83 DEGs, we determined a list of eight genes that have previously been implicated in learning and memory<sup>257-264</sup>. The gene expression of these eight candidate genes was downregulated in the FC + vehicle group and upregulated in the FC + ZL006 group (Figure 10A). Among these, recent studies report that *Igf2* and *Igfbp2* are important molecules in fear memory consolidation<sup>258,259</sup>. To subsequently investigate the roles of *Igf2* and *Igfbp2*, we examined protein expression levels of IGF2 and IGFBP2 in our 2x2 design. We found directionally consistent differences in the protein levels of both IGF2 and IGFBP2 between the FC + vehicle group (decreased IGF2 and IGFBP2: IGF2: 75%; IGFBP2: 53% compared to 100% for tone + vehicle;  $p < 0.05$ ) and the FC + ZL006 group (increased IGF2: 1462%; IGFBP2: 692%, compared to 100% for tone + ZL006;  $p < 0.01$ ) (Figure 10B). To gain further insight, we used the RNA-sequencing results to determine upstream transcription factors in the FC + vehicle and FC + ZL006 groups (Figure 10C). Of these, we discovered two important transcription factors in the FC + vehicle group that are not significantly affected in the FC + ZL006 group: *Nfkb1* and *Hif1a*. Both transcription factors regulate IGF2 and IGFBP2 transcription<sup>265-267</sup>. Remarkably, nNOS negatively regulates *Nfkb1*, *Hif1a*, and IGF1-receptor (IGF1R)



activity, while IGF1R positively regulates *Nfkb1* and *Hif1a*<sup>268-272</sup>. Additionally, IGF2 has differing downstream effects based on the receptor it binds. While IGF2 binding to IGF1R activates intracellular signaling cascades, IGF2 binding to IGF2R results in IGF2 internalization and degradation, in addition to possible downstream signaling<sup>273-276</sup>. Thus, IGF2 and IGFBP2 expression patterns were distinctly regulated during fear conditioning and affected by ZL006 treatment, possibly via transcriptional and post-translational machinery and degradation dynamics. Using this information, we propose a potential mechanism involving the NMDAR-PSD95-nNOS-NO axis and IGF2/IGFBP2 in Figure 10E.

We also explored protein-protein interactions (PPI) of IGF2 and IGFBP2 using immediate-neighbor clusters of IGF2 and IGFBP2. With this, we showed that IGF2 interacts with a complex network of proteins in the FC + vehicle group, including IGFBP2, but that the complexity of the IGF2 PPI greatly diminishes in the FC + ZL006 group (Figure 10D). Therefore, *Igf2* and *Igfbp2* gene and protein expressions were significantly and differentially altered in the FC + vehicle and FC + ZL006 groups, suggesting that these molecules likely play pivotal roles in the NMDAR-PSD95-nNOS-NO axis regulation of fear consolidation in the amygdala.

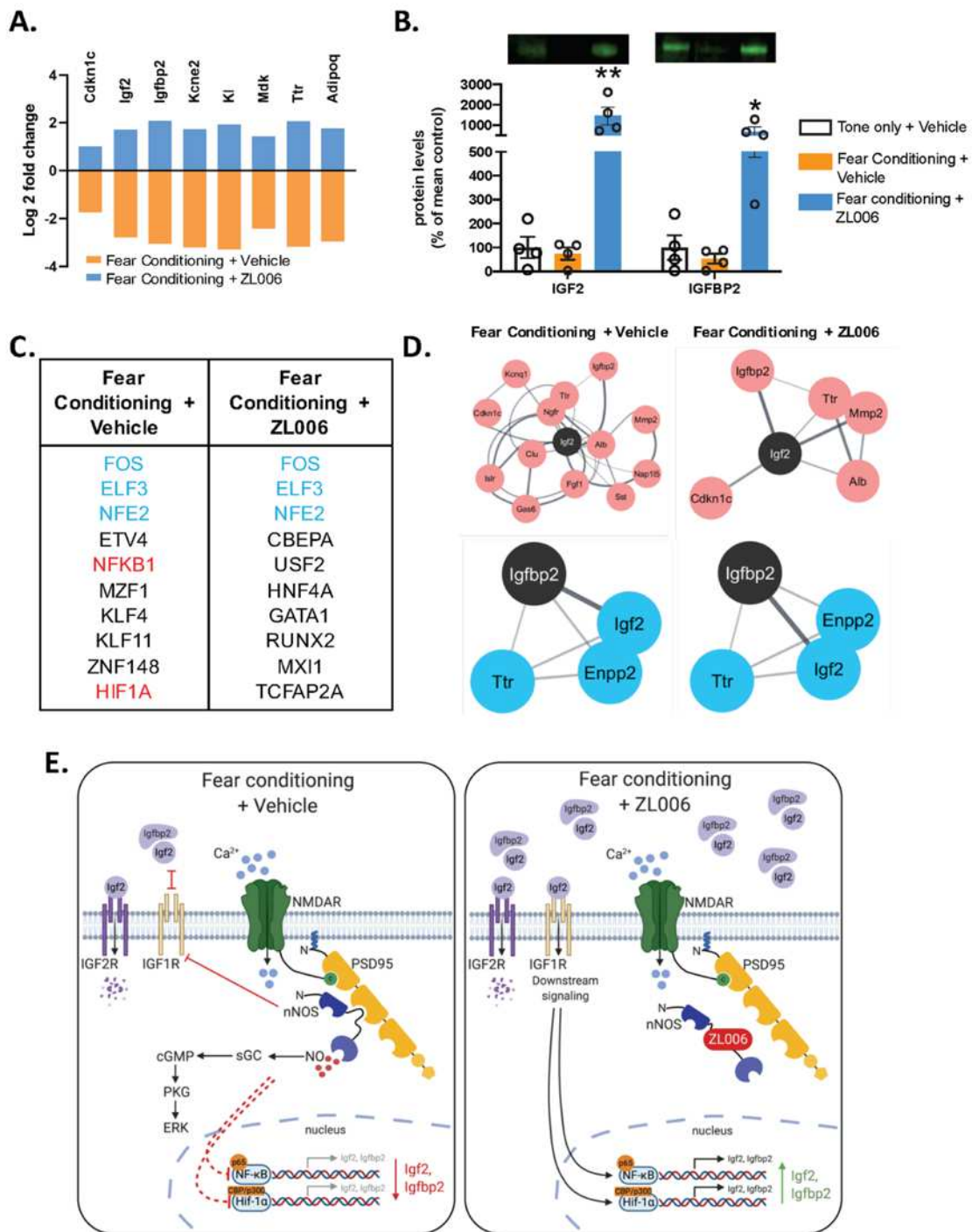


**Figure 10. Key genes, proteins, and transcription factors: putative role of the NMDAR-PSD95-nNOS-NO axis and IGF2/IGFBP2 in cued fear consolidation.** A) Gene expression levels from RNA-sequencing of multiple learning and memory-related genes. B) Protein expression levels of IGF2 and IGFBP2, two proteins important for fear memory. Values for FC + vehicle are percent of tone + vehicle; values for FC + ZL006 are as percent of tone + ZL006. \* $p < 0.05$ ; \*\* $p < 0.01$  relative to tone + vehicle and FC +

vehicle groups C) DEGs in FC + vehicle and FC + ZL006 groups were used to identify significantly altered transcription factors, using TRANSFAC and JASPAR. Transcription factors common between the groups are highlighted in blue, while two important transcription factors found in the FC + vehicle group but not in the FC + ZL006 group are in red. D) Gene networks showing a cluster of all genes correlating with *Igf2* and *Igfbp2* expression in FC + vehicle and FC + ZL006 groups. Each node represents a gene, and each line represents an interaction. E) Based on RNA-sequencing, protein expression levels, and transcription factor analysis, a suggested mechanism of how nNOS mediates the IGF system in cued fear conditioning (left panel). With ZL006 blocking nNOS-mediated inhibition of NF- $\kappa$ B and HIF-1 $\alpha$ , IGF2 and IGFBP2 transcription and IGF2/IGF1R signaling increases, which could be key in attenuating cued fear consolidation (right panel).

## 2.4 Discussion

Numerous studies have found that NMDAR signaling in the BLA regulates the consolidation of cued fear memory<sup>45,162,277,278</sup>. Our initial RNA-sequencing data showed distinct transcriptomic changes in the BLA following cued fear consolidation (i.e., 24 h after cued fear conditioning). Upon gene ontology and pathway analyses of significantly regulated genes, we found three distinct clusters of biological processes, molecular functions, and canonical pathways: response to stress, NMDAR/glutamatergic signaling, and intracellular signaling downstream of NMDAR activation. Specifically, upon evaluating the genes involved in these pathways, we found that 7 out of 12 pathways included *nNos*.

This is a potentially important clue towards therapeutic approaches to treat fear-related disorders. Approaches that target NMDAR function to ameliorate fear memory utilize antagonists like MK-801 and ketamine but are limited by these drugs also affecting motor, cognitive, and memory functions<sup>279-281</sup>. However, nNOS is downstream of NMDAR activation, and we previously reported that inhibiting nNOS activation by disrupting PSD95-nNOS interaction attenuates cued fear consolidation without affecting other memory or motor functions<sup>162</sup>. Validating our previous results, Figure 6 shows that disrupting the NMDAR-PSD95-nNOS-NO axis plays an important role in cued fear memory consolidation. We have previously also demonstrated that site-specific blockade of this axis within the BLA fully disrupts fear consolidation 24 h later<sup>8</sup>. However, the molecular mechanism by which the NMDAR-PSD95-nNOS-NO axis in the BLA affects cued fear consolidation remains largely unexplored. As a first step in elucidating these molecular mechanisms, we applied a transcriptomic-wide approach in a 2x2 design and

utilized ZL006, a small molecule protein-protein inhibitor of the PSD95-nNOS interaction that was previously shown to decrease consolidation of cued fear memory<sup>162</sup>. Understanding the BLA transcriptome post-fear consolidation in normal versus fear-attenuated animals will help identify potential molecular pathways and specific therapeutic targets.

By disrupting the PSD95-nNOS interaction using ZL006, we impaired cued fear consolidation (Figure 7), as previously reported.<sup>162</sup> Using RNA-sequencing, we cross-evaluated gene expression patterns in rats with normal fear consolidation and rats with impaired fear consolidation to determine pathways and genes uniquely important in the consolidation of cued fear.

In doing so, we observed distinct gene expression patterns (Figures 8 and 9), indicating that by inhibiting the PSD95-nNOS-NO axis, ZL006 could modify transcriptional machinery in the BLA that is required for the consolidation of cued fear.

After finding that cued fear conditioning and ZL006 treatment alter gene expression in the BLA in a unique, mutually opposing pattern, we turned to the mechanistic pathways and functional changes in the FC + vehicle and FC + ZL006 groups. We performed a broad analysis of gene enrichment from all DEGs in the FC + vehicle and FC + ZL006 groups. Overall, we found enrichment in processes and functions consistent with conditioned fear (Figure 9C). For example, fear conditioning resulted in enrichment of the behavioral fear response, response to corticosterone, and regulation of glutamate; this substantiates studies reporting on the importance of corticosterone and glutamate in the BLA for fear memory consolidation<sup>282,283</sup>. Importantly, fear conditioning also resulted in enrichment of nitrogen metabolism and

cGMP effects pathways in the BLA. This effect was subsequently eliminated with ZL006 treatment after fear conditioning. Nitrogen metabolism is the cycle that produces nitrogenous compounds, and notably, nNOS is a source of endogenous nitric oxide<sup>284</sup>. The production of nitric oxide in the brain further activates cGMP, a second messenger that plays a role in long-term potentiation and depression and is also required for fear memory consolidation<sup>204,285-287</sup>. Observing enrichment of the nitrogen metabolism and cGMP effects, both pathways downstream of nNOS activation, in the FC + vehicle group alone reveals that a primary mechanism for cued fear consolidation is via nNOS activity in the BLA. These enriched processes validate our use of the PSD95-nNOS disruption as a tool to further elucidate molecular mechanisms underlying fear consolidation in the amygdala.

Next, we found several biological processes and molecular functions that were enriched in downregulated gene sets of the FC + vehicle group and upregulated gene sets of the FC + ZL006 group. This suggests that fear conditioning and ZL006 treatment enrich these pathways, but via different mechanisms. One important pathway that emerged in this analysis is the regulation of insulin-like growth factor (IGF) transport and uptake by IGF binding proteins (IGFBPs), a pathway shown to be important in fear learning and memory.<sup>258,259</sup>

Focusing on genes within the IGF pathway, insulin-like growth factor 2 (*Igf2*) and insulin-like growth factor-binding protein 2 (*Igfbp2*) were both significantly downregulated in the FC + vehicle group and upregulated to control levels in the FC + ZL006 group (Figure 10A). Recent studies of contextual fear memories show that IGF2 and IGFBP2 in the hippocampus play a role in regulating fear responses, and its potential

as a therapeutic target is emerging<sup>258,259</sup>. Thus, we further explored IGF2 and IGFBP2 by quantifying protein expression levels in our 2x2 design. We found that relative to control groups, protein levels of IGF2 and IGFBP2 decreased in the FC + vehicle group and increased well beyond control levels in the FC + ZL006 group, correlating with gene expression data (Figure 10B). One explanation for the significant upregulation in protein levels in the FC + ZL006 group is that blocking nNOS signaling not only increases *Igf2* and *Igfbp2* gene transcription, but it may also regulate IGF receptor affinity for IGF2 and IGFBP2, in such a way that there is less IGF2 and IGFBP2 degraded and therefore more soluble protein available.

To further explain the relationship between gene and protein expression levels of IGF2 and IGFBP2, we generated a list of upstream transcription factors from the FC + vehicle and FC + ZL006 groups (Figure 10C). We identified two transcription factors, *Nfkb1* and *Hif1a*, that are relevant for IGF2 and IGFBP2 function. It is reported that nNOS negatively regulates *Nfkb1* and *Hif1a*; nNOS also inhibits IGF1R activity, which binds IGF2 and initiates downstream signaling cascades<sup>268-270,273-275</sup>. On the other hand, IGF1R positively regulates *Nfkb1* and *Hif1a*<sup>271,272</sup>. Additionally, *Igf2* and *Igfbp2* are both target genes of *Nfkb1* and *Hif1a*<sup>265-267</sup>.

Thus, we hypothesize that cued fear consolidation involves NMDAR-PSD95-nNOS-NO-mediated transcriptional regulation of the IGF system, which, in addition to regulating transcription, may also regulate intracellular signaling and degradation of IGF2 and IGFBP2. Figure 10E proposes that nNOS activation after fear conditioning leads to cGMP signaling and negative regulation of NF-kB, HIF1a, and IGF1R. With IGF1R no longer able to bind IGF2 and activate downstream signaling, IGF2 primarily

binds to IGF2 receptor (IGF2R), which is reported to internalize and degrade IGF2 upon binding<sup>276</sup>. As a result, there is reduced overall *Igf2* and *Igfbp2* transcription and extracellular IGF2 and IGFBP2 protein. Additionally, the IGF2/IGF2R complex is reported to enhance spine maturation and synapse formation<sup>265</sup>. Thus, after fear conditioning, the nNOS-activated cGMP pathway and IGF2/IGF2R-activated downstream signaling may play a role in increased fear memory consolidation. In contrast, with ZL006 treatment, nNOS activity is inhibited, and IGF1R can now positively regulate NF- $\kappa$ B and HIF1 $\alpha$ . As a result, there is increased *Igf2* and *Igfbp2* transcription. Thus, it appears that cued fear consolidation is a process mediated by the NMDAR-PSD95-nNOS signal transduction pathway, with IGF2 and IGFBP2 as potential downstream target molecules. Meanwhile, with ZL006 administration, nNOS may no longer inhibit IGF1R activity, allowing for distinctly separate regulation of the IGF system compared to cued fear conditioning. Further validating their diverse roles, the protein-protein interaction networks of *Igf2* and *Igfbp2* varied greatly between the FC + vehicle and FC + ZL006 groups (Figure 10D). Importantly, this indicates that IGF2 and IGFBP2 interact with different sets of proteins during fear conditioning and that those interactions are greatly diminished with ZL006 treatment. Ultimately, while there are certainly numerous pathways activated during fear conditioning, IGF2- and IGFBP2-mediated plasticity may be one of the key mechanisms explaining the downstream effects of NMDAR-PSD95-nNOS-NO activity in cued fear consolidation.

In addition, *Fos*, *Nfe2*, and *Elf3* were three key transcriptional regulators that were also implicated in both FC + vehicle and FC + ZL006 groups (Figure 10C). While *Fos* has been well-characterized in the BLA and is specifically important for fear learning,



*Nfe2* and *Elf3* are novel findings here<sup>288,289</sup>. These transcription factors may be working in concert to regulate genes within both the FC + vehicle and FC + ZL006 groups.

Finally, we identified several enriched pathways and processes that can be further explored in future studies. Our results revealed enriched D3 receptor (D3R) and D4 receptor (D4R) activity and dopaminergic synaptic transmission in the FC + vehicle group. Previous studies have shown that blocking D3R and D4R in the lateral amygdala reduces anxiety and freezing behavior<sup>290-292</sup>. We also found enrichment of mu-type opioid receptor (MOR) binding. The role of MORs in the BLA has been limited to studies on pain and addiction<sup>293,294</sup>. However, *Blaesse et al.* show that MOR activation can mitigate intercalated cells-mediated inhibition of the medial central nucleus of the amygdala (CeM)<sup>295</sup>. The CeM regulates the expression of conditioned fear, and as such, attenuated CeM inhibition would result in increased CeM output and, therefore, greater expression of conditioned fear, as observed in the FC + vehicle group<sup>296</sup>. This makes MORs in the BLA another potentially exciting target to explore further for its role in cued fear consolidation.

In conclusion, these data provide a transcriptomic-wide analysis of the molecular pathways regulated by the NMDAR-PSD95-nNOS-NO axis within BLA and its role in cued fear consolidation. Using a pharmacological approach to disrupt the PSD95-nNOS interaction and impair fear consolidation, we identified gene expression patterns, functional and transcriptional enrichment, and key genes and transcription factors in the BLA that may be crucial for fear consolidation. Of particular note is the role of IGF2 and IGFBP2 as key molecular mediators downstream of the NMDAR-PSD95-nNOS-NO axis within the amygdala during fear consolidation. These results provide additional insight

into the complex mechanisms of fear consolidation. By studying the indicated processes, pathways, and target genes further, we hope to elucidate a complete understanding of the transcriptional and molecular basis of fear consolidation and identify novel target therapeutics that may further impact and improve treatment of fear disorders such as PTSD.

## CHAPTER 3

### **Fear Consolidation Requires nNOS-Dependent, Sequentially Orchestrated Changes in AMPA and NMDA Mediated Glutamatergic Neurotransmission in the Basolateral Amygdala**

#### **3.1 Introduction**

Persistent aversive memories is a one of the key mechanisms in the pathophysiology of several severe psychiatric disorders such as post-traumatic stress disorder, phobias, and anxiety disorders<sup>247</sup>. In classical Pavlovian conditioning, fear consolidation is the process that encodes the long-term association of an intensely aversive experience (unconditioned stimulus) with concomitant non-aversive cues (such as spatial context, visual, auditory, olfactory cues etc., called conditioned stimuli)<sup>243,297</sup>. Consolidation of fear requires the release of the excitatory neurotransmitter glutamate, resulting in the activation of  $\alpha$ -amino-3-hydroxy-5-methyl-4-isoxazolepropionic acid (AMPA) and N-methyl-D-aspartate (NMDAR) receptors, and eventual increases in AMPA and NMDA receptor surface expression and function<sup>298-300</sup>. This cascade begins with activation of AMPARs, which depolarizes the cell<sup>65</sup>. NMDARs function as coincidence detectors of excitatory activity; under basal conditions, there is a magnesium block in the receptor pore<sup>65,301</sup>. As increased AMPAR activity depolarizes the neuron, the magnesium block is removed, and NMDAR activation permits influx of Na<sup>+</sup> and Ca<sup>2+</sup> ions<sup>65,301</sup>. Calcium signaling promotes many intracellular signaling mechanisms, including neuronal nitric oxide synthase (nNOS) interaction with postsynaptic density protein-95 (PSD95), an NMDAR scaffolding protein, at the plasma membrane<sup>249,250,302</sup>.

This organization promotes nNOS activity and nitric oxide (NO) production in a synapse-specific manner.

Previous experiments antagonizing NMDAR activity during critical periods of consolidation further highlight the requirement of NMDAR-dependent synaptic plasticity for consolidation to occur<sup>303-305</sup>. Several studies have demonstrated that NMDAR-PSD95-nNOS interaction is a critical step in fear memory and plasticity in the hippocampus and cortex<sup>231,251</sup>. A recent study from our group found that there is a specific pattern of PSD95-nNOS interaction immediately following fear acquisition in the basolateral amygdala (BLA), a brain region that plays a critical role in acquisition and consolidation of fear<sup>162</sup>. The interaction between PSD95 and nNOS is initiated upon fear-conditioning and increases 1-2 hours after fear acquisition. When the interaction is disrupted, both globally and locally in the BLA, using a small molecule protein-protein interaction inhibitor [ZL006 (4-(3,5-Dichloro-2-hydroxy-benzylamino)]], cued fear consolidation is attenuated<sup>162</sup>. Additionally, ZL006 is able to prevent high frequency stimulation-induced long-term potentiation (LTP) in BLA neurons<sup>162</sup>. The mechanism underlying these changes, however, remain unknown.

In the present study, we hypothesized that there are time-dependent changes in AMPAR and NMDAR signaling in the BLA initiated by cued fear conditioning, and that these sequential changes are critical for the consolidation of fear responses. Furthermore, we hypothesized that some aspects of these sequential glutamatergic molecular mechanisms underlying fear consolidation were dependent on the activity of nNOS. Therefore, we first reconfirmed that pharmacologically blocking PSD95-nNOS binding (with ZL006) blocked cued fear consolidation in rats. Next, we studied AMPAR- and

NMDAR-mediated current changes in the BLA after acquisition of fear and the role of nNOS in synaptic plasticity using brain slice electrophysiology. Specifically, we performed fear conditioning, administered either vehicle or ZL006 (intraperitoneal, i.p.), and examined AMPAR- and NMDAR-mediated current in the BLA of the rats at two key timepoints – immediately after fear conditioning and 24h after fear conditioning. We also evaluated the synaptosomal expression of GluR1 and NR2B subunits and phosphorylation of these receptor subunits at well described sites during fear consolidation. Our findings reported here suggest that there is a rapid (within 4-6 hours) activation of AMPAR-mediated currents and elevated GluR1 synaptosomal levels in the BLA, followed at 24 hours by sustained AMPAR-mediated current and increased NMDAR-mediated currents, accompanied by increases in not only GluR1 but also NR2B synaptosomal levels. Furthermore, levels of phosphorylated GluR1 and NR2B subunits were increased only after 24h following fear conditioning. All of these synaptic changes were blocked by pretreatment with ZL006 treatment. In conclusion, we use biochemical and electrophysiological methods to reveal a sequential molecular mechanism underlying cued fear consolidation in the amygdala and demonstrate that this sequence is nNOS dependent.

### **3.2 Materials and Methods**

Animals: Adult male Sprague-Dawley rats (250-300 g, Harlan, IN) were used for all experiments. Rats were housed in a temperature-controlled vivarium (22 °C) on a 12:12h light-dark cycle with food and water provided *ad libitum*. All rats were single-housed and given at least seven days to acclimate to new housing environment before handling and behavioral testing. Animal care was in accordance with NIH Guidelines for

the Care and Use of Laboratory Animals, and all procedures were approved by the IUPUI Institutional Animal Care and Use Committee.

Fear conditioning test: Rats were handled for five mins/day in the five days leading up to fear conditioning. On the first day of testing, rats were habituated to two contexts for 10 min. Both contexts were a 25.5 x 25.5 x 39.5 cm box, placed in a larger, soundproof Ugo Basile box with white 15-lux light and white noise at 4% volume (55 dB). Context A had transparent walls and a metal grid floor connected to a shock generator (Stoelting Co., Wood Dale, IL, USA) and was cleaned with 70% ethanol between all trials. Context B had patterned wall inserts, a plexiglass floor insert, and was cleaned with 1% acetic acid between all trials. Next, 24h after habituation, for fear conditioning, rats were placed in context A for a 100s habituation followed by three tones (20s, 4kHz, 80dB) that co-terminated with a shock (0.5s, 0.8mA). The inter-trial interval (ITI) was 100s, and the rat remained in the box for 60s after the last trial. The “tone-only” control group experienced the same protocol but without receiving foot-shocks. All rats received drug or vehicle intraperitoneal (i.p.) injections immediately after fear conditioning. After 24h, we tested for fear responses by placing rats in context B with the same protocol, without foot-shocks. Animal movement was tracked using an automated video recording and tracking system (ANYmaze, Stoelting Co., Wood Dale, IL, USA). Fear responses were calculated as percent time spent freezing during tones; freezing was defined as full immobility excluding respiration. A two-way ANOVA was used, with treatment as a between-subjects factor and tones as a within-subjects factor. *Post hoc* Fisher’s LSD test was used when  $p < 0.05$ .

Drugs and chemicals: For i.p. injections, ZL006 (Sigma Aldrich, St. Louis, MO, USA) was dissolved in a vehicle of 10% DMSO (Sigma Aldrich):90% of 100% ethanol (Fisher Scientific, Rockford, IL, USA), emulphor (Alkamuls EL-620, Solvay, Brussels, Belgium), and sterilized saline (1:1:8). Rats were injected with either the drug formulation (10 mg/kg) or vehicle alone at an injection volume of 1 ml/kg.

Electrophysiology: Either after fear acquisition or fear consolidation testing, rats were deeply anesthetized with isoflurane and trans-cardially perfused with protective artificial cerebrospinal fluid (aCSF) of the following composition (in mM): 93 N-methyl-D-glucamine (NMDG), 2.5 KCl, 1.2 NaH<sub>2</sub>PO<sub>4</sub>, 30 NaHCO<sub>3</sub>, 20 HEPES, 25 glucose, 2 thiourea, 5 Na-ascorbate, 3 Na-pyruvate, 0.5 CaCl<sub>2</sub>·4H<sub>2</sub>O, and 10 MgSO<sub>4</sub>·7H<sub>2</sub>O [30]. Brains were rapidly dissected and sectioned coronally (350 μm) on a Campden 7000smz-2 vibratome (Lafayette Instrument Co). For the initial recovery, slices were immersed in an oxygenated (mixture of 95% O<sub>2</sub>/5% CO<sub>2</sub>) NMDG-based aCSF at 30 °C for ≤11 min and then transferred to room temperature (RT) oxygenated aCSF of the following composition (in mM): 130 NaCl, 3.5 KCl, 1.1 KH<sub>2</sub>PO<sub>4</sub>, 1.3 MgCl<sub>2</sub>, 2.5 CaCl<sub>2</sub>, 10 glucose, 30 NaHCO<sub>3</sub>. The osmolality of all aCSF solutions used was adjusted to ~315 mOsm. Once transferred to a submersion-type slice chamber and perfused at a rate of 2–3 ml/min with oxygenated aCSF heated to 30 °C, individual BLA principal neurons were visualized using a Scientifica SliceScope Pro 6000 (Scientifica) upright microscope connected to the Hamamatsu ORCA-Flash4.0 digital CMOS camera (Hamamatsu, Japan). Whole-cell patch-clamp recordings were obtained using standard techniques with borosilicate glass electrodes (resistance 3–6 mΩ, WPI, Sarasota, FL) filled with a cesium methanesulfonate-based recording solution with the following composition (in mM): 120

CsMethanesulfonate, 15 HEPES, 0.4 EGTA, 2.9 NaCl, 5 TEA-Cl, 5 phosphocreatine, 2.5 Mg-ATP, 0.25 Na-GTP adjusted to pH 7.3 with KOH, and having an osmolality of 270–280 mOsm.

Individual neurons in the BLA were visualized using differential interference contrast microscopy with a 40x water immersion objective and displayed in real time on a monitor. Whole-cell recordings were made with a Multiclamp 700B amplifier using pClamp 10.3 software and a Digidata 1322A interface (Molecular Devices). To evoke postsynaptic currents, a concentric stimulating electrode (FHC) was placed ~500  $\mu\text{m}$  from the internal capsule to stimulate thalamic inputs to the BLA<sup>306</sup>. A stimulus of ~270 pA was repeated 15 times at a frequency of 0.2 Hz and then averaged for subsequent data analysis. The evoked excitatory post-synaptic potentials (eEPSPs) were recorded at -70 mV and measured at peak current to estimate AMPA currents, and then the holding potential was shifted to +40 mV and measured 50 ms after the initiation of current to estimate NMDA currents within the same cell. The time point of 50 ms after current initiation was chosen because NMDA currents are present at this time point, but AMPA currents have completely inactivated before 50 ms<sup>172,188</sup>. Access resistance was continuously monitored; recordings were excluded from analysis if resistance exceeded 20 M $\Omega$  or shifted by more than 15% during the experiment. A one-way ANOVA was used for statistical analysis. *Post hoc* Fisher's LSD test was used when  $p < 0.05$ .

Western Blotting: Rats were deeply anesthetized with isoflurane, followed by rapid decapitation. Brains were removed and rapidly frozen in iso-pentane (Fisher Scientific) on dry ice and stored in -80°C until ready to process. Brains were sectioned on a Leica CM1950 cryostat at 300  $\mu\text{m}$ , and punches of the BLA were collected using a 1



mm diameter Harris micro-punch (Electron Microscopy Sciences). The punches were homogenized in 10% w/v 0.32M HEPES sucrose and centrifuged for 500 g for 10 min. The supernatant was centrifuged at 12,500 g for 15 min and the resulting pellet contained synaptosomal membrane. The pellet was resuspended in 10% w/v of lysis buffer and Halt protease and phosphatase inhibitors cocktail (Thermo Scientific). A BCA assay (Thermo Scientific) was used to determine protein concentration, and 10 ug protein was loaded on 12% Bis-Tris Protein Gels (Bio-Rad) and transferred to nitrocellulose membrane (Amersham). After blocking, blots were incubated overnight at 4°C with anti-GluR1 (1:1000, ab109450, Abcam), anti-pGluR1 (S831, 1:500, 04-823, Millipore Sigma), anti-pGluR1 (Ser845, 1:500, OPA1-04118, Invitrogen), anti-NR2B (1:1000, ab65783, Abcam), anti-pNR2B (Ser1303, 1:500, 07-398, Millipore Sigma), anti-pNR2B (Tyr1472, 1:500, AB5403, Millipore Sigma), anti-pNR2B (Ser1480, 1:500, ab73014, Abcam), anti-nNOS (1:500; sc-5302, Santa Cruz Biotechnologies), and anti- $\beta$ -actin (housekeeping gene) (1:1000, sc-47778, Santa Cruz Biotechnology). Blots were washed, incubated 1h with secondary antibodies, and washed again. Blots were scanned using Odyssey CLx scanner (Li-cor), and Li-cor Image Studio software were used to perform densitometry. The densities of each protein of interest were normalized to the loading control ( $\beta$ -actin). A one-way ANOVA was used for statistical analysis. *Post hoc* Fisher's LSD test was used when  $p < 0.05$ .

### 3.3 Results

#### Cued fear acquisition results in immediate enhancement of AMPAR but not NMDAR subunit expression and function in the BLA and is blocked with systemic ZL006 treatment

In our fear conditioning paradigm, rats that received shocks paired with tones acquired cue-induced fear, observed by the increased freezing by the end of fear acquisition testing (average by tone/shock is 62% in vehicle treated and 49% in ZL006 treated groups) (Figure 11). Immediately after fear acquisition, rats were given an i.p injection of vehicle or ZL006. After 24h, rats were placed in a different context and presented with just tones to test for cued fear expression. The vehicle-treated group displayed freezing levels similar to their acquired freezing levels (75%). However, the ZL006-treated group expressed significantly lower freezing throughout the duration of the fear expression test (37%), compared to their respective acquired freezing levels (Figure 11). Rats that received tones without shocks during fear acquisition showed no gradual increases in freezing by end of fear acquisition nor during consolidation, as expected. These results corroborate our previous findings showing that administering ZL006 systemically immediately after cued fear acquisition disrupts cued fear memory consolidation in rats<sup>162</sup>.

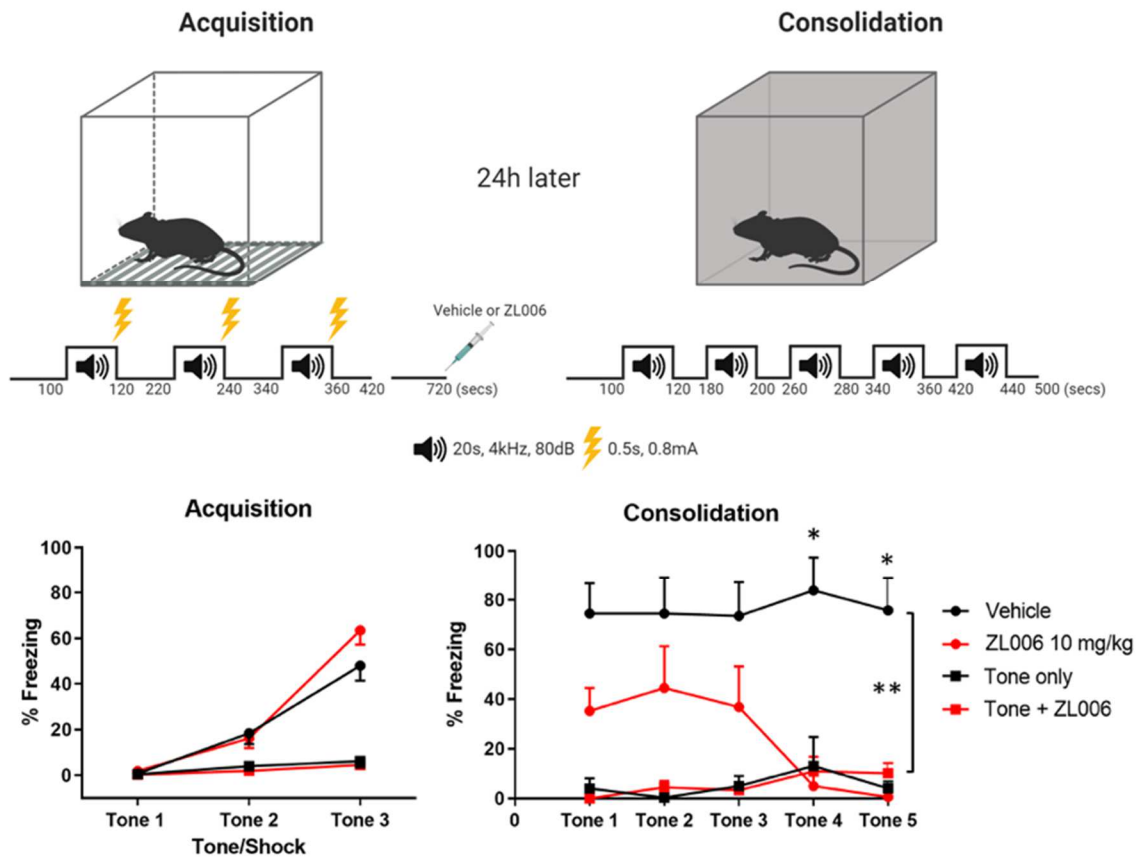


**Figure 11. Fear conditioning experimental schematic and behavior.** After habituation to both experimental contexts, rats were exposed to 3 tone-shock pairs for fear acquisition. Rats that were exposed to tone-shock pairs show normal acquisition, with freezing increasing up to  $55.8 \pm 10.3\%$  by the end of acquisition testing (Trial:  $F_{2,232} = 65.67$ ,  $p < 0.0001$ ). Immediately after acquisition, rats were given an i.p. injection of vehicle or ZL006. After 24h, during consolidation testing, rats given vehicle injections show freezing responses similar to end-of-acquisition responses. Rats given ZL006 treatment, however, show consistently and significantly lower freezing compared to vehicle-treated rats ( $37.4 \pm 5.2\%$ , averaged) compared to tone only control rats ( $3.0 \pm 1.2\%$ , averaged) (Treatment:  $F_{3,26} = 18.23$ ,  $p < 0.0001$ ). \* $p < 0.0001$  relative to tone only control group. (\* $p < 0.02$ , \*\* $p < 0.01$ ).

In our previous study, we showed BLA neurons treated with ZL006 exhibited impaired high-frequency stimulation induced LTP; we also showed that intra-BLA infusion of ZL006 impairs cued fear consolidation<sup>162</sup>. Thus, we sought to better understand selective AMPAR- and NMDAR-mediated synaptic transmission dynamics in the BLA following cued fear conditioning and systemic ZL006 treatment. To do this, we collected rat brains within 15 minutes of i.p injection (timepoint t0) and recorded amplitude of evoked and recorded AMPAR- and NMDAR-mediated currents in the BLA. We observed a significant increase in AMPAR-mediated currents in fear-conditioned animals, compared to the tone-only control group (Figure 12A). Surprisingly, AMPAR-mediated currents were restored to baseline levels in BLA neurons of ZL006-treated rats ( $p < 0.01$ ). Studies report that the AMPAR subunit, GluR1, is increasingly trafficked to the synaptosome in the BLA during the early stages of fear conditioning<sup>307-309</sup>. Additionally, loss of GluR1 function impairs consolidation of fear memories<sup>101,303,310,311</sup>. To understand if our findings were due to higher membrane expression of AMPARs, we next probed for GluR1 in BLA synaptosomes using Western blotting. We found increased expression of GluR1 on the synaptic membranes from the BLA in fear-conditioned rats ( $p < 0.01$ ), but ZL006 treatment did not significantly block this increase (Figure 12C).

In contrast to AMPAR, at t0, we did not observe any changes between the groups examined shortly after fear conditioning in either NMDAR-mediated currents or synaptic membrane expression of NR2B, an NMDAR subunit that is considered vital for fear consolidation (Figure 12B,D)<sup>304,312</sup>.

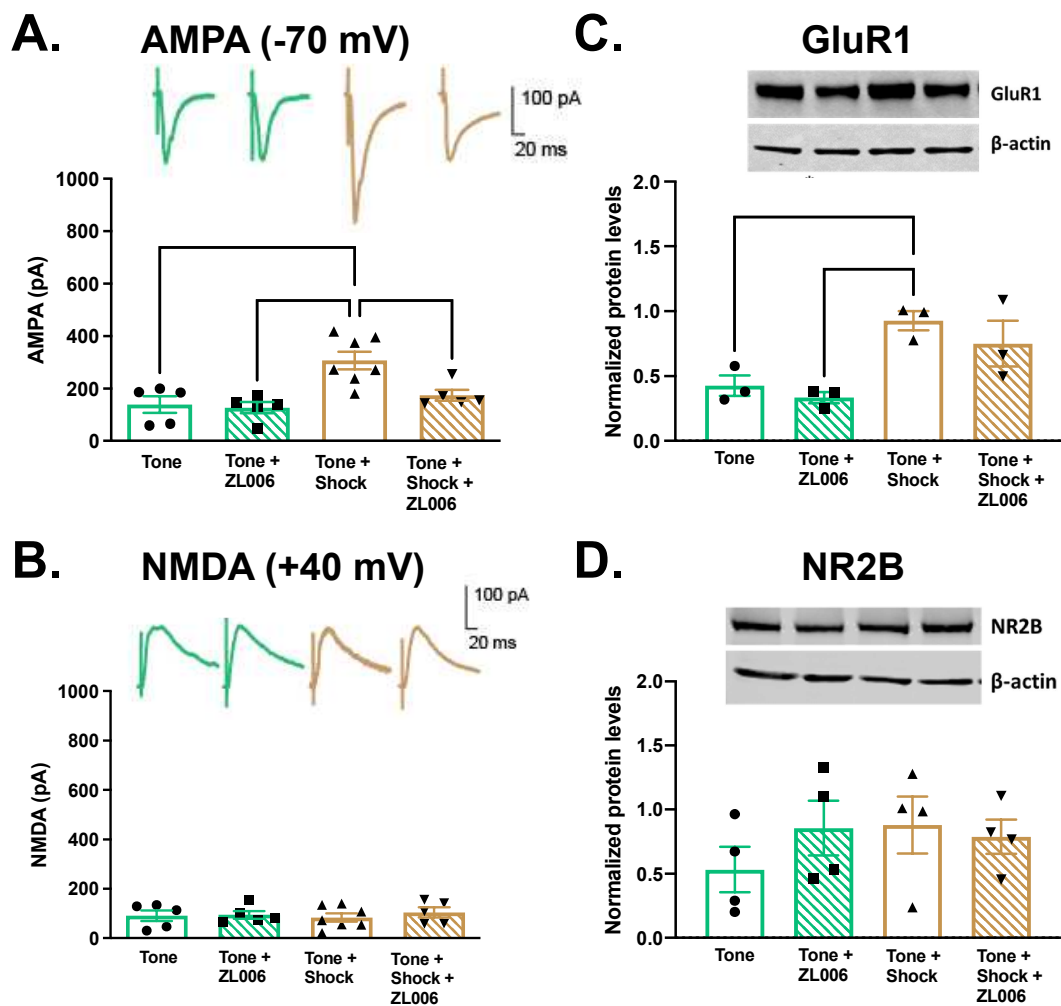


**Figure 12. AMPAR and NMDAR protein expression and function after fear acquisition.** A) AMPAR-mediated currents and representative traces recorded at a holding potential of -70 mV from BLA neurons in rats ( $p = 0.0007$ ). B) NMDAR-mediated currents and representative traces recorded at a holding potential of +40 mV from BLA neurons in rats. C) Synaptosomal GluR1 protein expression and representative bands obtained from BLA of rats ( $p = 0.01$ ). D) Synaptosomal NR2B protein expression and representative bands obtained from BLA of rats. \*\*  $< 0.01$ ; \*\*\* $p < 0.001$ . Note: Dr. Erik Dustrude collected the electrophysiological data.

Increased NMDAR surface expression and enhanced NMDAR-mediated synaptic transmission in the BLA 24 hours after cued fear acquisition, which is blocked with systemic ZL006 treatment

Noting the increases in AMPAR-mediated current and membrane expression after fear acquisition, we sought to understand if these changes were plastic and change over time. Since we test for fear expression 24h after training to confirm fear consolidation (t24), we hypothesized that there are differences in AMPAR and NMDAR surface expression and function immediately after training (acquisition) versus 24h after fear expression (consolidation) acquisition. To test this, we prepared brain slices immediately after the second day fear testing and again recorded AMPAR- and NMDAR-mediated synaptic transmission from BLA neurons.

Interestingly, the increase in AMPAR-mediated currents was sustained 24h after fear acquisition in the fear-conditioned and vehicle-treated group as was the blockade of AMPAR-mediated currents in the ZL006-treated group (Figure 13A). However, there were no significant differences in synaptosomal GluR1 expression in the BLA of any groups (Figure 13C). In other words, 24h after fear conditioning, AMPAR-mediated currents were increased in the BLA of fear-conditioned animals and restored to baseline in ZL006-treated rats. However, these changes could not be attributed to simply an increase in synaptosomal GluR1 levels.

Most interestingly, we found a significant increase in NMDAR-mediated currents in the BLA of fear-conditioned animals at t24, compared to tone-only controls ( $p < 0.0001$ ) (Figure 13B). This significant increase was mirrored in synaptosomal NR2B expression (Figure 13D) ( $p < 0.001$ ). In addition, in the BLA of ZL006-treated rats,

NMDAR-mediated currents and NR2B surface membrane expression remained at baseline levels, suggesting an important role for the PSD95-nNOS interaction in the temporal regulation of NMDAR-mediated glutamatergic signaling in the BLA after fear conditioning.

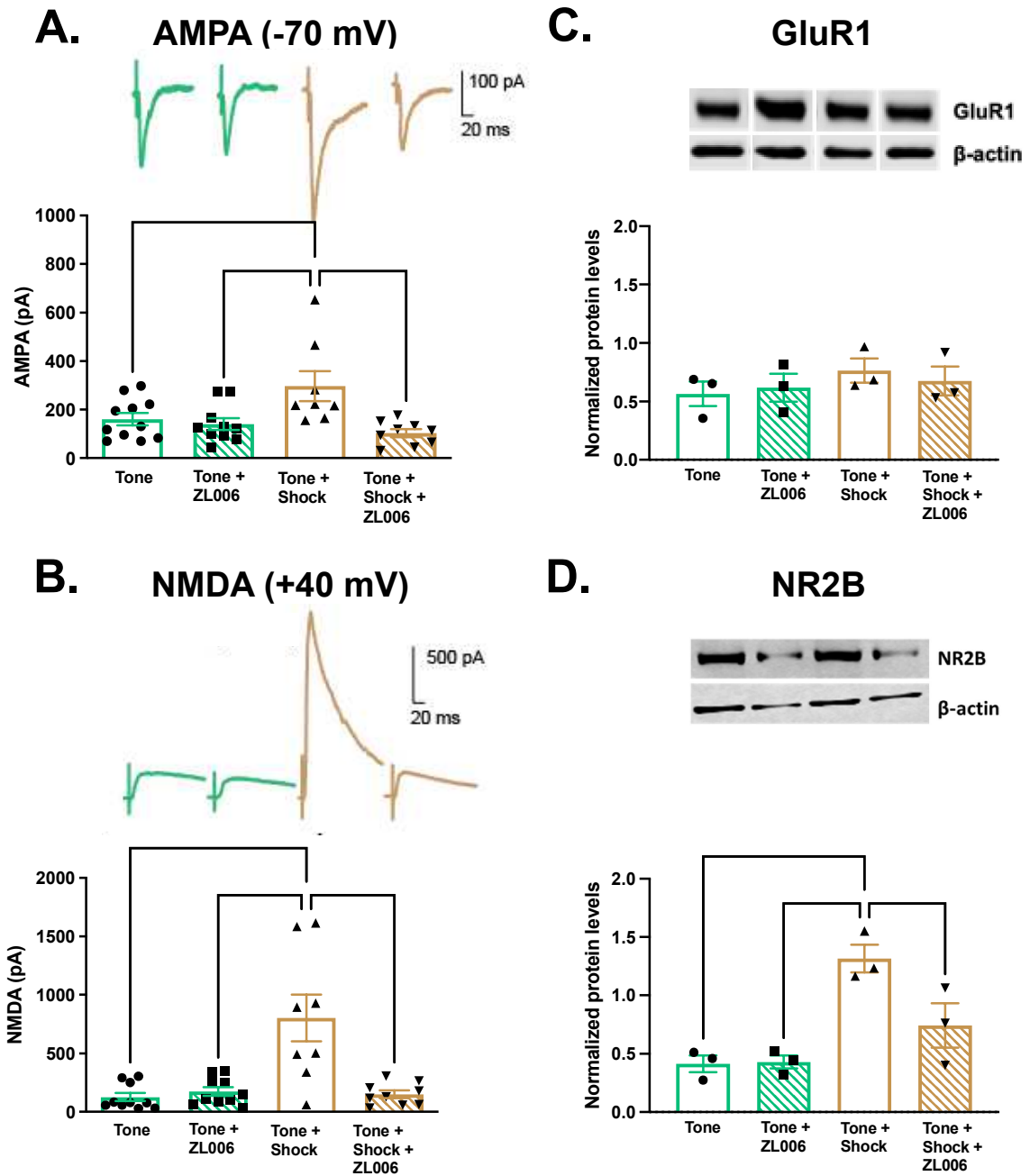


**Figure 13. AMPAR and NMDAR protein expression and function 24h after fear acquisition.** A) AMPAR-mediated currents and representative traces recorded at a holding potential of -70 mV from BLA neurons in rats ( $p = 0.003$ ). B) NMDAR-mediated currents and representative traces recorded at a holding potential of +40 mV from BLA neurons in rats ( $p < 0.0001$ ). C) Synaptosomal GluR1 protein expression and representative bands obtained from BLA of rats. D) Synaptosomal NR2B protein expression and representative bands obtained from BLA of rats ( $p = 0.003$ ). \* $p < 0.05$ ;



\*\*p < 0.01; \*\*\*p < 0.001; \*\*\*\*p < 0.0001. Note: Dr. Erik Dustrude collected the electrophysiological data.

### Expression levels of key phosphorylated sites on GluR1 and NR2B increase 24 hours after fear acquisition

At t24, although the changes in synaptosomal NR2B expression reflect changes in NMDAR-mediated currents, synaptosomal GluR1 expression does not reflect the same patterns as AMPAR-mediated currents. It appeared that total GluR1 levels were unchanged, yet we saw a clear functional increase in AMPAR-mediated currents. While receptor number is one explanation for receptor-mediated current alterations, phosphorylation of AMPAR and NMDAR subunits at specific sites is also reported to regulate receptor efficiency and conductance. Multiple phosphorylation sites on GluR1 and NR2B are known to be required for AMPAR and NMDAR synaptosomal trafficking and enhanced function, and as a result, are heavily implicated in synaptic plasticity and fear memory<sup>85,93,108,109,313-316</sup>. Using this information, we probed for five phosphorylation sites on the GluR1 and NR2B subunits – Ser831 and Ser845 on GluR1 and Tyr1472, Ser1480, and Ser1303 on NR2B.

At t0, we detected no significant differences in phosphorylation levels at any sites in our groups (Figure 14). At t24, however, we observed significant upregulation of phosphorylation at both sites of the GluR1 and two of the three sites, except for Tyr1472, of the NR2B subunit ( $p < 0.01$ ) (Figure 15). In comparison to the vehicle-treated group, increases in phosphorylation levels of these sites were not observed with ZL006 pre-treatment. This suggests that cued fear memory consolidation depends on the temporally concerted changes of not only absolute numbers but also phosphorylation of GluR1 and NR2B subunits. Remarkably, systemic ZL006 treatment blocked phosphorylation at all the sites we tested, indicating that the PSD95-nNOS interaction and presumably

downstream NO signaling is required for initiating these concerted changes in numbers and phosphorylation of GluR1 and NR2B. Figure 16 summarizes the levels of AMPAR and NMDAR-mediated currents, GluR1 and NR2B subunits, and phosphorylation after fear conditioning and shows that ZL006 blocks all the changes. Keeping this in mind, we provide a graphical mechanism in Figure 17, which suggests that mechanisms downstream of the PSD95-nNOS interaction are critical for regulation of AMPAR and NMDAR function and expression in the BLA.

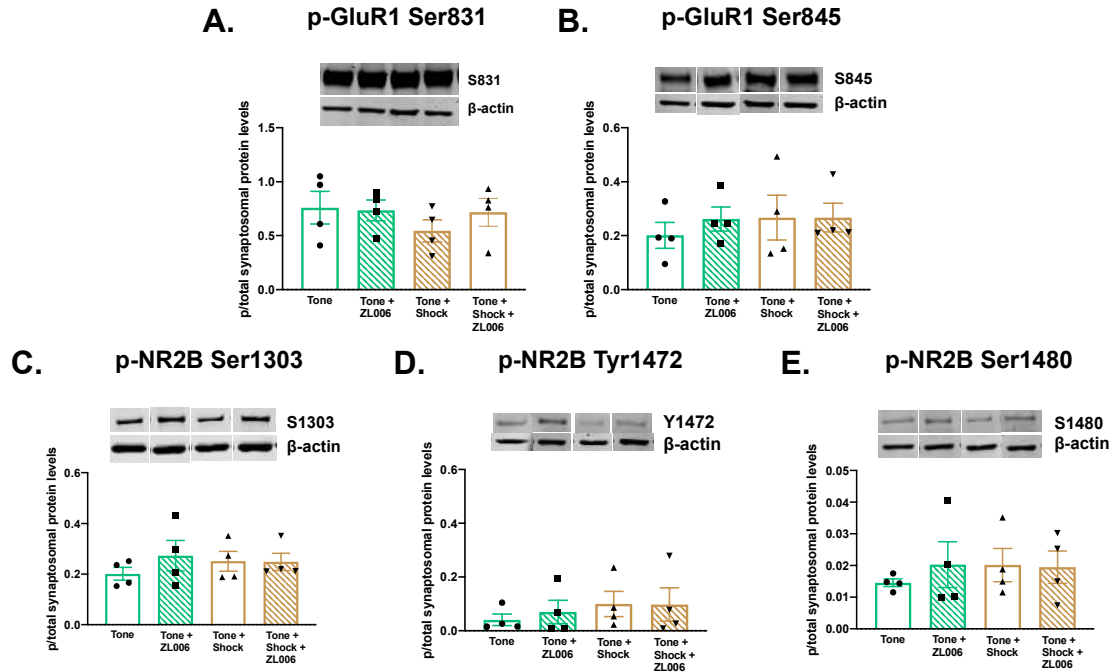


**Figure 14. Alterations in phosphorylation of key sites on the synaptosomal GluR1 and NR2B subunits after fear acquisition.** A) Expression levels of phosphorylated Ser831 on synaptosomal GluR1 in the BLA of rats after fear acquisition. B) Expression levels of phosphorylated Ser845 on synaptosomal GluR1 in the BLA of rats after fear acquisition. C) Expression levels of phosphorylated Ser1303 on synaptosomal NR2B in the BLA of rats after fear acquisition. D) Expression levels of phosphorylated Tyr1472 on synaptosomal NR2B in the BLA of rats after fear acquisition. E) Expression levels of phosphorylated Ser1480 on synaptosomal NR2B in the BLA of rats after fear acquisition. NO significant differences found between groups.

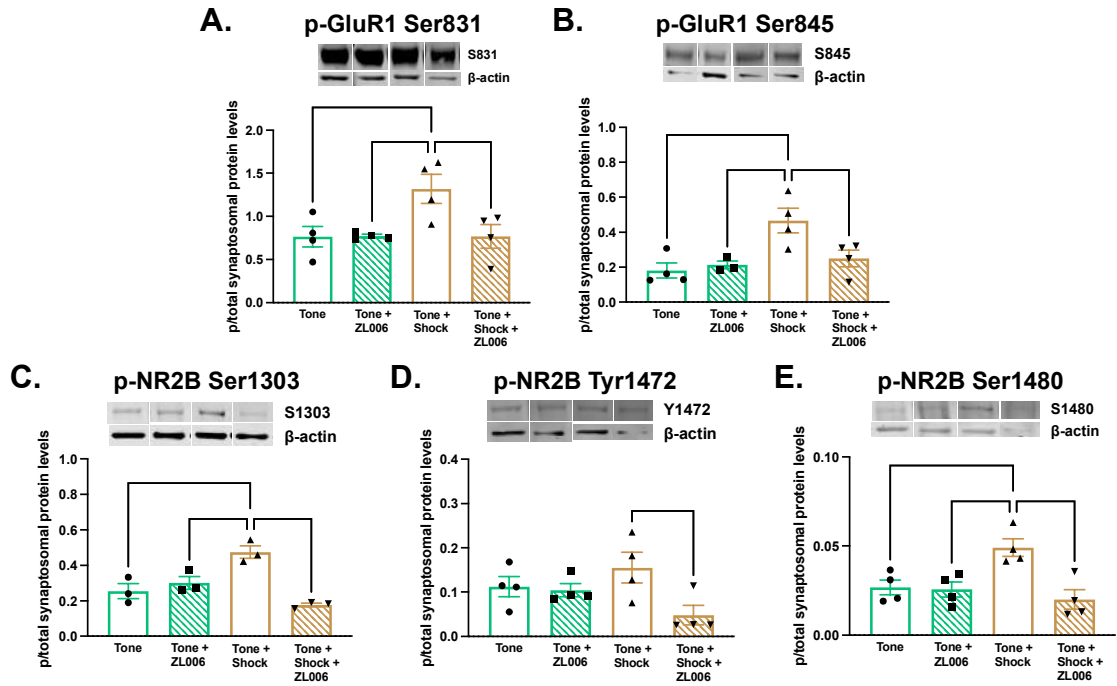


**Figure 15. Alterations in phosphorylation of key sites on the synaptosomal GluR1 and NR2B subunits 24h after fear acquisition.** A) Expression levels of phosphorylated Ser831 on synaptosomal GluR1 in the BLA of rats 24h after fear acquisition ( $p = 0.02$ ). B) Expression levels of phosphorylated Ser845 on synaptosomal GluR1 in the BLA of rats 24h after fear acquisition ( $p = 0.009$ ). C) Expression levels of phosphorylated Ser1303 on synaptosomal NR2B in the BLA of rats 24h after fear acquisition ( $p = 0.001$ ). D) Expression levels of phosphorylated Tyr1472 on synaptosomal NR2B in the BLA of rats 24h after fear acquisition ( $p = 0.06$ ). E) Expression levels of phosphorylated Ser1480 on synaptosomal NR2B in the BLA of rats 24h after fear acquisition ( $p = 0.005$ ). \* $p < 0.05$ ; \*\* $p < 0.01$ ; \*\*\* $p < 0.001$ .

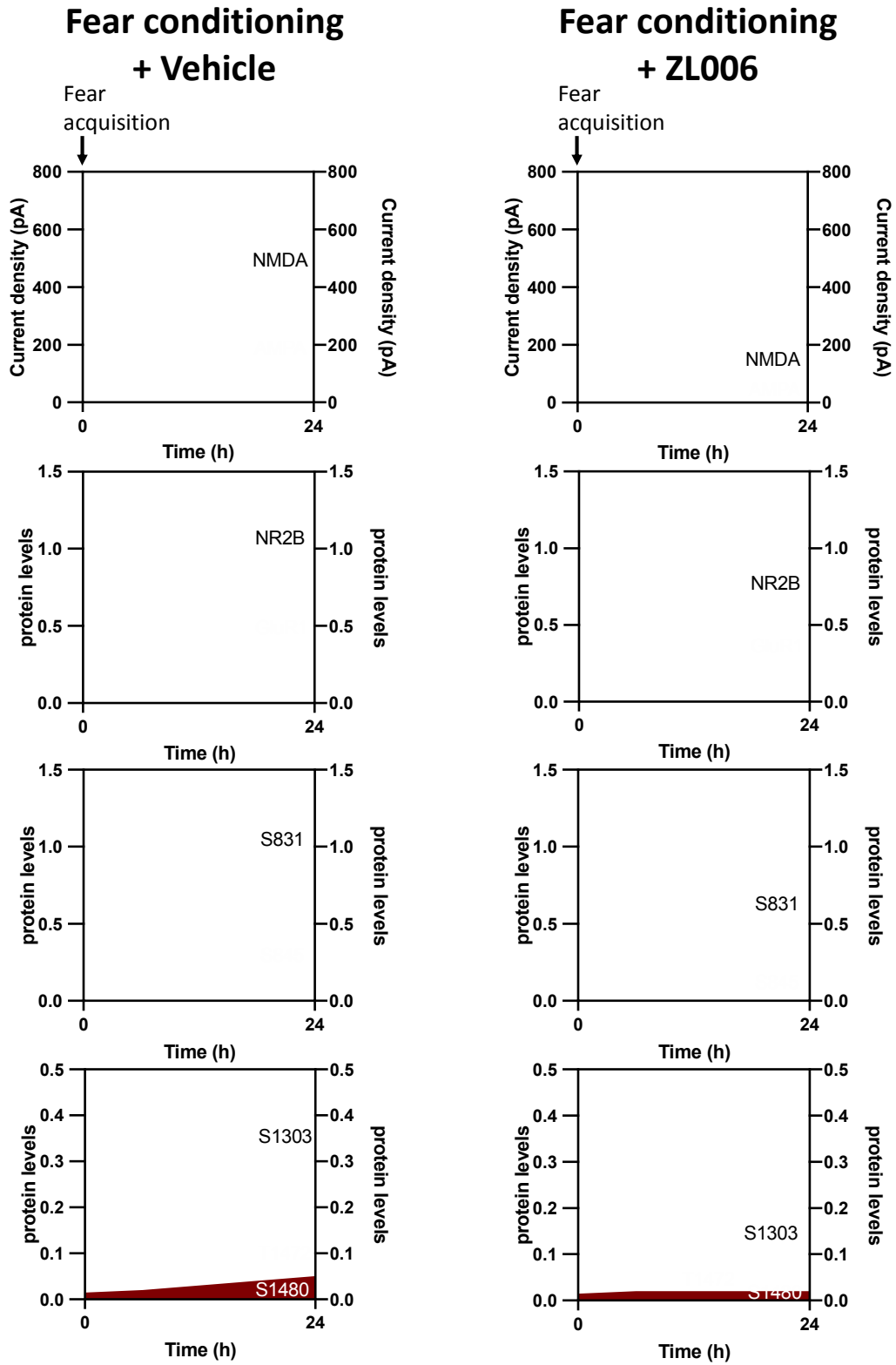


**Figure 16. Summary of AMPAR and NMDAR-mediated currents and GluR1 and NR2B total and phosphorylated expression levels immediately after and 24h after**

**fear acquisition.** Time-course summary of our findings, showing that there are unique changes in AMPAR- and NMDAR-mediated current densities and total and phosphorylated synaptosomal GluR1 and NR2B expression patterns in the BLA of rats over the first 24h after fear conditioning. These patterns are disrupted with ZL006 treatment after fear conditioning.

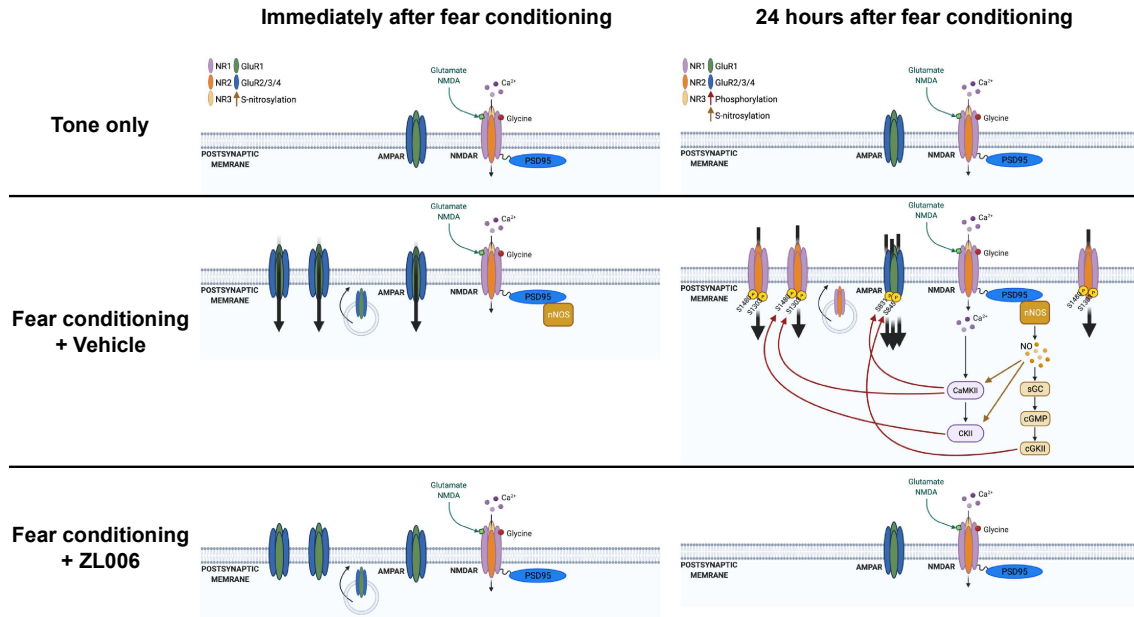


**Figure 17. Graphical summary of molecular changes occurring in the BLA during fear consolidation.** Based on our findings here, a suggested mechanism of how nNOS mediates synaptic function in the BLA during fear conditioning. The early stage of fear consolidation is marked by enhanced GluR1 subunit expression and AMPAR channel conductance. The late stage of fear consolidation is marked by enhanced AMPAR- and NMDAR-mediated currents, NR2B subunit expression, and phosphorylation of GluR1 and NR2B. These changes are mediated by nNOS activity, as evidenced by the significant reduction in currents, subunit expression, and phosphorylation of AMPARs and NMDARs with ZL006 administration. PSD95 = postsynaptic density 95; nNOS = neuronal nitric oxide synthase; NO = nitric oxide; sGC = soluble guanylyl cyclase; cGMP = cyclic guanosine monophosphate; cGKII = cGMP-dependent protein kinase II; CaMKII = calcium/calmodulin-dependent protein kinase II; CKII = casein kinase II.



### 3.4 Discussion

Previous studies by us and other groups have reported on the importance of the PSD95-nNOS interaction in modulating fear responses<sup>162,231,251</sup>. However, which synaptic and molecular mechanisms are regulated by the PSD95-nNOS interaction is still poorly understood. In previous studies, we have shown that both systemic and intra-BLA delivery of a small molecule inhibitor of PSD95-nNOS interaction, ZL006, sufficiently attenuates cued fear consolidation<sup>162</sup>. Additionally, we showed that ZL006 application impairs LTP in BLA neurons<sup>162</sup>. Using this information, we aimed to further elucidate the sequential synaptic function and receptor composition mechanisms within the BLA underlying cued fear conditioning that are modulated by PSD95-nNOS interaction-mediated signaling. To do this, we focused on two timepoints – immediately after fear conditioning (t0) and 24h after fear conditioning (t24), when fear consolidation is observed. In addition to parsing out AMPAR- and NMDAR-mediated synaptic currents at these timepoints, we also reasoned that any changes we observe in these specific glutamate receptor currents might be due to a unique pattern of total synaptosomal AMPAR and NMDAR expression and phosphorylation patterns of subunits of these receptors at specific sites that allow enhanced function at their respective ionophores. Thus, based on prior work, we chose to test for total levels of synaptosomal GluR1 and NR2B expression, phosphorylation at Ser831 and Ser845 for GluR1, and phosphorylation at Tyr1472, Ser1480, and Ser1303 for NR2B<sup>85,93,108,109,304,313-316</sup>.

Immediately after fear conditioning (t0) we observed an increase in AMPAR-mediated currents in BLA neurons of fear-conditioned and vehicle-treated animals compared to behavioral controls. However, this increase was mitigated when PSD95-

nNOS binding was inhibited in animals via ZL006 pre-treatment (Figure 12A). No such differences were found in NMDAR-mediated current in BLA neurons when recorded at t0 (Figure 12B). We also found increased synaptosomal GluR1 expression in the BLA of fear-conditioned animals at t0, regardless of ZL006 treatment (Figure 12C). Additionally, there were no differences in phosphorylation of the Ser831 and Ser845 sites on GluR1 at t0 (Figure 14A, B). First, this indicates that the initial spike in AMPAR-mediated current observed after fear conditioning is due primarily to increased synaptosomal GluR1 expression. Second, since ZL006-treatment did not block GluR1 expression nor phosphorylation levels on GluR1, and yet blocked the increase in AMPAR-mediated currents, it indicates that there are alternative mechanisms underlying ZL006-mediated blockade of AMPAR in the early stages after fear conditioning. These mechanisms could include nitrosylation, phosphorylation at alternative GluR1 sites, or effects on other AMPAR subunits.

When tested for cued fear expression 24h after fear conditioning, we observe attenuated cued fear consolidation in animals treated systemically with ZL006, validating a previous study (Figure 11)<sup>162</sup>. Investigating AMPAR and NMDAR function and expression patterns at t24, we found persistent increases in AMPAR-mediated current at t24, compared to tone only controls. These increases were blocked, however, in fear-conditioned animals given ZL006 treatment (Figure 13A). As noted before, AMPAR-mediated neurotransmission remained elevated to the same levels 24h after fear conditioning as they were immediately after fear conditioning, while inhibition of the PSD95-nNOS interaction blocked this increase. Importantly, unlike at t0, we also

observed a significant increase in NMDAR-mediated current in fear-conditioned animals at t24, which was also blocked with ZL006 treatment (Figure 13B).

Unlike t0, at t24, the total synaptosomal GluR1 levels were not altered in the BLA of fear-conditioned animals, suggesting that while acute increase in AMPAR function was accomplished by increasing total number of synaptic AMPARs, the functional increase in AMPAR function at t24 had a different molecular mechanism. Consistent with this assumption, we found that both p-Ser831 and p-Ser845 GluR1 levels in the BLA increased with fear conditioning and were subsequently blocked with ZL006 treatment (Figure 15A, B). This importantly suggests that phosphorylation at Ser831 and Ser845 plays a significant role in enhancing AMPAR function 24h after fear conditioning, and this role is likely mediated via the PSD95-nNOS interaction.

In studying the molecular mechanism underlying the NMDAR-mediated current increases in the BLA at t24 following fear conditioning, we found that the synaptosomal levels of NR2B also increased in vehicle treated fear-conditioned animals which were blocked in ZL006-treated animals (Figure 13D). Surprisingly, we found unique expression patterns of phosphorylation at our sites of interest in NR2B at t24. Phosphorylation levels of both Ser1303 and Ser1480 at t24 were elevated in fear-conditioned animals, but blocked in ZL006-treated animals, indicating the importance of these sites in enhancing and supporting NMDAR function in the late stages of fear memory consolidation (Figure 15C, E). In contrast, phosphorylation of Tyr1472 was unaltered in fear-conditioned animals, but significantly downregulated in ZL006-treated animals, suggesting that Tyr1472 does not necessarily play a role in the increase of NMDAR-mediated current we observed at t24 (Figure 15D). Phosphorylation of Tyr1472

may nonetheless be regulated in an activity-dependent manner, which could explain the downregulation of expression in fear-conditioned, ZL006-treated animals.

Our pharmacological approach here investigates nNOS-mediated effects on glutamatergic signaling within the BLA, a mechanism that appears critical to consolidation of cued fear. The interaction between PSD95 and nNOS activates nNOS and results in the production of nitric oxide (NO), which activates several downstream mechanisms enhancing plasticity, including S-nitrosylation via NO<sup>317</sup>. Fyn, a Src kinase that phosphorylates Tyr1472 on NR2B, requires S-nitrosylation for its kinase activity<sup>186</sup>. Another kinase whose activity is mediated by NO is calcium/calmodulin-dependent protein kinase II (CaMKII), which phosphorylates Ser1303 on NR2B as well as Ser831 on GluR1<sup>88,104,318</sup>. CamKII also activates casein kinase 2 (CK2), which further phosphorylates Ser1480 on NR2B<sup>91,92</sup>. Upon production, NO also activates soluble guanylate cyclase (sGC), which then catalyzes production of cGMP, a second messenger signaling molecule<sup>192,319</sup>. cGMP-dependent activation of cGMP-dependent protein kinase II (cGKII) is vital for phosphorylation of Ser845 on GluR1<sup>198</sup>. This suggests that nNOS is crucial for regulation of activity of multiple kinases. In addition to these studies, we found that blocking nNOS activity, whether pharmacologically or genetically, inhibits activity-dependent increases in phosphorylation of most of our tested sites on GluR1 and NR2B in the BLA. Our findings further support and elucidate the details of nNOS-mediated downstream mechanisms that ultimately control GluR1 and NR2B trafficking and conductance following fear conditioning.

Our findings specify a time- and experience-dependent NMDAR-PSD95-nNOS signaling mechanism underlying cued fear memory consolidation and show that a

pharmacological and genetic blockade of nNOS activity is able to inhibit this mechanism. We provide evidence for the role of nNOS in the BLA in the rapid increases in total synaptic AMPAR levels in the acute stage of fear conditioning, and phosphorylation of Ser831 and Ser845 of GluR1 and Ser1303 of NR2B for the sustained increases in AMPAR and NMDAR conductance during the late stages of fear memory consolidation. Moreover, we show that blocking nNOS activity within the BLA is able to prevent the phosphorylation of these sites at 24h after fear conditioning, sufficient to inhibit the increases in AMPAR- and NMDAR-mediated currents and attenuate cued fear consolidation.

There appears to be further nuances to the phosphorylation of the various sites on the NR2B subunit. For example, while we do not see a significant increase in phosphorylation of Tyr1472 on NR2B at t24, this may be because S-nitrosylation of Fyn kinase, which phosphorylates Tyr1472, has been shown to peak in activity 6h after stimulation of NO<sup>186</sup>. Importantly, though, we observe that ZL006 treatment reduced the phosphorylation of Tyr1472. Thus, it is possible that Tyr1472 levels changed between 0 and 24h after fear conditioning but were returned to normal by 24h. This would indicate that ZL006 treatment possibly blocked phosphorylation of Tyr1472 at some point after fear conditioning, which was sustained and later observed at t24.

The other phosphorylation site that showed unexpected expression patterns is Ser1480 on NR2B. Interestingly, it is reported that phosphorylation of Ser1480 on NR2B localizes it to the extrasynaptic membrane, where it may be endocytosed<sup>93</sup>. However, we observed an increase in synaptosomal NR2B levels and NMDAR-mediated currents at t24 that correlated with increased p-Ser1480 levels in our fear-conditioned and vehicle-

treated animals at t24, all of which were blocked with ZL006 treatment. This suggests that phosphorylation at NR2B at Ser1480 ensures a pool of extrasynaptic NR2B that is readily available to be trafficked to the synapse. As ZL006 blocked phosphorylation at Ser1480, nNOS may also modulate the availability of an extrasynaptic pool of NR2B.

In summary, our findings identify an NMDAR-PSD95-nNOS axis-regulated pattern of time-dependent changes in AMPAR and NMDAR functions, surface expressions, and phosphorylation states that appears to be critical for the molecular mechanism in the BLA underlying cued fear acquisition. We were able to impair cued fear consolidation and block most of the synaptic and molecular changes via systemic administration of a small molecule inhibitor of the PSD95-nNOS interaction. These findings further demonstrate that activities of synaptic AMPARs and NMDARs within the BLA are temporarily orchestrated to ensure proper fear memory formation and stabilization. Within the BLA, this concerted activity is largely regulated via activation of the NMDAR-PSD95-nNOS axis and its downstream signaling. Our findings reveal a series of temporally and spatially specific molecular mechanisms underlying the consolidation of cued fear memory, and as such, serves as an important pathway to target for developing novel treatment of fear disorders.

## CHAPTER 4

### **Intra-Basolateral Amygdala Knockdown of nNOS Weakens Auditory Fear Consolidation and Alters the Synaptosomal Expression and Phosphorylation Levels of GluR1 and NR2B**

#### **4.1 Introduction**

Neuronal nitric oxide synthase (nNOS) is an enzyme implicated in regulation of fear memory consolidation<sup>162</sup>. nNOS is expressed abundantly in the central nervous system and is activated downstream of N-Methyl-D-aspartic acid receptor (NMDAR) activation in neuronal cells<sup>118,249,250</sup>. Upon presynaptic release, glutamate binds to and opens NMDARs, which allows for calcium influx<sup>65,301</sup>. Postsynaptic density protein 95 (PSD95) is a scaffolding protein that binds to NMDARs and nNOS to form the macromolecular NMDAR-PSD95-nNOS complex<sup>118,249,250</sup>. nNOS contains a calcium/calmodulin (CaM)-binding domain<sup>137,138</sup>. When intracellular calcium levels rise due to NMDAR activation, CaM binds and conformationally alters nNOS<sup>152,153</sup>. These conformational changes activate nNOS to catalyze the production of nitric oxide (NO), which regulates multiple synaptic plasticity mechanisms<sup>169,172,175,178,180,192,193</sup>. Several studies report that inhibiting nNOS activity alters auditory fear consolidation, and I showed in chapter 3 that this might be due to the unique effects of the NMDAR-PSD95-nNOS axis on glutamatergic neurotransmission in the BLA, a central region for fear memory consolidation<sup>16,162,204,231</sup>.

The results in chapters 2 and 3 are based on a model of systemic administration of an inhibitor of PSD95-nNOS interaction; however, we observed transcriptional and molecular changes specifically within the BLA. These discoveries support the results

from our laboratory's recent publication, in which we demonstrated that an intra-BLA inhibition of PSD95-nNOS interaction sufficiently attenuated fear consolidation<sup>162</sup>.

Therefore, we wondered if blocking nNOS altogether in the BLA would also result in the same behavioral and synaptic phenotype we observed in chapter 3.

Here, we injected AAV5-nNOS-siRNA-CMV-GFP into the BLA of rats to knockdown nNOS expression. In addition to auditory fear conditioning, we tested animals in numerous other behavioral tests to investigate motor function, social and anxiety-like behavior, and spatial memory. Finally, in the BLA, we examined the synaptosomal expression levels of GluR1 and NR2B as well as the levels of phosphorylation at the sites previously probed in chapter 3. We demonstrated that the AAV-mediated knockdown of nNOS in the BLA reduces cued fear consolidation, does not affect motor function, social and anxiety-like behaviors, or spatial memory, and prevents experience-dependent increases of total and phosphorylated levels of synaptosomal GluR1 and NR2B in the BLA.

## **4.2 Materials and Methods**

Animals: Adult male Sprague-Dawley rats (250-300 g, Harlan, IN) were used for all experiments. Rats were housed in a temperature-controlled vivarium (22 °C) on a 12:12h light-dark cycle with food and water provided *ad libitum*. All rats were single-housed and given at least seven days to acclimate to new housing environment before handling and behavioral testing. Animal care was in accordance with NIH Guidelines for the Care and Use of Laboratory Animals, and all procedures were approved by the IUPUI Institutional Animal Care and Use Committee.



Fear conditioning test: Rats were handled for five min/day in the five days leading up to fear conditioning. On the first day of testing, rats were habituated to two contexts for 10 min. Both contexts were a 25.5 x 25.5 x 39.5 cm box, placed in a larger, soundproof Ugo Basile box with white 15-lux light and white noise at 4% volume (55 dB). Context A had transparent walls and a metal grid floor connected to a shock generator (Stoelting Co., Wood Dale, IL, USA) and was cleaned with 70% ethanol between all trials. Context B had patterned wall inserts, a plexiglass floor insert and was cleaned with 1% acetic acid between all trials. Twenty-four hours after habituation, rats were placed in context A for a 100s habituation followed by fear conditioning with three tones (20s, 4kHz, 80dB) that co-terminated with a shock (0.5s, 0.8mA). The inter-trial interval (ITI) was 100s, and the rat remained in the box for 60s after the last trial. After 24h, we tested for fear responses by placing rats in context B with the same protocol but without foot-shocks. Animal movement was tracked using an automated video recording and tracking system (ANY-maze, Stoelting Co., Wood Dale, IL, USA). Fear responses were calculated as the percentage of time spent freezing during tones; freezing was defined as full immobility excluding respiration. A two-way ANOVA was used, with treatment as a between-subjects factor and tones as a within-subjects factor. The *post hoc* Fisher's LSD test was used when  $p < 0.05$ .

Open field (OF) test: Rats were habituated to a dark testing room illuminated with a red lightbulb for at least 30 min prior to the beginning of testing. For the OF test, rats were placed in the center of the OF box (91.5 x 91.5 x 30.5 cm, open-topped) and allowed to explore the box for 5 min. A ceiling-mounted CCD camera was used to record

the test, which was later analyzed using the ANY-maze automated tracking system (Stoelting Co.). We used distance traveled to measure locomotor activity.

Social interaction (SI) test: Rats were again habituated to a dark testing room illuminated with a red lightbulb for at least 30 min prior to the beginning of testing. For the SI test, subject rats and a sex-, age-, and weight-matched partner were placed into the OF box together. The fur of subject rats was marked to discern them more easily from the partner rat. Testing was conducted for 5 min and was recorded in the same manner as the OF test. An observer blinded to the treatment groups manually scored all videos using ODlog v2.6.1. All non-aggressive interaction with or investigation of the partner rat initiated by the subject rat was scored as SI. This included sniffing, anogenital investigation, climbing over or under the partner rat, grooming, or chasing/following the partner rat.

Elevated plus maze (EPM) test: The EPM consisted of 2 sets of perpendicular arms elevated 25 inches from the ground; one set of arms was open, and the other was closed (55 x 4 in and 55 x 4 x 6 in). For testing, rats were placed in the center area and allowed to explore for 5 min. A ceiling-mounted CCD camera was used to record all testing. ANY-maze software (Stoelting Co.) was used to analyze the videos and determine the timing and number of entries into each arm.

Y-maze test: The Y-maze consisted of a cylindrical center chamber with 3 adjacent arms (34 x 8 x 14.5 cm) in the shape of a Y, with visual cues at the end of each arm as well as consistent distal cues around the room. Rats were habituated to the room for at least 30 min prior to testing. For acquisition training, rats were placed in a start arm (the same start arm was used for all rats throughout testing) and allowed to explore the

start arm, center, and a familiar arm (which was the same for all rats throughout testing) for 10 min. The novel arm was blocked for acquisition training. After 1h, the novel arm was opened, and rats were placed in the start arm and allowed to explore all arms for 5 min. A ceiling-mounted CCD camera was used to record all testing. Videos were manually analyzed by an observer blinded to the treatment groups using ODlog v2.6.1 to record the number and duration of arm entries for each arm.

Viral knockdown of nNOS: Rats (~65 g) were anesthetized in a chamber with 5% isoflurane and placed in a stereotaxic frame. Isoflurane was maintained at 2.5% throughout the surgery. Using sterile technique, the skull was exposed to drill holes for targeting the BLA. Using a Hamilton syringe, 400 nL of either AAV5-nNOS-siRNA-CMV-GFP or AAV5-scrambled-CMV-GFP virus was bilaterally delivered at a rate of 80 nL/min into the BLA (AP -1.48, ML 4.25, DV -8). The syringe was left in place for 10 min to minimize off-target leakage and was removed very slowly afterward. Rats were tested in behavioral paradigms (order of testing: open field, social interaction, elevated plus maze, Y-maze, fear conditioning) 4 weeks after surgery.

Western blotting: Rats were sacrificed by deep anesthesia with isoflurane followed by rapid decapitation. The brains were removed and rapidly frozen in isopentane (Fisher Scientific) on dry ice and stored at -80°C until processing. The brains were sectioned on a Leica CM1950 cryostat at 300 µm, and punches of the BLA were collected using a 1 mm diameter Harris micro-punch (Electron Microscopy Sciences). The punches were homogenized in 10% w/v 0.32M HEPES sucrose and centrifuged at 500 g for 10 min. The supernatant was centrifuged at 12,500 g for 15 min and the resulting pellet contained the synaptosomal membrane. The pellet was resuspended in

10% w/v lysis buffer supplemented with the Halt protease and phosphatase inhibitors cocktail (Thermo Scientific). A BCA assay (Thermo Scientific) was used to determine protein concentration. Ten micrograms of protein per sample were loaded onto 12% Bis-Tris protein gels (Bio-Rad) and transferred to a nitrocellulose membrane (Amersham). The blots were blocked for 1h and then incubated overnight at 4°C with anti-GluR1 (1:1000, ab109450, Abcam), anti-pGluR1 (S831, 1:500, 04-823, Millipore Sigma), anti-pGluR1 (Ser845, 1:500, OPA1-04118, Invitrogen), anti-NR2B (1:1000, ab65783, Abcam), anti-pNR2B (Ser1303, 1:500, 07-398, Millipore Sigma), anti-pNR2B (Tyr1472, 1:500, AB5403, Millipore Sigma), anti-pNR2B (Ser1480, 1:500, ab73014, Abcam), anti-nNOS (1:500; sc-5302, Santa Cruz Biotechnologies), and anti- $\beta$ -actin (housekeeping gene) (1:1000, sc-47778, Santa Cruz Biotechnology) antibodies. Blots were washed, incubated for 1h with secondary antibodies, and washed again. Blots were scanned using an Odyssey CLx scanner (Li-cor), and Li-cor Image Studio software was used to perform densitometry. The densities of each protein of interest were normalized to the loading control ( $\beta$ -actin). A one-way ANOVA was used for statistical analysis. *Post hoc* Fisher's LSD test was used when  $p < 0.05$ .

Immunohistochemistry: The brains from animals injected with nNOS-siRNA or scrambled virus were collected ~15 mins after fear consolidation testing ended. Rats were deeply anesthetized with isoflurane and perfused trans-cardially with phosphate-buffered saline (PBS, pH 7.4) followed by 4% paraformaldehyde (PFA) in PBS (pH 7.4). The brains were placed in 30% sucrose in PBS at 4°C until they sank, sectioned coronally at 35  $\mu$ m using a freezing microtome, protected from light, and stored in cryoprotectant at -20°C. Alternate sections containing the BLA were rinsed with PBS (3x, 10 min),

incubated with mouse anti-nNOS (1:500; sc-5302, Santa Cruz Biotechnologies) in PBS-T overnight, and then rinsed in PBS-T (3x, 10 min). Next, sections were incubated at RT for 90 min with goat anti-mouse IgG (1:500; A-11004, Thermo Fisher Scientific) in PBS-T and then rinsed in PBS-T (3x, 10 min). Sections were mounted on slides, air-dried, and cover-slipped. A Leica confocal microscope was used to obtain images of the BLA.

### **4.3 Results**

#### Viral siRNA-mediated knockdown of nNOS in the BLA impairs cued fear consolidation

Knowing that systemic blockade of the PSD95-nNOS interaction alters AMPAR- and NMDAR-mediated currents as well as expression and phosphorylation states of GluR1 and NR2B subunits specifically in the BLA, we sought to determine if a BLA-specific knockdown of nNOS interferes with fear consolidation and the underlying molecular sequence of events in a manner similar to ZL006 treatment.

To do this, rats were bilaterally infused with an AAV, AAV5-nNOS-siRNA-CMV-GFP, that targeted the *nNos* gene. Four weeks later, we found that the virus was expressed in the BLA and was associated with an overall decrease in BLA-localized nNOS protein expression (Figure 18A). The rats were tested in the same cued fear conditioning paradigm as in chapters 2 and 3. We observed normal fear acquisition in the control and nNOS knockdown rats. However, during the fear expression test 24h later, the nNOS knockdown group displayed significantly reduced freezing (Figure 18B). We also tested for other behavioral effects of the nNOS knockdown. We found no differences between control and nNOS knockdown rats in locomotor activity, social interaction behaviors, anxiety-like behavior, and spatial memory (Figure 18C, D).

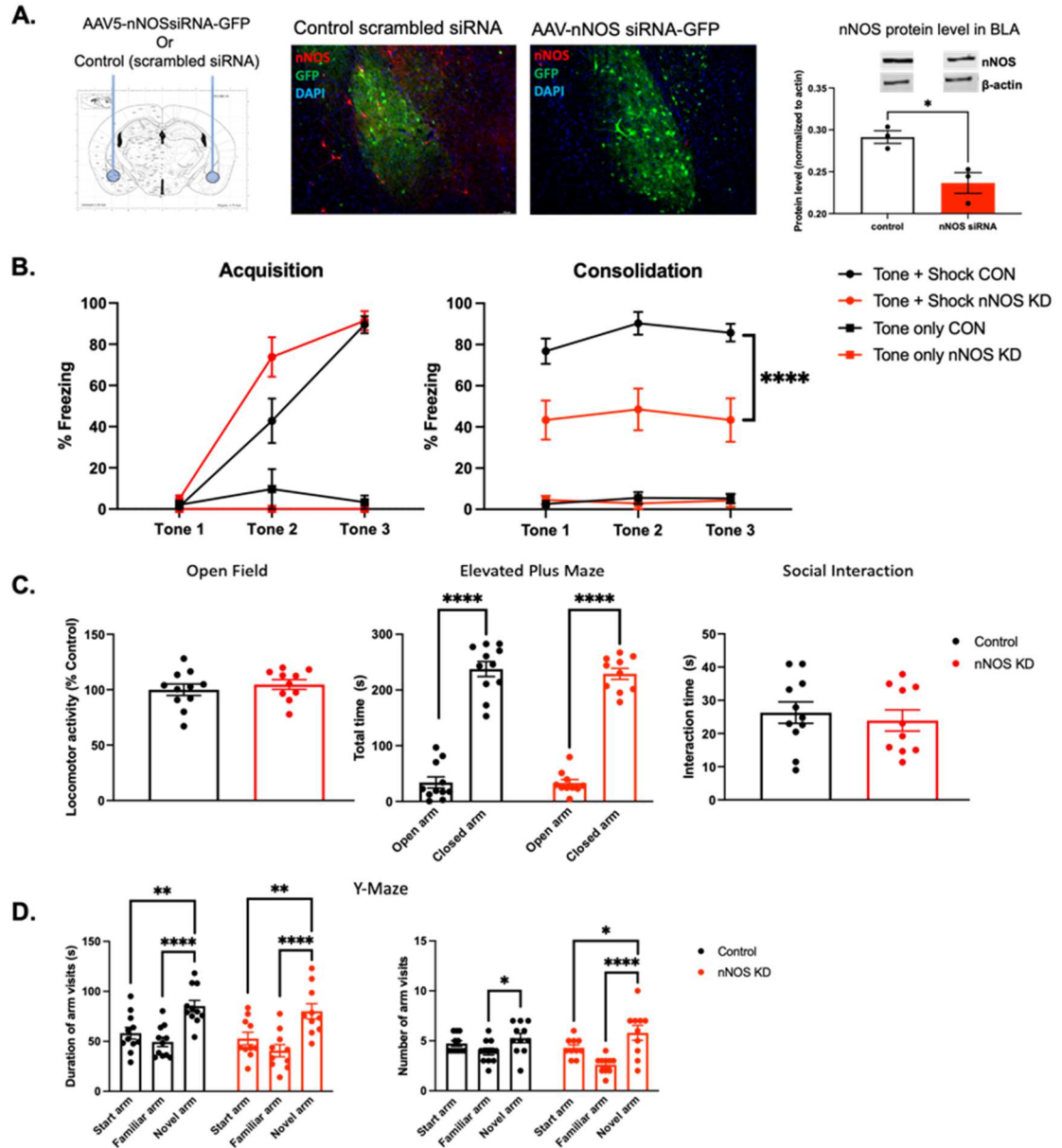


**Figure 18. siRNA-mediated knockdown of nNOS in the BLA disrupts cued fear consolidation.** A) Immunofluorescence images and Western blot results show successful localization and knockdown of nNOS in the BLA (\* $p < 0.05$ ). B) Rats that were exposed to tone-shock pairs show normal acquisition, with freezing increasing up to  $91.3 \pm 14.3\%$  by the end of acquisition testing (Trial:  $F_{2,50} = 44.98$ ,  $p < 0.0001$ ). After 24h, during consolidation testing, nNOS knockdown animals show consistently and significantly lower freezing ( $45.1 \pm 29.1\%$ , averaged) compared to viral control rats ( $84.9 \pm 16.7\%$ , averaged) and tone only control rats ( $2.6 \pm 3.4\%$ , averaged) (Treatment:  $F_{3,24} = 30.37$ ,  $p < 0.0001$ ). C) No significant differences were found between control and nNOS knockdown animals in locomotion, anxiety-like behaviors, and social interaction (as tested using the open field test, elevated plus maze, and social interaction test, respectively). D) In the Y-maze test, the number and duration of novel arm visits were

significantly greater in control and nNOS knockdown rats. \* $p < 0.05$ ; \*\* $p < 0.01$ ; \*\*\*\* $p < 0.0001$ .

Viral siRNA-mediated knockdown of nNOS in the BLA alters synaptosomal expression and phosphorylation of GluR1 and NR2B

We subsequently tested whether the knockdown of the nNOS gene in the BLA disrupted synaptosomal protein expression patterns in a similar manner to the ZL006 treatment. After testing for cued fear consolidation, we probed for GluR1, NR2B, and the phosphorylation sites of interest (Ser831 and Ser845 on GluR1 and Tyr1472, Ser1480, and Ser1303 on NR2B) within the BLA. Analogous to t24 (24 hours after fear conditioning) in our ZL006-treatment study, we found that the total expression of synaptosomal NR2B is significantly decreased in the BLA of the nNOS knockdown group, compared to that of the control group (Figure 19B). There were no changes in synaptosomal GluR1 expression in the BLA of nNOS knockdown animals, which is in agreement with our observations of ZL006-treated groups at t24 (Figure 19A). We detected similar trends in the expression levels of all but one synaptosomal phosphorylated subunits. Compared with phosphorylation levels in the control group, in the nNOS knockdown group, phosphorylation levels of Ser831 and Ser845 on GluR1 and Tyr1472 and Ser1303 on NR2B decreased significantly at t24 (Figure 19C-F). However, expression levels of Ser1480 on NR2B were not significantly different between the two groups (Figure 19G). Overall, our findings show that nNOS activity plays a major role in regulating downstream signaling pathways that impact synaptic AMPAR and NMDAR functions and expressions in the BLA and that nNOS plays a unique role in the consolidation of cue-induced fear without affecting motor or other memory functions.



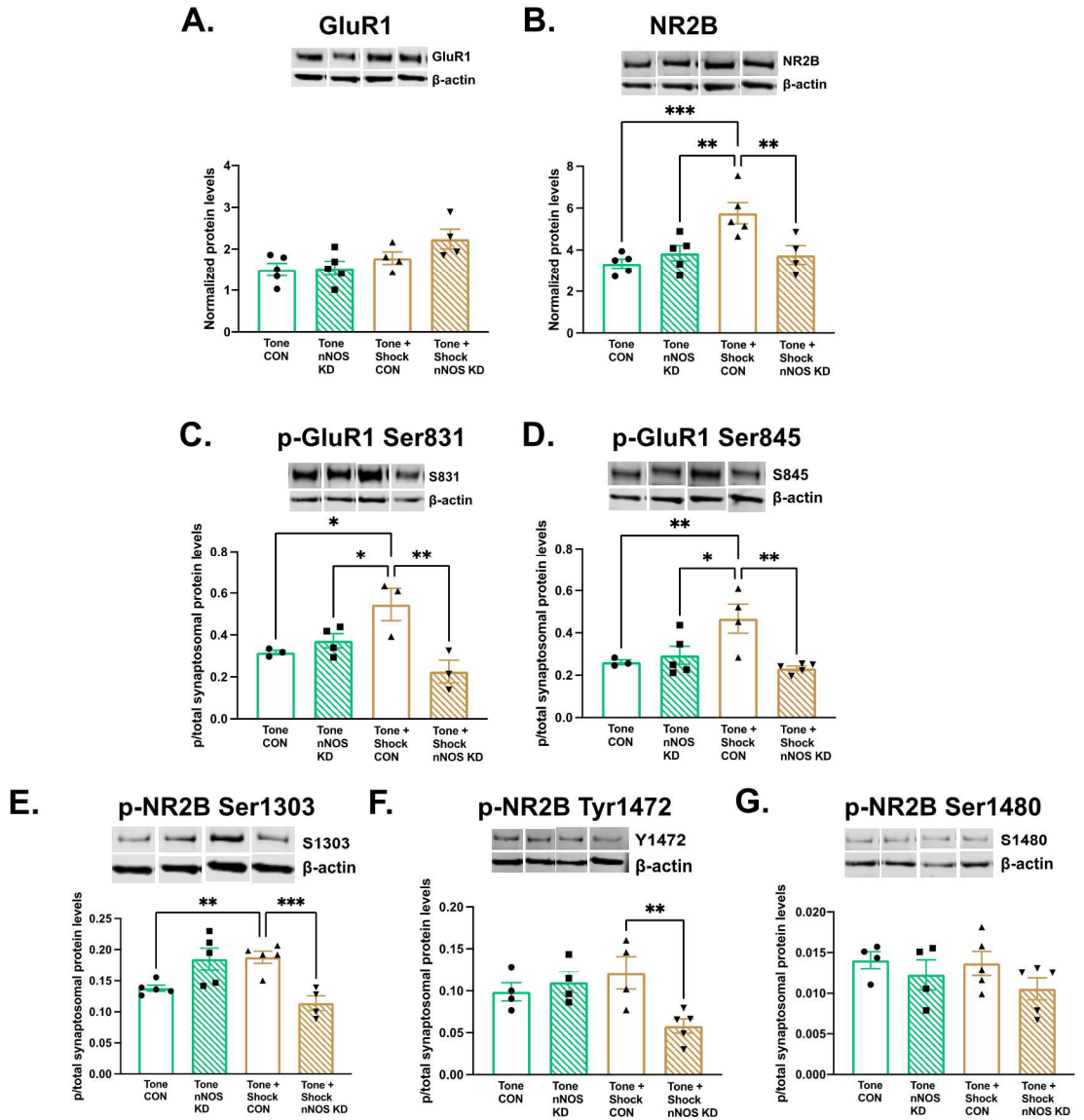


**Figure 19. Alterations in phosphorylation of key sites on the synaptosomal GluR1 and NR2B subunits 24h after fear acquisition in nNOS knockdown animals.** A) Expression levels of synaptosomal GluR1 in the BLA of rats 24h after fear acquisition. B) Expression levels of synaptosomal NR2B in the BLA of rats 24h after fear acquisition ( $p = 0.002$ ). C) Expression levels of phosphorylated Ser831 on synaptosomal GluR1 in the BLA of rats 24h after fear acquisition ( $p = 0.009$ ). D) Expression levels of phosphorylated Ser845 on synaptosomal GluR1 in the BLA of rats 24h after fear acquisition ( $p = 0.008$ ). E) Expression levels of phosphorylated Ser1303 on synaptosomal NR2B in the BLA of rats 24h after fear acquisition ( $p = 0.001$ ). F) Expression levels of phosphorylated Tyr1472 on synaptosomal NR2B in the BLA of rats 24h after fear acquisition ( $p = 0.02$ ). G) Expression levels of phosphorylated Ser1480 on synaptosomal NR2B in the BLA of rats 24h after fear acquisition. \* $p < 0.05$ ; \*\* $p < 0.01$ ; \*\*\* $p < 0.001$ .

#### 4.4 Discussion

After determining in chapter 3 that systemic delivery of ZL006 attenuated cued fear consolidation in a rat model and uniquely altered glutamatergic neurotransmission within the BLA in a time-dependent manner in chapter 3, we next determined whether a BLA-specific genetic knockdown of nNOS would have similar outcomes. To do this, we injected the BLA of rats with either AAV5-nNOS-siRNA-CMV-GFP or scrambled control constructs.

We found significantly reduced expression of nNOS protein in the BLA of rats with AAV-mediated nNOS knockdown. Additionally, we showed that rats with nNOS knocked down had diminished consolidation of cued fear memory and no deficits in motor function, social and anxiety-like behaviors, spatial memory, and fear acquisition (Figure 18). Similar to what we found in the BLA from ZL006-treated animals at t24 in chapter 3, the BLA from rats with nNOS knocked down displayed decreased levels of total NR2B, p-Ser831, p-Ser845, p-Ser1303, and p-Tyr1472. However, we saw no differences in p-Ser1480 levels (Figure 19).

Interestingly, it has been reported that the phosphorylation of Ser1480 by CaMKII-activated CK2 on NR2B localizes it to the extrasynaptic membrane, where it may be endocytosed<sup>91-93</sup>. In contrast with our results in chapter 3, we found that Ser1480 phosphorylation remained unchanged in scrambled control and nNOS knockdown animals. These differences could be due to virus-specific compensatory mechanisms or other regulatory mechanisms that modulate Ser1480 phosphorylation in a complex, unknown manner. However, since rats with nNOS knocked down were behaviorally

similar to the ZL006-treated rats, we conclude that Ser1480 phosphorylation does not directly impact the reductions of fear consolidation in the genetic knockdown model.

Several recent studies have shown that disrupted fear learning is a common phenotypic effect of knocking down or knocking out nNOS<sup>160,231,320</sup>. Our findings in this chapter revealed that knockdown of nNOS in the BLA impaired cued fear consolidation, which validates existing studies and provides novel data on the importance of nNOS activity specifically in the BLA for auditory fear consolidation. We are the first to report that an nNOS knockdown in the BLA alters the expression levels and phosphorylation states of synaptosomal GluR1 and NR2B in fear-conditioned animals, indicating that nNOS is involved in the regulation of glutamatergic receptor trafficking and phosphorylation states. Overall, the experiments in this chapter utilized the silencing of *nNos* in the BLA via an AAV-mediated knockdown to substantiate the importance of nNOS-mediated signaling in the BLA for auditory fear consolidation.

The silencing of genes, termed RNA interference (RNAi), has been a successful tool to study molecular and cellular mechanisms downstream of a single gene of interest<sup>321</sup>. More recently, the appeal of RNAi drugs in clinical settings has been reignited. Three RNAi drugs have been approved in the European Union and the United States in the last three years, and seven other RNAi drugs are in Phase 3 clinical trials<sup>322</sup>. RNAi therapeutics offer a way to target and utilize endogenous machinery to silence pathogenic genes and can be further localized to specific organs or cell types. Thus far, RNAi drugs have been developed to target rare genetic conditions<sup>322</sup>. However, studies using RNAi of nNOS have reported neuroprotective effects in Parkinson's disease and astrocytic brain tumors in pre-clinical models<sup>323,324</sup>. Adding to our findings in this

chapter, targeting nNOS via RNAi holds therapeutic potential that should be explored in future studies.

In summary, our experiments in the nNOS knockdown model recapitulated the behavioral and molecular phenotypes we observed in the ZL006-treated animals 24h after fear conditioning (chapter 3). Thus, we conclude that BLA-specific nNOS signaling plays an important role in auditory fear consolidation, likely via the regulation of glutamatergic receptors expression and phosphorylation levels.

## CHAPTER 5

### Conclusion

#### 5.1 General Summary

The research in this dissertation investigated multiple molecular mechanisms underlying the NMDAR-PSD95-nNOS axis in the BLA and its role in auditory fear consolidation in a rodent model.

The NMDAR-PSD95-nNOS axis mediates transcriptional regulation in the BLA during fear consolidation

First, we utilized a whole transcriptomic approach to study the BLA 24 hours after fear conditioning. We chose this timepoint based on previous studies of fear consolidation. In Pavlovian fear behavioral models, 24 hours after fear conditioning, animals expressing fear in response to the CS are considered to have consolidated the long-term fear memory. This timepoint also allowed us to behaviorally confirm that disrupting the NMDAR-PSD95-nNOS axis impaired fear consolidation before we evaluated transcriptomic changes in the BLA.

In chapter 2, we showed that the BLA transcriptome was altered during fear consolidation. Additionally, we showed that pathways downstream of the NMDAR-PSD95-nNOS axis were especially enriched. Due to these findings, we decided to do a similar study treating animals with ZL006, a small molecule inhibitor of PSD95-nNOS interaction, to determine how disrupting the NMDAR-PSD95-nNOS axis modifies gene and pathway enrichment in the BLA during fear consolidation. In doing so, we observed that ZL006 treatment restored gene expression to control-like levels. Thus, we revealed

that the NMDAR-PSD95-nNOS axis is involved in transcriptional regulation in the BLA during fear consolidation.

There are at least two reported time periods when transcription occurs in memory consolidation: one immediately after a learning event and another that begins 3-6 hours after a learning event and lasts for more than 24 hours but less than 48 hours after the event<sup>13,205</sup>. As our laboratory has shown, the PSD95-nNOS interaction peaks 1-2 hours after fear conditioning, an effect which ZL006 prevents<sup>162</sup>. Putting this in the context of chapter 2, the PSD95-nNOS interaction may regulate at least the second transcription event that occurs after initial learning. This hypothesis is further supported by recent studies that showed that nNOS interacts with and regulates the activity of transcription factors such as HIF-1 $\alpha$ , NF $\kappa$ B, SOX2, and PGC-1 $\alpha$ <sup>268,325-327</sup>.

We also discovered key genes and pathways altered in the BLA during fear consolidation with and without treatment of ZL006 and revealed that IGF2 and IGFBP2 signaling might be a crucial mechanism downstream of nNOS activation. Over the last 10 years, multiple studies have investigated the roles of IGF2 and IGFBP2 in memory consolidation, indicating a new and exciting mechanism that should continue to be explored. In summary, IGF2 enhances fear memory consolidation, promotes neurogenesis, and is increased in response to fear extinction, indicating the importance of IGF2 signaling in memory formation and stabilization<sup>258,328,329</sup>. Similarly, IGFBP2 plays a role in neurodegeneration, spatial learning, mature dendritic spine formation, and early-life hippocampal LTP<sup>259,330,331</sup>. IGFBP2 is also reduced in models of depressive-like behavior and has therapeutic effects in animal models of PTSD<sup>259,332</sup>. Taken together,

these results show that IGF2/IGFBP2 signaling may be a translationally significant pathway to study further.

In summary, we determined that a unique transcriptomic profile of the BLA during fear consolidation was altered with disruption of the NMDAR-PSD95-nNOS axis. Therefore, we established that the NMDAR-PSD95-nNOS axis plays an important role in fear consolidation via transcriptional regulation of the BLA.

The NMDAR-PSD95-nNOS axis regulates time-dependent AMPAR and NMDAR expression, phosphorylation, and conductance in the BLA during fear consolidation

Next, we sought to understand the effects of disrupting the NMDAR-PSD95-nNOS axis on neurotransmission within the BLA. As our laboratory has shown previously, ZL006 impairs LTP in BLA neurons. Another study utilizing intra-amygdalar infusion of an NOS inhibitor, 7-nitroindazole, and a PKG inhibitor, Rp-8-Br-PET-cGMPS, showed that these inhibitors blocked fear conditioning-induced increases in amygdalar GluR1 levels<sup>223</sup>. In the fear circuit, NMDAR activity plays an important role in neurotransmission, and NMDAR-mediated AMPAR trafficking in the BLA can further modulate activity-dependent synaptic potentiation<sup>310,333</sup>. Therefore, we explored AMPAR and NMDAR conductance and surface expression in the BLA after fear conditioning. In doing so, we discovered that AMPARs and NMDARs in the BLA worked in concert over time after an initial fear learning event to ensure sufficient consolidation of the memory.

Two recent studies in PSD95-deficient mice showed that AMPAR/NMDAR current ratios were decreased in the mPFC and hippocampus, accompanied by correlating changes in subunit expression (reduced GluR1 levels and increased NR2B levels)<sup>334,335</sup>. These studies suggest that PSD95 and its downstream signaling may be important for

regulating AMPAR- and NMDAR-mediated currents and subunit expression. Moreover, multiple studies have reported that NO signaling upregulated the trafficking of AMPARs to the surface membrane, specifically of the GluR1 subunit<sup>188,189,336,337</sup>. Furthermore, a study on NO regulation of NMDAR activity showed that NO had no effects on synaptic NMDAR-mediated current or expression, although this study, similar to the others mentioned above, was performed in tissue slices and did not include an experience-dependent factor<sup>338</sup>. Our study showed that disrupting the PSD95-nNOS interaction can have similar inhibitory effects on both AMPAR-mediated current and synaptosomal GluR1 expression; however, our findings of reduced NMDAR-mediated current and expression levels contradict the literature. This contradiction is likely due to differences in rodent models, behavioral phenotypes, and the time- and experience-dependent changes we focused on. Thus, our work in chapter 3 is novel and concludes that AMPAR- and NMDAR-mediated currents and synaptosomal expression levels are altered over time after fear conditioning and that the PSD95-nNOS interaction plays an important role in regulating these changes.

Genetic knockdown of the *nNos* gene in the BLA sufficiently blocks auditory fear consolidation and alters GluR1 and NR2B synaptosomal expression and phosphorylation levels in the BLA

The above studies utilized ZL006 as a small molecule inhibitor of the PSD95-nNOS interaction to study the downstream effects of the PSD95-nNOS interaction in fear consolidation. Pharmacological agents that are effective against consolidation of fear, such as ZL006, are useful tools to functionally analyze the effects of inhibiting a protein, or in this case, a protein-protein interaction and to further analyze the druggability of a



therapeutic target. However, systemic administration of a drug can have off-target phenotypic effects, form pharmacological intermediates that affect experimental results, and alter or inhibit another protein or pathway. Additionally, while ZL006 blocks the PSD95-nNOS interaction, nNOS may still bind other proteins and form macromolecular complexes.

Generally, using multiple approaches to answer the same questions is ideal for experimental rigor. As such, we decided to utilize a BLA-specific knockdown of the *nNos* gene to validate the behavioral and molecular phenotypes we observed in chapter 3. To do this, we used an AAV-siRNA-mediated knockdown, which degrades the *nNos* mRNA and leads to decreased nNOS protein levels. Knocking down nNOS in the BLA resulted in impaired auditory fear consolidation and reduced NR2B synaptosomal expression, corroborating the results in chapter 3.

Multiple studies in nNOS-deficient models have displayed impairments in both contextual and cued fear learning. The Song laboratory demonstrated deficits in social interaction and anxiety-like behaviors, as well as reduced synaptosomal NR2B levels (but no changes in GluR1 levels) in a study involving an intra-BLA knockdown of nNOS in mice<sup>160,231,339</sup>. While our results in chapter 4 substantiated the fear behavioral phenotype and changes in synaptosomal GluR1 and NR2B levels, we discovered no effects on social or anxiety-like behaviors. Two key differences that may have led to these discrepancies are that we studied rats instead of mice and used different testing paradigms for assessing social and anxiety-like behaviors.

It is also interesting to note that while we used the BLA from fear-conditioned rats in our biochemical investigation of GluR1 and NR2B levels, the Song group utilized

fluorescence-activated cell sorting and thus only studied nNOS-negative interneurons from the BLA of behaviorally naïve mice. However, both protocols yielded similar results. Therefore, it may be valuable to use the model we established in chapter 4 to fluorescently sort and study nNOS-negative neurons in the BLA, as pooling all BLA neurons regardless of whether nNOS expression has been successfully knocked down could dilute the output of our biochemical assays.

## **5.2 Significance**

The work in this thesis provides the novel finding that disrupting the NMDAR-PSD95-nNOS axis, both pharmacologically and genetically, alters the BLA transcriptome and glutamatergic neurotransmission, in addition to specifically mitigating fear memory consolidation.

We chose to study the presented fear conditioning model to study the molecular effects of a traumatic event on associative fear learning in the BLA. The more PTSD is studied as a neuropsychiatric illness, the greater the variety of causes, risk factors, and identified symptoms. Once popularly known as a mental illness affecting soldiers, it is now redefined as something that can affect anyone and can be caused by a single traumatic incident.

While traumatic events are not preventable, studies show that treating patients immediately after trauma with a  $\beta$ -adrenergic receptor antagonist reduces their likelihood of developing PTSD<sup>340</sup>. However, if the antagonist was given anytime up to 48 hours after trauma, there were no effects, providing clinical evidence for a time frame after trauma when drug administration can successfully prevent PTSD<sup>341</sup>. On the other hand, patients with PTSD that are well-beyond this narrow time frame still benefit from

treatments paired with cognitive behavioral therapy or exposure therapy<sup>342</sup>. Applying this to my research, it is clear that fear memory consolidation requires temporally-regulated molecular mechanisms. Studying the effects of these events on focal neural circuits and molecular pathways, as I have done here, may help us to understand how and when to best treat patients who are high-risk for developing PTSD. It also brings us a step closer to developing therapeutics that treat very specific symptoms of PTSD with minimum side-effects. Additionally, these treatments could be paired with behavioral therapy to have better outcomes in patients with protracted or delayed PTSD symptoms and diagnoses.

### **5.3 Limitations & Future Directions**

An important limitation of the work presented in this thesis is that it was done in male rats. Studies in nNOS knockout females showed impairments in short-term and long-term memory after fear conditioning, similar to male counterparts<sup>160</sup>. However, corticosterone levels returned to pre-fear conditioning levels much quicker in females than males, and overall synaptic plasticity differed between nNOS knockout male and female mice<sup>160,343</sup>. Thus, while there were no sex-specific differences in behavior, there may be sex-specific differences in the nNOS-dependent molecular mechanisms we studied in this thesis. Therefore, it is vital to include females in future studies, especially considering the differences in PTSD symptomology and pathophysiology between males and females<sup>344,345</sup>.

Another limitation is that the studies using ZL006 and nNOS knockdown in this thesis assumed that both methods reduced NO synthesis in target regions, although it was not tested in these animals. Previous studies using ZL006 have determined that ZL006

administration does reduce NO levels<sup>149,150</sup>. However, it would be ideal to confirm this in our models using an NO detection assay. This experiment would also help to determine whether NO from eNOS or iNOS might be compensating for NO levels in our models.

The RNA-sequencing study in chapter 2 provided numerous opportunities for future studies. Primarily, IGF2/IGFBP2 signaling seems to be, as described in detail in chapter 2, a significant pathway in fear learning that is gaining traction in the field and could be a potential therapeutic target downstream of nNOS signaling. Since our results showed elevated IGF2 and IGFBP2 levels in the BLA with systemic ZL006 treatment, it would be interesting, for example, to overexpress IGF2 and/or IGFBP2 only in BLA neurons and investigate the effects on fear consolidation and downstream molecular mechanisms.

Additionally, finding novel pathways and gene targets using RNA-sequencing and inhibition of nNOS signaling provides value for using similar methods to begin to parse out, in more detail, the transcriptional regulation that underlies fear consolidation. In the amygdala, histone deacetylase and DNA methyltransferase, both of which mediate epigenetic mechanisms via histone deacetylation and DNA methylation, respectively, regulate cued fear memory consolidation<sup>346</sup>. Furthermore, modulating chromatin remodeling in the amygdala can alter fear memory formation<sup>347</sup>. In the BLA specifically, inhibiting histone deacetylase enhances memory consolidation<sup>348</sup>. Overall, there is evidence to indicate that epigenetic mechanisms play a role in memory consolidation. However, there is a need to understand how the epigenome in the BLA is altered in response to fear conditioning. Thus, future studies in our model should utilize tools to analyze the epigenome of the BLA.

Similarly, single-cell RNA-sequencing is another tool that would provide a comprehensive study of the BLA transcriptome that moves a step beyond what we presented in chapter 2. The cell population in the BLA is heterogeneous, and as such, RNA-sequencing provides a snapshot of gene expression levels in the BLA. With single-cell RNA-sequencing, we would be able to define cell-type specific gene expression levels, as well as define splicing patterns and gene co-expression networks on the single-cell level. This could be paired with, for example, the nNOS knockdown model in chapter 4, to sort and analyze the single-cell transcriptome of nNOS-positive neurons. A study like this would also offer cell-type specific information about some of the gene targets from chapter 2, like IGF2 and IGF2BP2. In summary, future studies in our model could utilize epigenomic and single-cell RNA-sequencing analyses to determine more detailed, single-cell level information that could be used to define new targets and regulatory mechanisms underlying nNOS-mediated cued fear consolidation.

In chapter 3, we found that the NMDAR-PSD95-nNOS axis altered neurotransmission in an experience- and time-dependent manner. This alteration could be via cGMP signaling effects, S-nitrosylation, NO retrograde signaling, or a combination of all three. These are the primary downstream effects of NO production; however, it is not clear whether these pathways compete or work in concert to result in the changes we observed in chapter 3. Therefore, it would be worthwhile to do a series of studies where each pathway is studied separately. For example, to isolate cGMP-mediated effects, one could use an nNOS knockdown model, exogenously apply cGMP, and study its effects. Similarly, an informative method to study S-nitrosylation would be a mass spectrometry-based analysis of S-nitrosylation sites; on a smaller scale, biotin switch assays can be

used to study S-nitrosylation of specific proteins. Last, numerous studies have shown that NO scavengers disrupt fear conditioning and LTP<sup>172,349,350</sup>. Thus, future studies in our model could use NO scavengers to answer various questions related to the impact of retrograde NO signaling.

Finally, the nNOS knockdown model in chapter 4 successfully recapitulated the behavioral phenotype observed with ZL006-treatment, and as such, it can be used to study a wide variety of mechanisms downstream of nNOS activity. A simple yet helpful experiment using our nNOS knockdown model would be to investigate the effects of fear conditioning on LTP and AMPAR and NMDAR conductance in nNOS-negative BLA neurons. This experiment would help validate the results in chapter 3 and further justify using this model to continue studying nNOS-specific effects on fear consolidation. It would also help characterize the electrophysiological properties of nNOS-negative BLA neurons.

#### **5.4 Final Remarks**

This dissertation provides novel evidence to support the importance of the NMDAR-PSD95-nNOS axis in the BLA for fear consolidation. We established that the pharmacological and genetic manipulation of the NMDAR-PSD95-nNOS axis resulted in fear consolidation impairments, transcriptional alterations in the BLA, and time-dependent changes in glutamatergic neurotransmission in the BLA. It is my hope that this research will contribute to the development of more effective therapeutics and ultimately the provision of better care and treatment for patients with fear disorders.

## REFERENCES

- 1 Abdul-Hamid, W. K. & Hughes, J. H. Nothing new under the sun: post-traumatic stress disorders in the ancient world. *Early Sci Med* **19**, 549-557, doi:10.1163/15733823-00196p02 (2014).
- 2 Association, A. P. *Diagnostic and statistical manual of mental disorders (5th ed.)*. (American Psychiatric Publishing, 2013).
- 3 Parsons, R. G. & Ressler, K. J. Implications of memory modulation for post-traumatic stress and fear disorders. *Nat Neurosci* **16**, 146-153, doi:10.1038/nn.3296 (2013).
- 4 Maren, S. Neurobiology of Pavlovian fear conditioning. *Annu Rev Neurosci* **24**, 897-931, doi:10.1146/annurev.neuro.24.1.897 (2001).
- 5 Blanchard, D. C. & Blanchard, R. J. Innate and conditioned reactions to threat in rats with amygdaloid lesions. *J Comp Physiol Psychol* **81**, 281-290, doi:10.1037/h0033521 (1972).
- 6 Clugnet, M. C. & LeDoux, J. E. Synaptic plasticity in fear conditioning circuits: induction of LTP in the lateral nucleus of the amygdala by stimulation of the medial geniculate body. *The Journal of Neuroscience* **10**, 2818-2824, doi:10.1523/jneurosci.10-08-02818.1990 (1990).
- 7 Maren, S. & Fanselow, M. S. Synaptic plasticity in the basolateral amygdala induced by hippocampal formation stimulation in vivo. *The Journal of Neuroscience* **15**, 7548-7564, doi:10.1523/jneurosci.15-11-07548.1995 (1995).
- 8 McGaugh, J. L. Memory--a century of consolidation. *Science* **287**, 248-251, doi:10.1126/science.287.5451.248 (2000).
- 9 Goddard, G. V. Amygdaloid Stimulation and Learning in the Rat. *J Comp Physiol Psychol* **58**, 23-30, doi:10.1037/h0049256 (1964).
- 10 LeDoux, J. E. Emotion circuits in the brain. *Annu Rev Neurosci* **23**, 155-184, doi:10.1146/annurev.neuro.23.1.155 (2000).
- 11 Gold, P. E., Zornetzer, S. F. & McGaugh, J. L. Electrical stimulation of the brain: effects on memory storage. *Adv Psychobiol* **2**, 193-224 (1974).
- 12 Bourchouladze, R. *et al.* Different training procedures recruit either one or two critical periods for contextual memory consolidation, each of which requires protein synthesis and PKA. *Learn Mem* **5**, 365-374 (1998).
- 13 Igaz, L. M., Vianna, M. R. M., Medina, J. H. & Izquierdo, I. Two Time Periods of Hippocampal mRNA Synthesis Are Required for Memory Consolidation of Fear-Motivated Learning. *The Journal of Neuroscience* **22**, 6781-6789, doi:10.1523/jneurosci.22-15-06781.2002 (2002).
- 14 Rogan, M. T. & LeDoux, J. E. LTP is accompanied by commensurate enhancement of auditory-evoked responses in a fear conditioning circuit. *Neuron* **15**, 127-136, doi:10.1016/0896-6273(95)90070-5 (1995).
- 15 Schroeder, B. W. & Shinnick-Gallagher, P. Fear learning induces persistent facilitation of amygdala synaptic transmission. *Eur J Neurosci* **22**, 1775-1783, doi:10.1111/j.1460-9568.2005.04343.x (2005).
- 16 Overeem, K. A., Ota, K. T., Monsey, M. S., Ploski, J. E. & Schafe, G. E. A role for nitric oxide-driven retrograde signaling in the consolidation of a fear memory. *Front Behav Neurosci* **4**, 2, doi:10.3389/neuro.08.002.2010 (2010).

- 17 Davis, M. in *Neurobiology of Learning and Memory* 381-425 (2007).
- 18 Schafe, G. E., Nader, K., Blair, H. T. & LeDoux, J. E. Memory consolidation of Pavlovian fear conditioning: a cellular and molecular perspective. *Trends in Neurosciences* **24**, 540-546, doi:10.1016/s0166-2236(00)01969-x (2001).
- 19 Sigurdsson, T., Doyere, V., Cain, C. K. & LeDoux, J. E. Long-term potentiation in the amygdala: a cellular mechanism of fear learning and memory. *Neuropharmacology* **52**, 215-227, doi:10.1016/j.neuropharm.2006.06.022 (2007).
- 20 Debiec, J., Diaz-Mataix, L., Bush, D. E., Doyere, V. & Ledoux, J. E. The amygdala encodes specific sensory features of an aversive reinforcer. *Nat Neurosci* **13**, 536-537, doi:10.1038/nn.2520 (2010).
- 21 Shekhar, A., Truitt, W., Rainnie, D. & Sajdyk, T. Role of stress, corticotrophin releasing factor (CRF) and amygdala plasticity in chronic anxiety. *Stress* **8**, 209-219, doi:10.1080/10253890500504557 (2005).
- 22 Johansen, J. P. *et al.* Optical activation of lateral amygdala pyramidal cells instructs associative fear learning. *Proc Natl Acad Sci U S A* **107**, 12692-12697, doi:10.1073/pnas.1002418107 (2010).
- 23 Morris, J. S., Ohman, A. & Dolan, R. J. Conscious and unconscious emotional learning in the human amygdala. *Nature* **393**, 467-470, doi:10.1038/30976 (1998).
- 24 Vargas, J. P., López, J. C. & Portavella, M. in *The Amygdala - A Discrete Multitasking Manager* (2012).
- 25 Janak, P. H. & Tye, K. M. From circuits to behaviour in the amygdala. *Nature* **517**, 284-292, doi:10.1038/nature14188 (2015).
- 26 Zhang, W.-H., Zhang, J.-Y., Holmes, A. & Pan, B.-X. Amygdala circuit substrates for stress adaptation and adversity. *Biological Psychiatry*, doi:10.1016/j.biopsych.2020.12.026 (2021).
- 27 Duvarci, S. & Pare, D. Amygdala microcircuits controlling learned fear. *Neuron* **82**, 966-980, doi:10.1016/j.neuron.2014.04.042 (2014).
- 28 Spampanato, J., Polepalli, J. & Sah, P. Interneurons in the basolateral amygdala. *Neuropharmacology* **60**, 765-773, doi:10.1016/j.neuropharm.2010.11.006 (2011).
- 29 Romanski, L. M. & LeDoux, J. E. Equipotentiality of thalamo-amygdala and thalamo-cortico-amygdala circuits in auditory fear conditioning. *The Journal of Neuroscience* **12**, 4501-4509, doi:10.1523/jneurosci.12-11-04501.1992 (1992).
- 30 Fendt, M. & Fanselow, M. S. The neuroanatomical and neurochemical basis of conditioned fear. *Neuroscience & Biobehavioral Reviews* **23**, 743-760, doi:10.1016/s0149-7634(99)00016-0 (1999).
- 31 Fanselow, M. S. Conditioned and unconditional components of post-shock freezing. *Pavlov J Biol Sci* **15**, 177-182, doi:10.1007/BF03001163 (1980).
- 32 Hitchcock, J. & Davis, M. Lesions of the amygdala, but not of the cerebellum or red nucleus, block conditioned fear as measured with the potentiated startle paradigm. *Behav Neurosci* **100**, 11-22, doi:10.1037//0735-7044.100.1.11 (1986).
- 33 Royer, S., Martina, M. & Paré, D. An Inhibitory Interface Gates Impulse Traffic between the Input and Output Stations of the Amygdala. *The Journal of Neuroscience* **19**, 10575-10583, doi:10.1523/jneurosci.19-23-10575.1999 (1999).
- 34 Busti, D. *et al.* Different fear states engage distinct networks within the intercalated cell clusters of the amygdala. *J Neurosci* **31**, 5131-5144, doi:10.1523/JNEUROSCI.6100-10.2011 (2011).



- 35 Rogan, M. T., Stäubli, U. V. & LeDoux, J. E. AMPA Receptor Facilitation Accelerates Fear Learning without Altering the Level of Conditioned Fear Acquired. *The Journal of Neuroscience* **17**, 5928-5935, doi:10.1523/jneurosci.17-15-05928.1997 (1997).
- 36 Barot, S. K., Kyono, Y., Clark, E. W. & Bernstein, I. L. Visualizing stimulus convergence in amygdala neurons during associative learning. *Proc Natl Acad Sci U S A* **105**, 20959-20963, doi:10.1073/pnas.0808996106 (2008).
- 37 Kim, J. J. & Jung, M. W. Neural circuits and mechanisms involved in Pavlovian fear conditioning: a critical review. *Neurosci Biobehav Rev* **30**, 188-202, doi:10.1016/j.neubiorev.2005.06.005 (2006).
- 38 Anglada-Figueroa, D. & Quirk, G. J. Lesions of the basal amygdala block expression of conditioned fear but not extinction. *J Neurosci* **25**, 9680-9685, doi:10.1523/JNEUROSCI.2600-05.2005 (2005).
- 39 Vazdarjanova, A. & McGaugh, J. L. Basolateral Amygdala Is Involved in Modulating Consolidation of Memory for Classical Fear Conditioning. *The Journal of Neuroscience* **19**, 6615-6622, doi:10.1523/jneurosci.19-15-06615.1999 (1999).
- 40 Amano, T., Duvarci, S., Popa, D. & Pare, D. The fear circuit revisited: contributions of the basal amygdala nuclei to conditioned fear. *J Neurosci* **31**, 15481-15489, doi:10.1523/JNEUROSCI.3410-11.2011 (2011).
- 41 Fanselow, M. S. & LeDoux, J. E. Why We Think Plasticity Underlying Pavlovian Fear Conditioning Occurs in the Basolateral Amygdala. *Neuron* **23**, 229-232, doi:10.1016/s0896-6273(00)80775-8 (1999).
- 42 LaBar, K. S., Gatenby, J. C., Gore, J. C., LeDoux, J. E. & Phelps, E. A. Human Amygdala Activation during Conditioned Fear Acquisition and Extinction: a Mixed-Trial fMRI Study. *Neuron* **20**, 937-945, doi:10.1016/s0896-6273(00)80475-4 (1998).
- 43 Rogan, M. T., Staubli, U. V. & LeDoux, J. E. Fear conditioning induces associative long-term potentiation in the amygdala. *Nature* **390**, 604-607, doi:10.1038/37601 (1997).
- 44 Schafe, G. E., Nadel, N. V., Sullivan, G. M., Harris, A. & LeDoux, J. E. Memory Consolidation for Contextual and Auditory Fear Conditioning Is Dependent on Protein Synthesis, PKA, and MAP Kinase. *Learn Mem* **6**, 97-110, doi:10.1101/lm.6.2.97 (1999).
- 45 Schafe, G. E. & LeDoux, J. E. Memory Consolidation of Auditory Pavlovian Fear Conditioning Requires Protein Synthesis and Protein Kinase A in the Amygdala. *The Journal of Neuroscience* **20**, RC96-RC96, doi:10.1523/JNEUROSCI.20-18-j0003.2000 (2000).
- 46 Duvarci, S., Nader, K. & LeDoux, J. E. De novo mRNA synthesis is required for both consolidation and reconsolidation of fear memories in the amygdala. *Learn Mem* **15**, 747-755, doi:10.1101/lm.1027208 (2008).
- 47 Ueda, T. in *Excitatory Amino Acids* Ch. Chapter 12, 173-195 (1986).
- 48 Pape, H. C. & Pare, D. Plastic synaptic networks of the amygdala for the acquisition, expression, and extinction of conditioned fear. *Physiol Rev* **90**, 419-463, doi:10.1152/physrev.00037.2009 (2010).

- 49 Mahanty, N. K. & Sah, P. Excitatory synaptic inputs to pyramidal neurons of the lateral amygdala. *Eur J Neurosci* **11**, 1217-1222, doi:10.1046/j.1460-9568.1999.00528.x (1999).
- 50 Takagi, H. Roles of ion channels in EPSP integration at neuronal dendrites. *Neuroscience Research* **37**, 167-171, doi:10.1016/s0168-0102(00)00120-6 (2000).
- 51 Meldrum, B. S. Glutamate as a neurotransmitter in the brain: review of physiology and pathology. *J Nutr* **130**, 1007S-1015S, doi:10.1093/jn/130.4.1007S (2000).
- 52 Miserendino, M. J., Sananes, C. B., Melia, K. R. & Davis, M. Blocking of acquisition but not expression of conditioned fear-potentiated startle by NMDA antagonists in the amygdala. *Nature* **345**, 716-718, doi:10.1038/345716a0 (1990).
- 53 Goosens, K. A. & Maren, S. NMDA receptors are essential for the acquisition, but not expression, of conditional fear and associative spike firing in the lateral amygdala. *Eur J Neurosci* **20**, 537-548, doi:10.1111/j.1460-9568.2004.03513.x (2004).
- 54 Rousseaux, C. G. A Review of Glutamate Receptors I: Current Understanding of Their Biology. *Journal of Toxicologic Pathology* **21**, 25-51, doi:10.1293/tox.21.25 (2008).
- 55 Laube, B., Kuhse, J. & Betz, H. Evidence for a Tetrameric Structure of Recombinant NMDA Receptors. *The Journal of Neuroscience* **18**, 2954-2961, doi:10.1523/jneurosci.18-08-02954.1998 (1998).
- 56 Gan, Q., Salussolia, C. L. & Wollmuth, L. P. Assembly of AMPA receptors: mechanisms and regulation. *J Physiol* **593**, 39-48, doi:10.1113/jphysiol.2014.273755 (2015).
- 57 Forsythe, I. D. & Westbrook, G. L. Slow excitatory postsynaptic currents mediated by N-methyl-D-aspartate receptors on cultured mouse central neurones. *J Physiol* **396**, 515-533, doi:10.1113/jphysiol.1988.sp016975 (1988).
- 58 Bekkers, J. M. & Stevens, C. F. NMDA and non-NMDA receptors are co-localized at individual excitatory synapses in cultured rat hippocampus. *Nature* **341**, 230-233, doi:10.1038/341230a0 (1989).
- 59 Stern, P., Behe, P., Schoepfer, R. & Colquhoun, D. Single-channel conductances of NMDA receptors expressed from cloned cDNAs: comparison with native receptors. *Proc Biol Sci* **250**, 271-277, doi:10.1098/rspb.1992.0159 (1992).
- 60 Rao, V. R. & Finkbeiner, S. NMDA and AMPA receptors: old channels, new tricks. *Trends Neurosci* **30**, 284-291, doi:10.1016/j.tins.2007.03.012 (2007).
- 61 Hubert, G. W., Li, C., Rainnie, D. G. & Muly, E. C. Effects of stress on AMPA receptor distribution and function in the basolateral amygdala. *Brain Struct Funct* **219**, 1169-1179, doi:10.1007/s00429-013-0557-z (2014).
- 62 Lee, H. & Kim, J. J. Amygdalar NMDA Receptors are Critical for New Fear Learning in Previously Fear-Conditioned Rats. *The Journal of Neuroscience* **18**, 8444-8454, doi:10.1523/jneurosci.18-20-08444.1998 (1998).
- 63 Delaney, A. J., Sedlak, P. L., Autuori, E., Power, J. M. & Sah, P. Synaptic NMDA receptors in basolateral amygdala principal neurons are triheteromeric proteins: physiological role of GluN2B subunits. *J Neurophysiol* **109**, 1391-1402, doi:10.1152/jn.00176.2012 (2013).

- 64 Nowak, L., Bregestovski, P., Ascher, P., Herbet, A. & Prochiantz, A. Magnesium gates glutamate-activated channels in mouse central neurones. *Nature* **307**, 462-465, doi:10.1038/307462a0 (1984).
- 65 Mayer, M. L., Westbrook, G. L. & Guthrie, P. B. Voltage-dependent block by Mg<sup>2+</sup> of NMDA responses in spinal cord neurones. *Nature* **309**, 261-263, doi:10.1038/309261a0 (1984).
- 66 Cooke, S. F. & Bliss, T. V. Plasticity in the human central nervous system. *Brain* **129**, 1659-1673, doi:10.1093/brain/awl082 (2006).
- 67 Arai, A. C., Xia, Y. F. & Suzuki, E. Modulation of AMPA receptor kinetics differentially influences synaptic plasticity in the hippocampus. *Neuroscience* **123**, 1011-1024, doi:10.1016/j.neuroscience.2003.10.033 (2004).
- 68 Bliss, T. V. & Collingridge, G. L. A synaptic model of memory: long-term potentiation in the hippocampus. *Nature* **361**, 31-39, doi:10.1038/361031a0 (1993).
- 69 Malenka, R. C., Kauer, J. A., Zucker, R. S. & Nicoll, R. A. Postsynaptic calcium is sufficient for potentiation of hippocampal synaptic transmission. *Science* **242**, 81-84, doi:10.1126/science.2845577 (1988).
- 70 Paoletti, P., Bellone, C. & Zhou, Q. NMDA receptor subunit diversity: impact on receptor properties, synaptic plasticity and disease. *Nat Rev Neurosci* **14**, 383-400, doi:10.1038/nrn3504 (2013).
- 71 Malenka, R. C. Synaptic plasticity in the hippocampus: LTP and LTD. *Cell* **78**, 535-538, doi:10.1016/0092-8674(94)90517-7 (1994).
- 72 Bashir, Z. I., Alford, S., Davies, S. N., Randall, A. D. & Collingridge, G. L. Long-term potentiation of NMDA receptor-mediated synaptic transmission in the hippocampus. *Nature* **349**, 156-158, doi:10.1038/349156a0 (1991).
- 73 Bauer, E. P. & LeDoux, J. E. Heterosynaptic long-term potentiation of inhibitory interneurons in the lateral amygdala. *J Neurosci* **24**, 9507-9512, doi:10.1523/JNEUROSCI.3567-04.2004 (2004).
- 74 Bauer, E. P., LeDoux, J. E. & Nader, K. Fear conditioning and LTP in the lateral amygdala are sensitive to the same stimulus contingencies. *Nat Neurosci* **4**, 687-688, doi:10.1038/89465 (2001).
- 75 Lee, H. J., Choi, J.-S., Brown, T. H. & Kim, J. J. Amygdalar NMDA Receptors Are Critical for the Expression of Multiple Conditioned Fear Responses. *The Journal of Neuroscience* **21**, 4116-4124, doi:10.1523/jneurosci.21-11-04116.2001 (2001).
- 76 Cull-Candy, S., Brickley, S. & Farrant, M. NMDA receptor subunits: diversity, development and disease. *Current Opinion in Neurobiology* **11**, 327-335, doi:10.1016/s0959-4388(00)00215-4 (2001).
- 77 Schuler, T., Mesic, I., Madry, C., Bartholomaeus, I. & Laube, B. Formation of NR1/NR2 and NR1/NR3 heterodimers constitutes the initial step in N-methyl-D-aspartate receptor assembly. *J Biol Chem* **283**, 37-46, doi:10.1074/jbc.M703539200 (2008).
- 78 Rauner, C. & Kohr, G. Triheteromeric NR1/NR2A/NR2B receptors constitute the major N-methyl-D-aspartate receptor population in adult hippocampal synapses. *J Biol Chem* **286**, 7558-7566, doi:10.1074/jbc.M110.182600 (2011).

- 79 Ulbrich, M. H. & Isacoff, E. Y. Subunit counting in membrane-bound proteins. *Nat Methods* **4**, 319-321, doi:10.1038/nmeth1024 (2007).
- 80 Furukawa, H., Singh, S. K., Mancusso, R. & Gouaux, E. Subunit arrangement and function in NMDA receptors. *Nature* **438**, 185-192, doi:10.1038/nature04089 (2005).
- 81 Ulbrich, M. H. & Isacoff, E. Y. Rules of engagement for NMDA receptor subunits. *Proc Natl Acad Sci U S A* **105**, 14163-14168, doi:10.1073/pnas.0802075105 (2008).
- 82 Valenzuela-Harrington, M., Gruart, A. & Delgado-Garcia, J. M. Contribution of NMDA receptor NR2B subunit to synaptic plasticity during associative learning in behaving rats. *Eur J Neurosci* **25**, 830-836, doi:10.1111/j.1460-9568.2007.05325.x (2007).
- 83 von Engelhardt, J. *et al.* Contribution of hippocampal and extra-hippocampal NR2B-containing NMDA receptors to performance on spatial learning tasks. *Neuron* **60**, 846-860, doi:10.1016/j.neuron.2008.09.039 (2008).
- 84 Kiyama, Y. *et al.* Increased Thresholds for Long-Term Potentiation and Contextual Learning in Mice Lacking the NMDA-type Glutamate Receptor  $\epsilon$ 1 Subunit. *The Journal of Neuroscience* **18**, 6704-6712, doi:10.1523/jneurosci.18-17-06704.1998 (1998).
- 85 Farinelli, M. *et al.* Selective regulation of NR2B by protein phosphatase-1 for the control of the NMDA receptor in neuroprotection. *PLoS One* **7**, e34047, doi:10.1371/journal.pone.0034047 (2012).
- 86 Rodrigues, S. M., Schafe, G. E. & LeDoux, J. E. Intra-Amygdala Blockade of the NR2B Subunit of the NMDA Receptor Disrupts the Acquisition But Not the Expression of Fear Conditioning. *The Journal of Neuroscience* **21**, 6889-6896, doi:10.1523/jneurosci.21-17-06889.2001 (2001).
- 87 Prabhu Ramya, R., Suma Priya, S., Mayadevi, M. & Omkumar, R. V. Regulation of phosphorylation at Ser(1303) of GluN2B receptor in the postsynaptic density. *Neurochem Int* **61**, 981-985, doi:10.1016/j.neuint.2012.08.016 (2012).
- 88 Omkumar, R. V., Kiely, M. J., Rosenstein, A. J., Min, K. T. & Kennedy, M. B. Identification of a phosphorylation site for calcium/calmodulindependent protein kinase II in the NR2B subunit of the N-methyl-D-aspartate receptor. *J Biol Chem* **271**, 31670-31678, doi:10.1074/jbc.271.49.31670 (1996).
- 89 Nakazawa, T. *et al.* Characterization of Fyn-mediated tyrosine phosphorylation sites on GluR epsilon 2 (NR2B) subunit of the N-methyl-D-aspartate receptor. *J Biol Chem* **276**, 693-699, doi:10.1074/jbc.M008085200 (2001).
- 90 Nakazawa, T. *et al.* NR2B tyrosine phosphorylation modulates fear learning as well as amygdaloid synaptic plasticity. *EMBO J* **25**, 2867-2877, doi:10.1038/sj.emboj.7601156 (2006).
- 91 Chung, H. J., Huang, Y. H., Lau, L. F. & Haganir, R. L. Regulation of the NMDA receptor complex and trafficking by activity-dependent phosphorylation of the NR2B subunit PDZ ligand. *J Neurosci* **24**, 10248-10259, doi:10.1523/JNEUROSCI.0546-04.2004 (2004).
- 92 Sanz-Clemente, A., Gray, J. A., Ogilvie, K. A., Nicoll, R. A. & Roche, K. W. Activated CaMKII couples GluN2B and casein kinase 2 to control synaptic NMDA receptors. *Cell Rep* **3**, 607-614, doi:10.1016/j.celrep.2013.02.011 (2013).

- 93 Chiu, A. M. *et al.* NMDAR-Activated PP1 Dephosphorylates GluN2B to Modulate NMDAR Synaptic Content. *Cell Rep* **28**, 332-341 e335, doi:10.1016/j.celrep.2019.06.030 (2019).
- 94 Raman, I. M. & Trussell, L. O. The mechanism of alpha-amino-3-hydroxy-5-methyl-4-isoxazolepropionate receptor desensitization after removal of glutamate. *Biophysical Journal* **68**, 137-146, doi:10.1016/s0006-3495(95)80168-2 (1995).
- 95 Clements, J. D., Feltz, A., Sahara, Y. & Westbrook, G. L. Activation Kinetics of AMPA Receptor Channels Reveal the Number of Functional Agonist Binding Sites. *The Journal of Neuroscience* **18**, 119-127, doi:10.1523/jneurosci.18-01-00119.1998 (1998).
- 96 Henley, J. M. & Wilkinson, K. A. Synaptic AMPA receptor composition in development, plasticity and disease. *Nat Rev Neurosci* **17**, 337-350, doi:10.1038/nrn.2016.37 (2016).
- 97 Boulter, J. *et al.* Molecular cloning and functional expression of glutamate receptor subunit genes. *Science* **249**, 1033-1037, doi:10.1126/science.2168579 (1990).
- 98 Egebjerg, J., Bettler, B., Hermans-Borgmeyer, I. & Heinemann, S. Cloning of a cDNA for a glutamate receptor subunit activated by kainate but not AMPA. *Nature* **351**, 745-748, doi:10.1038/351745a0 (1991).
- 99 Ogoshi, F. & Weiss, J. H. Heterogeneity of Ca<sup>2+</sup>-Permeable AMPA/Kainate Channel Expression in Hippocampal Pyramidal Neurons: Fluorescence Imaging and Immunocytochemical Assessment. *The Journal of Neuroscience* **23**, 10521-10530, doi:10.1523/jneurosci.23-33-10521.2003 (2003).
- 100 Isaac, J. T., Ashby, M. C. & McBain, C. J. The role of the GluR2 subunit in AMPA receptor function and synaptic plasticity. *Neuron* **54**, 859-871, doi:10.1016/j.neuron.2007.06.001 (2007).
- 101 Humeau, Y. *et al.* A pathway-specific function for different AMPA receptor subunits in amygdala long-term potentiation and fear conditioning. *J Neurosci* **27**, 10947-10956, doi:10.1523/JNEUROSCI.2603-07.2007 (2007).
- 102 Mao, S. C., Hsiao, Y. H. & Gean, P. W. Extinction training in conjunction with a partial agonist of the glycine site on the NMDA receptor erases memory trace. *J Neurosci* **26**, 8892-8899, doi:10.1523/JNEUROSCI.0365-06.2006 (2006).
- 103 Blackstone, C., Murphy, T. H., Moss, S. J., Baraban, J. M. & Huganir, R. L. Cyclic AMP and synaptic activity-dependent phosphorylation of AMPA-preferring glutamate receptors. *The Journal of Neuroscience* **14**, 7585-7593, doi:10.1523/jneurosci.14-12-07585.1994 (1994).
- 104 Mammen, A. L., Kameyama, K., Roche, K. W. & Huganir, R. L. Phosphorylation of the alpha-amino-3-hydroxy-5-methylisoxazole4-propionic acid receptor GluR1 subunit by calcium/calmodulin-dependent kinase II. *J Biol Chem* **272**, 32528-32533, doi:10.1074/jbc.272.51.32528 (1997).
- 105 McGlade-McCulloh, E., Yamamoto, H., Tan, S. E., Brickey, D. A. & Soderling, T. R. Phosphorylation and regulation of glutamate receptors by calcium/calmodulin-dependent protein kinase II. *Nature* **362**, 640-642, doi:10.1038/362640a0 (1993).
- 106 Derkach, V., Barria, A. & Soderling, T. R. Ca<sup>2+</sup>/calmodulin-kinase II enhances channel conductance of alpha-amino-3-hydroxy-5-methyl-4-isoxazolepropionate

- type glutamate receptors. *Proc Natl Acad Sci U S A* **96**, 3269-3274, doi:10.1073/pnas.96.6.3269 (1999).
- 107 Roche, K. W., O'Brien, R. J., Mammen, A. L., Bernhardt, J. & Huganir, R. L. Characterization of Multiple Phosphorylation Sites on the AMPA Receptor GluR1 Subunit. *Neuron* **16**, 1179-1188, doi:10.1016/s0896-6273(00)80144-0 (1996).
- 108 Shukla, K., Kim, J., Blundell, J. & Powell, C. M. Learning-induced glutamate receptor phosphorylation resembles that induced by long term potentiation. *J Biol Chem* **282**, 18100-18107, doi:10.1074/jbc.M702906200 (2007).
- 109 Shi, Y. W., Fan, B. F., Xue, L., Wen, J. L. & Zhao, H. Regulation of Fear Extinction in the Basolateral Amygdala by Dopamine D2 Receptors Accompanied by Altered GluR1, GluR1-Ser845 and NR2B Levels. *Front Behav Neurosci* **11**, 116, doi:10.3389/fnbeh.2017.00116 (2017).
- 110 Lee, H. K., Barbarosie, M., Kameyama, K., Bear, M. F. & Huganir, R. L. Regulation of distinct AMPA receptor phosphorylation sites during bidirectional synaptic plasticity. *Nature* **405**, 955-959, doi:10.1038/35016089 (2000).
- 111 Dosemeci, A., Weinberg, R. J., Reese, T. S. & Tao-Cheng, J. H. The Postsynaptic Density: There Is More than Meets the Eye. *Front Synaptic Neurosci* **8**, 23, doi:10.3389/fnsyn.2016.00023 (2016).
- 112 McGee, A. W. & Brecht, D. S. Identification of an intramolecular interaction between the SH3 and guanylate kinase domains of PSD-95. *J Biol Chem* **274**, 17431-17436, doi:10.1074/jbc.274.25.17431 (1999).
- 113 Cho, K.-O., Hunt, C. A. & Kennedy, M. B. The rat brain postsynaptic density fraction contains a homolog of the drosophila discs-large tumor suppressor protein. *Neuron* **9**, 929-942, doi:10.1016/0896-6273(92)90245-9 (1992).
- 114 Chen, X. *et al.* PSD-95 is required to sustain the molecular organization of the postsynaptic density. *J Neurosci* **31**, 6329-6338, doi:10.1523/JNEUROSCI.5968-10.2011 (2011).
- 115 Kornau, H. C., Schenker, L. T., Kennedy, M. B. & Seeburg, P. H. Domain interaction between NMDA receptor subunits and the postsynaptic density protein PSD-95. *Science* **269**, 1737-1740, doi:10.1126/science.7569905 (1995).
- 116 Chen, L. *et al.* Stargazin regulates synaptic targeting of AMPA receptors by two distinct mechanisms. *Nature* **408**, 936-943, doi:10.1038/35050030 (2000).
- 117 McCann, J. J. *et al.* Supertertiary structure of the synaptic MAGuK scaffold proteins is conserved. *Proc Natl Acad Sci U S A* **109**, 15775-15780, doi:10.1073/pnas.1200254109 (2012).
- 118 Christopherson, K. S., Hillier, B. J., Lim, W. A. & Brecht, D. S. PSD-95 assembles a ternary complex with the N-methyl-D-aspartic acid receptor and a bivalent neuronal NO synthase PDZ domain. *J Biol Chem* **274**, 27467-27473, doi:10.1074/jbc.274.39.27467 (1999).
- 119 Toto, A. *et al.* Ligand binding to the PDZ domains of postsynaptic density protein 95. *Protein Eng Des Sel* **29**, 169-175, doi:10.1093/protein/gzw004 (2016).
- 120 Cheng, D. *et al.* Relative and absolute quantification of postsynaptic density proteome isolated from rat forebrain and cerebellum. *Mol Cell Proteomics* **5**, 1158-1170, doi:10.1074/mcp.D500009-MCP200 (2006).

- 121 Kim, E., Cho, K.-O., Rothschild, A. & Sheng, M. Heteromultimerization and NMDA Receptor-Clustering Activity of Chapsyn-110, a Member of the PSD-95 Family of Proteins. *Neuron* **17**, 103-113, doi:10.1016/s0896-6273(00)80284-6 (1996).
- 122 Roche, K. W. *et al.* Molecular determinants of NMDA receptor internalization. *Nat Neurosci* **4**, 794-802, doi:10.1038/90498 (2001).
- 123 Opazo, P., Sainlos, M. & Choquet, D. Regulation of AMPA receptor surface diffusion by PSD-95 slots. *Curr Opin Neurobiol* **22**, 453-460, doi:10.1016/j.conb.2011.10.010 (2012).
- 124 Xu, W. *et al.* Molecular dissociation of the role of PSD-95 in regulating synaptic strength and LTD. *Neuron* **57**, 248-262, doi:10.1016/j.neuron.2007.11.027 (2008).
- 125 Colledge, M. *et al.* Ubiquitination Regulates PSD-95 Degradation and AMPA Receptor Surface Expression. *Neuron* **40**, 595-607, doi:10.1016/s0896-6273(03)00687-1 (2003).
- 126 Sturgill, J. F., Steiner, P., Czervionke, B. L. & Sabatini, B. L. Distinct domains within PSD-95 mediate synaptic incorporation, stabilization, and activity-dependent trafficking. *J Neurosci* **29**, 12845-12854, doi:10.1523/JNEUROSCI.1841-09.2009 (2009).
- 127 Bhattacharyya, S., Biou, V., Xu, W., Schluter, O. & Malenka, R. C. A critical role for PSD-95/AKAP interactions in endocytosis of synaptic AMPA receptors. *Nat Neurosci* **12**, 172-181, doi:10.1038/nn.2249 (2009).
- 128 Carlisle, H. J., Fink, A. E., Grant, S. G. & O'Dell, T. J. Opposing effects of PSD-93 and PSD-95 on long-term potentiation and spike timing-dependent plasticity. *J Physiol* **586**, 5885-5900, doi:10.1113/jphysiol.2008.163469 (2008).
- 129 Migaud, M. *et al.* Enhanced long-term potentiation and impaired learning in mice with mutant postsynaptic density-95 protein. *Nature* **396**, 433-439, doi:10.1038/24790 (1998).
- 130 Nagura, H. *et al.* Impaired synaptic clustering of postsynaptic density proteins and altered signal transmission in hippocampal neurons, and disrupted learning behavior in PDZ1 and PDZ2 ligand binding-deficient PSD-95 knockin mice. *Mol Brain* **5**, 43, doi:10.1186/1756-6606-5-43 (2012).
- 131 Mittal, C. K. Nitric oxide synthase: involvement of oxygen radicals in conversion of L-arginine to nitric oxide. *Biochem Biophys Res Commun* **193**, 126-132, doi:10.1006/bbrc.1993.1599 (1993).
- 132 Forstermann, U. & Sessa, W. C. Nitric oxide synthases: regulation and function. *Eur Heart J* **33**, 829-837, 837a-837d, doi:10.1093/eurheartj/ehr304 (2012).
- 133 Alderton, W. K., Cooper, C. E. & Knowles, R. G. Nitric oxide synthases: structure, function and inhibition. *Biochem J* **357**, 593-615, doi:10.1042/0264-6021:3570593 (2001).
- 134 Ghosh, D. K. & Stuehr, D. J. Macrophage NO synthase: characterization of isolated oxygenase and reductase domains reveals a head-to-head subunit interaction. *Biochemistry* **34**, 801-807, doi:10.1021/bi00003a013 (1995).
- 135 Crane, B. R. *et al.* Structure of nitric oxide synthase oxygenase dimer with pterin and substrate. *Science* **279**, 2121-2126, doi:10.1126/science.279.5359.2121 (1998).

- 136 Roman, L. J., Martasek, P. & Masters, B. S. Intrinsic and extrinsic modulation of nitric oxide synthase activity. *Chem Rev* **102**, 1179-1190, doi:10.1021/cr000661e (2002).
- 137 Smith, B. C., Underbakke, E. S., Kulp, D. W., Schief, W. R. & Marletta, M. A. Nitric oxide synthase domain interfaces regulate electron transfer and calmodulin activation. *Proc Natl Acad Sci U S A* **110**, E3577-3586, doi:10.1073/pnas.1313331110 (2013).
- 138 Venema, R. C., Sayegh, H. S., Kent, J. D. & Harrison, D. G. Identification, characterization, and comparison of the calmodulin-binding domains of the endothelial and inducible nitric oxide synthases. *J Biol Chem* **271**, 6435-6440, doi:10.1074/jbc.271.11.6435 (1996).
- 139 Gunther, M., Al Nimer, F., Gahm, C., Piehl, F. & Mathiesen, T. iNOS-mediated secondary inflammatory response differs between rat strains following experimental brain contusion. *Acta Neurochir (Wien)* **154**, 689-697, doi:10.1007/s00701-012-1297-1 (2012).
- 140 Simic, G. *et al.* nNOS expression in reactive astrocytes correlates with increased cell death related DNA damage in the hippocampus and entorhinal cortex in Alzheimer's disease. *Exp Neurol* **165**, 12-26, doi:10.1006/exnr.2000.7448 (2000).
- 141 Galea, E., Feinstein, D. L. & Reis, D. J. Induction of calcium-independent nitric oxide synthase activity in primary rat glial cultures. *Proc Natl Acad Sci U S A* **89**, 10945-10949, doi:10.1073/pnas.89.22.10945 (1992).
- 142 Endoh, M., Maiese, K. & Wagner, J. Expression of the inducible form of nitric oxide synthase by reactive astrocytes after transient global ischemia. *Brain Research* **651**, 92-100, doi:10.1016/0006-8993(94)90683-1 (1994).
- 143 Stanarius, A., Töpel, I., Schulz, S., Noack, H. & Wolf, G. Immunocytochemistry of endothelial nitric oxide synthase in the rat brain: a light and electron microscopical study using the tyramide signal amplification technique. *Acta Histochemica* **99**, 411-429, doi:10.1016/s0065-1281(97)80034-7 (1997).
- 144 Barna, M., Komatsu, T. & Reiss, C. S. Activation of type III nitric oxide synthase in astrocytes following a neurotropic viral infection. *Virology* **223**, 331-343, doi:10.1006/viro.1996.0484 (1996).
- 145 Steinert, J. R., Chernova, T. & Forsythe, I. D. Nitric oxide signaling in brain function, dysfunction, and dementia. *Neuroscientist* **16**, 435-452, doi:10.1177/1073858410366481 (2010).
- 146 Kone, B. C. Protein-protein interactions controlling nitric oxide synthases. *Acta Physiol Scand* **168**, 27-31, doi:10.1046/j.1365-201x.2000.00629.x (2000).
- 147 Chaudhury, A., He, X. D. & Goyal, R. K. Role of PSD95 in membrane association and catalytic activity of nNOS $\alpha$  in nitrenergic varicosities in mice gut. *Am J Physiol Gastrointest Liver Physiol* **297**, G806-813, doi:10.1152/ajpgi.00279.2009 (2009).
- 148 Bodnarova, M., Martasek, P. & Moroz, L. L. Calcium/calmodulin-dependent nitric oxide synthase activity in the CNS of *Aplysia californica*: biochemical characterization and link to cGMP pathways. *J Inorg Biochem* **99**, 922-928, doi:10.1016/j.jinorgbio.2005.01.012 (2005).
- 149 Tillmann, S., Pereira, V. S., Liebenberg, N., Christensen, A. K. & Wegener, G. ZL006, a small molecule inhibitor of PSD-95/nNOS interaction, does not induce



- antidepressant-like effects in two genetically predisposed rat models of depression and control animals. *PLoS One* **12**, e0182698, doi:10.1371/journal.pone.0182698 (2017).
- 150 Tao, W. Y. *et al.* Neuroprotective effects of ZL006 in Abeta1-42-treated neuronal cells. *Neural Regen Res* **15**, 2296-2305, doi:10.4103/1673-5374.285006 (2020).
- 151 Florio, S. K. *et al.* Disruption of nNOS-PSD95 protein-protein interaction inhibits acute thermal hyperalgesia and chronic mechanical allodynia in rodents. *Br J Pharmacol* **158**, 494-506, doi:10.1111/j.1476-5381.2009.00300.x (2009).
- 152 Panda, K., Ghosh, S. & Stuehr, D. J. Calmodulin activates intersubunit electron transfer in the neuronal nitric-oxide synthase dimer. *J Biol Chem* **276**, 23349-23356, doi:10.1074/jbc.M100687200 (2001).
- 153 Abu-Soud, H. M., Yoho, L. L. & Stuehr, D. J. Calmodulin controls neuronal nitric-oxide synthase by a dual mechanism. Activation of intra- and interdomain electron transfer. *Journal of Biological Chemistry* **269**, 32047-32050, doi:10.1016/s0021-9258(18)31597-7 (1994).
- 154 Bocchio, M. *et al.* Sleep and Serotonin Modulate Paracapsular Nitric Oxide Synthase Expressing Neurons of the Amygdala. *eNeuro* **3**, doi:10.1523/ENEURO.0177-16.2016 (2016).
- 155 Wang, X. *et al.* Decreased Number and Expression of nNOS-Positive Interneurons in Basolateral Amygdala in Two Mouse Models of Autism. *Front Cell Neurosci* **12**, 251, doi:10.3389/fncel.2018.00251 (2018).
- 156 Wang, X., Liu, C., Wang, X., Gao, F. & Zhan, R. Z. Density and neurochemical profiles of neuronal nitric oxide synthase-expressing interneuron in the mouse basolateral amygdala. *Brain Res* **1663**, 106-113, doi:10.1016/j.brainres.2017.02.009 (2017).
- 157 Walton, J. C., Selvakumar, B., Weil, Z. M., Snyder, S. H. & Nelson, R. J. Neuronal nitric oxide synthase and NADPH oxidase interact to affect cognitive, affective, and social behaviors in mice. *Behav Brain Res* **256**, 320-327, doi:10.1016/j.bbr.2013.08.003 (2013).
- 158 Trainor, B. C., Workman, J. L., Jessen, R. & Nelson, R. J. Impaired nitric oxide synthase signaling dissociates social investigation and aggression. *Behav Neurosci* **121**, 362-369, doi:10.1037/0735-7044.121.2.362 (2007).
- 159 Tanda, K. *et al.* Abnormal social behavior, hyperactivity, impaired remote spatial memory, and increased D1-mediated dopaminergic signaling in neuronal nitric oxide synthase knockout mice. *Mol Brain* **2**, 19, doi:10.1186/1756-6606-2-19 (2009).
- 160 Kelley, J. B., Balda, M. A., Anderson, K. L. & Itzhak, Y. Impairments in fear conditioning in mice lacking the nNOS gene. *Learn Mem* **16**, 371-378, doi:10.1101/lm.1329209 (2009).
- 161 O'Dell, T. J. *et al.* Endothelial NOS and the blockade of LTP by NOS inhibitors in mice lacking neuronal NOS. *Science* **265**, 542-546, doi:10.1126/science.7518615 (1994).
- 162 Li, L. P. *et al.* PSD95 and nNOS interaction as a novel molecular target to modulate conditioned fear: relevance to PTSD. *Transl Psychiatry* **8**, 155, doi:10.1038/s41398-018-0208-5 (2018).

- 163 Lee, H. J. & Zheng, J. J. PDZ domains and their binding partners: structure, specificity, and modification. *Cell Commun Signal* **8**, 8, doi:10.1186/1478-811X-8-8 (2010).
- 164 Brenman, J. E. *et al.* Interaction of Nitric Oxide Synthase with the Postsynaptic Density Protein PSD-95 and  $\alpha$ 1-Syntrophin Mediated by PDZ Domains. *Cell* **84**, 757-767, doi:10.1016/s0092-8674(00)81053-3 (1996).
- 165 Morais Cabral, J. H. *et al.* Crystal structure of a PDZ domain. *Nature* **382**, 649-652, doi:10.1038/382649a0 (1996).
- 166 Cui, H. *et al.* PDZ protein interactions underlying NMDA receptor-mediated excitotoxicity and neuroprotection by PSD-95 inhibitors. *J Neurosci* **27**, 9901-9915, doi:10.1523/JNEUROSCI.1464-07.2007 (2007).
- 167 Tochio, H. *et al.* Formation of nNOS/PSD-95 PDZ dimer requires a preformed beta-finger structure from the nNOS PDZ domain. *J Mol Biol* **303**, 359-370, doi:10.1006/jmbi.2000.4148 (2000).
- 168 Stricker, N. L. *et al.* PDZ domain of neuronal nitric oxide synthase recognizes novel C-terminal peptide sequences. *Nat Biotechnol* **15**, 336-342, doi:10.1038/nbt0497-336 (1997).
- 169 Campbell, M. G., Smith, B. C., Potter, C. S., Carragher, B. & Marletta, M. A. Molecular architecture of mammalian nitric oxide synthases. *Proc Natl Acad Sci U S A* **111**, E3614-3623, doi:10.1073/pnas.1413763111 (2014).
- 170 Rao, Y. M., Chaudhury, A. & Goyal, R. K. Active and inactive pools of nNOS in the nerve terminals in mouse gut: implications for nitrergic neurotransmission. *Am J Physiol Gastrointest Liver Physiol* **294**, G627-634, doi:10.1152/ajpgi.00519.2007 (2008).
- 171 Cossenza, M. *et al.* Nitric oxide in the nervous system: biochemical, developmental, and neurobiological aspects. *Vitam Horm* **96**, 79-125, doi:10.1016/B978-0-12-800254-4.00005-2 (2014).
- 172 Arancio, O. *et al.* Nitric Oxide Acts Directly in the Presynaptic Neuron to Produce Long-Term Potentiation in Cultured Hippocampal Neurons. *Cell* **87**, 1025-1035, doi:10.1016/s0092-8674(00)81797-3 (1996).
- 173 Meffert, M. Nitric oxide stimulates Ca<sup>2+</sup>-independent synaptic vesicle release. *Neuron* **12**, 1235-1244, doi:10.1016/0896-6273(94)90440-5 (1994).
- 174 Meffert, M. K., Calakos, N. C., Scheller, R. H. & Schulman, H. Nitric Oxide Modulates Synaptic Vesicle Docking/Fusion Reactions. *Neuron* **16**, 1229-1236, doi:10.1016/s0896-6273(00)80149-x (1996).
- 175 Micheva, K. D., Buchanan, J., Holz, R. W. & Smith, S. J. Retrograde regulation of synaptic vesicle endocytosis and recycling. *Nat Neurosci* **6**, 925-932, doi:10.1038/nn1114 (2003).
- 176 Kovacs, I. & Lindermayr, C. Nitric oxide-based protein modification: formation and site-specificity of protein S-nitrosylation. *Front Plant Sci* **4**, 137, doi:10.3389/fpls.2013.00137 (2013).
- 177 Foster, M. W., Hess, D. T. & Stamler, J. S. Protein S-nitrosylation in health and disease: a current perspective. *Trends Mol Med* **15**, 391-404, doi:10.1016/j.molmed.2009.06.007 (2009).
- 178 Seth, D. & Stamler, J. S. The SNO-proteome: causation and classifications. *Curr Opin Chem Biol* **15**, 129-136, doi:10.1016/j.cbpa.2010.10.012 (2011).

- 179 Doulias, P. T. *et al.* Site specific identification of endogenous S-nitrosocysteine proteomes. *J Proteomics* **92**, 195-203, doi:10.1016/j.jprot.2013.05.033 (2013).
- 180 Okamoto, S. *et al.* S-nitrosylation-mediated redox transcriptional switch modulates neurogenesis and neuronal cell death. *Cell Rep* **8**, 217-228, doi:10.1016/j.celrep.2014.06.005 (2014).
- 181 Ho, G. P. *et al.* S-nitrosylation and S-palmitoylation reciprocally regulate synaptic targeting of PSD-95. *Neuron* **71**, 131-141, doi:10.1016/j.neuron.2011.05.033 (2011).
- 182 Riccio, A. *et al.* A nitric oxide signaling pathway controls CREB-mediated gene expression in neurons. *Mol Cell* **21**, 283-294, doi:10.1016/j.molcel.2005.12.006 (2006).
- 183 Sen, N. & Snyder, S. H. Neurotrophin-mediated degradation of histone methyltransferase by S-nitrosylation cascade regulates neuronal differentiation. *Proc Natl Acad Sci U S A* **108**, 20178-20183, doi:10.1073/pnas.1117820108 (2011).
- 184 Stroissnigg, H. *et al.* S-nitrosylation of microtubule-associated protein 1B mediates nitric-oxide-induced axon retraction. *Nat Cell Biol* **9**, 1035-1045, doi:10.1038/ncb1625 (2007).
- 185 Palmer, L. A. *et al.* Hypoxia-induced changes in protein s-nitrosylation in female mouse brainstem. *Am J Respir Cell Mol Biol* **52**, 37-45, doi:10.1165/rcmb.2013-0359OC (2015).
- 186 Hao, L., Wei, X., Guo, P., Zhang, G. & Qi, S. Neuroprotective Effects of Inhibiting Fyn S-Nitrosylation on Cerebral Ischemia/Reperfusion-Induced Damage to CA1 Hippocampal Neurons. *Int J Mol Sci* **17**, doi:10.3390/ijms17071100 (2016).
- 187 Ba, M., Ding, W., Guan, L., Lv, Y. & Kong, M. S-nitrosylation of Src by NR2B-nNOS signal causes Src activation and NR2B tyrosine phosphorylation in levodopa-induced dyskinetic rat model. *Hum Exp Toxicol* **38**, 303-310, doi:10.1177/0960327118806633 (2019).
- 188 Selvakumar, B. *et al.* S-nitrosylation of AMPA receptor GluA1 regulates phosphorylation, single-channel conductance, and endocytosis. *Proc Natl Acad Sci U S A* **110**, 1077-1082, doi:10.1073/pnas.1221295110 (2013).
- 189 Selvakumar, B., Haganir, R. L. & Snyder, S. H. S-nitrosylation of stargazin regulates surface expression of AMPA-glutamate neurotransmitter receptors. *Proc Natl Acad Sci U S A* **106**, 16440-16445, doi:10.1073/pnas.0908949106 (2009).
- 190 Huang, Y. *et al.* S-nitrosylation of N-ethylmaleimide sensitive factor mediates surface expression of AMPA receptors. *Neuron* **46**, 533-540, doi:10.1016/j.neuron.2005.03.028 (2005).
- 191 Sha, Y. & Marshall, H. E. S-nitrosylation in the regulation of gene transcription. *Biochim Biophys Acta* **1820**, 701-711, doi:10.1016/j.bbagen.2011.05.008 (2012).
- 192 Underbakke, E. S. *et al.* Nitric oxide-induced conformational changes in soluble guanylate cyclase. *Structure* **22**, 602-611, doi:10.1016/j.str.2014.01.008 (2014).
- 193 Gudi, T., Hong, G. K. P., Vaandrager, A. B., Lohmann, S. M. & Pilz, R. B. Nitric oxide and cGMP regulate gene expression in neuronal and glial cells by activating type II cGMP-dependent protein kinase. *The FASEB Journal* **13**, 2143-2152, doi:10.1096/fasebj.13.15.2143 (1999).

- 194 Matsumoto, Y., Unoki, S., Aonuma, H. & Mizunami, M. Critical role of nitric oxide-cGMP cascade in the formation of cAMP-dependent long-term memory. *Learn Mem* **13**, 35-44, doi:10.1101/lm.130506 (2006).
- 195 Kleppisch, T. & Feil, R. cGMP signalling in the mammalian brain: role in synaptic plasticity and behaviour. *Handb Exp Pharmacol*, 549-579, doi:10.1007/978-3-540-68964-5\_24 (2009).
- 196 Feil, R. & Kleppisch, T. NO/cGMP-dependent modulation of synaptic transmission. *Handb Exp Pharmacol*, 529-560, doi:10.1007/978-3-540-74805-2\_16 (2008).
- 197 Serulle, Y., Arancio, O. & Ziff, E. B. A role for cGMP-dependent protein kinase II in AMPA receptor trafficking and synaptic plasticity. *Channels (Austin)* **2**, 230-232, doi:10.4161/chan.2.4.6391 (2008).
- 198 Serulle, Y. *et al.* A GluR1-cGKII interaction regulates AMPA receptor trafficking. *Neuron* **56**, 670-688, doi:10.1016/j.neuron.2007.09.016 (2007).
- 199 Wang, H. G. *et al.* Presynaptic and postsynaptic roles of NO, cGK, and RhoA in long-lasting potentiation and aggregation of synaptic proteins. *Neuron* **45**, 389-403, doi:10.1016/j.neuron.2005.01.011 (2005).
- 200 Haghikia, A. *et al.* Long-term potentiation in the visual cortex requires both nitric oxide receptor guanylyl cyclases. *J Neurosci* **27**, 818-823, doi:10.1523/JNEUROSCI.4706-06.2007 (2007).
- 201 Luo, C. *et al.* Presynaptically localized cyclic GMP-dependent protein kinase 1 is a key determinant of spinal synaptic potentiation and pain hypersensitivity. *PLoS Biol* **10**, e1001283, doi:10.1371/journal.pbio.1001283 (2012).
- 202 Bon, C. L. M. & Garthwaite, J. On the Role of Nitric Oxide in Hippocampal Long-Term Potentiation. *The Journal of Neuroscience* **23**, 1941-1948, doi:10.1523/jneurosci.23-05-01941.2003 (2003).
- 203 Nugent, F. S., Niehaus, J. L. & Kauer, J. A. PKG and PKA signaling in LTP at GABAergic synapses. *Neuropsychopharmacology* **34**, 1829-1842, doi:10.1038/npp.2009.5 (2009).
- 204 Ota, K. T., Pierre, V. J., Ploski, J. E., Queen, K. & Schafe, G. E. The NO-cGMP-PKG signaling pathway regulates synaptic plasticity and fear memory consolidation in the lateral amygdala via activation of ERK/MAP kinase. *Learn Mem* **15**, 792-805, doi:10.1101/lm.1114808 (2008).
- 205 Taubenfeld, S. M., Milekic, M. H., Monti, B. & Alberini, C. M. The consolidation of new but not reactivated memory requires hippocampal C/EBPbeta. *Nat Neurosci* **4**, 813-818, doi:10.1038/90520 (2001).
- 206 Bekinschtein, P. *et al.* Persistence of long-term memory storage requires a late protein synthesis- and BDNF- dependent phase in the hippocampus. *Neuron* **53**, 261-277, doi:10.1016/j.neuron.2006.11.025 (2007).
- 207 Alberini, C. M. & Kandel, E. R. The regulation of transcription in memory consolidation. *Cold Spring Harb Perspect Biol* **7**, a021741, doi:10.1101/cshperspect.a021741 (2014).
- 208 Eckel-Mahan, K. L. & Storm, D. R. Circadian rhythms and memory: not so simple as cogs and gears. *EMBO Rep* **10**, 584-591, doi:10.1038/embor.2009.123 (2009).

- 209 Wang, G., Grone, B., Colas, D., Appelbaum, L. & Mourrain, P. Synaptic plasticity in sleep: learning, homeostasis and disease. *Trends Neurosci* **34**, 452-463, doi:10.1016/j.tins.2011.07.005 (2011).
- 210 Tononi, G. & Cirelli, C. Sleep and the price of plasticity: from synaptic and cellular homeostasis to memory consolidation and integration. *Neuron* **81**, 12-34, doi:10.1016/j.neuron.2013.12.025 (2014).
- 211 Krivanek, J. & McGaugh, J. L. Effects of pentylentetrazol on memory storage in mice. *Psychopharmacologia* **12**, 303-321, doi:10.1007/BF00401409 (1968).
- 212 Luttges, M. W. & McGaugh, J. L. Facilitation of avoidance conditioning in mice by posttraining administration of bemegrade. *Agents Actions* **2**, 118-121, doi:10.1007/BF01966749 (1971).
- 213 Han, J. H. *et al.* Selective erasure of a fear memory. *Science* **323**, 1492-1496, doi:10.1126/science.1164139 (2009).
- 214 Alberini, C. M., Ghirardl, M., Metz, R. & Kandel, E. R. C/EBP is an immediate-early gene required for the consolidation of long-term facilitation in Aplysia. *Cell* **76**, 1099-1114, doi:10.1016/0092-8674(94)90386-7 (1994).
- 215 Arguello, A. A. *et al.* CCAAT enhancer binding protein delta plays an essential role in memory consolidation and reconsolidation. *J Neurosci* **33**, 3646-3658, doi:10.1523/JNEUROSCI.1635-12.2013 (2013).
- 216 Taubenfeld, S. M. *et al.* Fornix-Dependent Induction of Hippocampal CCAAT Enhancer-Binding Protein  $\beta$  and  $\delta$  Co-Localizes with Phosphorylated cAMP Response Element-Binding Protein and Accompanies Long-Term Memory Consolidation. *The Journal of Neuroscience* **21**, 84-91, doi:10.1523/jneurosci.21-01-00084.2001 (2001).
- 217 Lonze, B. E. & Ginty, D. D. Function and Regulation of CREB Family Transcription Factors in the Nervous System. *Neuron* **35**, 605-623, doi:10.1016/s0896-6273(02)00828-0 (2002).
- 218 Zhang, J. W., Klemm, D. J., Vinson, C. & Lane, M. D. Role of CREB in transcriptional regulation of CCAAT/enhancer-binding protein beta gene during adipogenesis. *J Biol Chem* **279**, 4471-4478, doi:10.1074/jbc.M311327200 (2004).
- 219 Ressler, K. J., Paschall, G., Zhou, X.-l. & Davis, M. Regulation of Synaptic Plasticity Genes during Consolidation of Fear Conditioning. *The Journal of Neuroscience* **22**, 7892-7902, doi:10.1523/jneurosci.22-18-07892.2002 (2002).
- 220 Guan, Z. *et al.* Integration of Long-Term-Memory-Related Synaptic Plasticity Involves Bidirectional Regulation of Gene Expression and Chromatin Structure. *Cell* **111**, 483-493, doi:10.1016/s0092-8674(02)01074-7 (2002).
- 221 Sung, Y. J., Walters, E. T. & Ambron, R. T. A neuronal isoform of protein kinase G couples mitogen-activated protein kinase nuclear import to axotomy-induced long-term hyperexcitability in Aplysia sensory neurons. *J Neurosci* **24**, 7583-7595, doi:10.1523/JNEUROSCI.1445-04.2004 (2004).
- 222 Pilz, R. B. & Casteel, D. E. Regulation of gene expression by cyclic GMP. *Circ Res* **93**, 1034-1046, doi:10.1161/01.RES.0000103311.52853.48 (2003).
- 223 Ota, K. T., Monsey, M. S., Wu, M. S., Young, G. J. & Schafe, G. E. Synaptic plasticity and NO-cGMP-PKG signaling coordinately regulate ERK-driven gene expression in the lateral amygdala and in the auditory thalamus following

- Pavlovian fear conditioning. *Learn Mem* **17**, 221-235, doi:10.1101/lm.1592510 (2010).
- 224 Lu, Y.-F., Kandel, E. R. & Hawkins, R. D. Nitric Oxide Signaling Contributes to Late-Phase LTP and CREB Phosphorylation in the Hippocampus. *The Journal of Neuroscience* **19**, 10250-10261, doi:10.1523/jneurosci.19-23-10250.1999 (1999).
- 225 Liu, J. L. *et al.* A NMDA receptor antagonist, MK-801 impairs consolidating extinction of auditory conditioned fear responses in a Pavlovian model. *PLoS One* **4**, e7548, doi:10.1371/journal.pone.0007548 (2009).
- 226 Kishioka, A., Uemura, T., Fukushima, F. & Mishina, M. Consolidation of auditory fear memories formed by weak unconditioned stimuli requires NMDA receptor activation and de novo protein synthesis in the striatum. *Mol Brain* **6**, 17, doi:10.1186/1756-6606-6-17 (2013).
- 227 McGowan, J. C. *et al.* Prophylactic Ketamine Attenuates Learned Fear. *Neuropsychopharmacology* **42**, 1577-1589, doi:10.1038/npp.2017.19 (2017).
- 228 Sachser, R. M. *et al.* Forgetting of long-term memory requires activation of NMDA receptors, L-type voltage-dependent Ca<sup>2+</sup> channels, and calcineurin. *Sci Rep* **6**, 22771, doi:10.1038/srep22771 (2016).
- 229 Lipton, S. A. Failures and successes of NMDA receptor antagonists: molecular basis for the use of open-channel blockers like memantine in the treatment of acute and chronic neurologic insults. *NeuroRx* **1**, 101-110, doi:10.1602/neurorx.1.1.101 (2004).
- 230 Zorumski, C. F., Izumi, Y. & Mennerick, S. Ketamine: NMDA Receptors and Beyond. *J Neurosci* **36**, 11158-11164, doi:10.1523/JNEUROSCI.1547-16.2016 (2016).
- 231 Cai, C. Y. *et al.* PSD-95-nNOS Coupling Regulates Contextual Fear Extinction in the Dorsal CA3. *Sci Rep* **8**, 12775, doi:10.1038/s41598-018-30899-4 (2018).
- 232 Luo, H., Han, L. & Tian, S. Effect of nitric oxide synthase inhibitor L-NAME on fear extinction in rats: a task-dependent effect. *Neurosci Lett* **572**, 13-18, doi:10.1016/j.neulet.2014.04.031 (2014).
- 233 Lisboa, S. F. *et al.* Increased Contextual Fear Conditioning in iNOS Knockout Mice: Additional Evidence for the Involvement of Nitric Oxide in Stress-Related Disorders and Contribution of the Endocannabinoid System. *Int J Neuropsychopharmacol* **18**, doi:10.1093/ijnp/pyv005 (2015).
- 234 Song, S., Lee, J., Park, S. & Choi, S. Fear renewal requires nitric oxide signaling in the lateral amygdala. *Biochem Biophys Res Commun* **523**, 86-90, doi:10.1016/j.bbrc.2019.12.038 (2020).
- 235 Xue, F. *et al.* Structure-based design, synthesis, and biological evaluation of lipophilic-tailed monocationic inhibitors of neuronal nitric oxide synthase. *Bioorg Med Chem* **18**, 6526-6537, doi:10.1016/j.bmc.2010.06.074 (2010).
- 236 Labby, K. J. *et al.* Intramolecular hydrogen bonding: a potential strategy for more bioavailable inhibitors of neuronal nitric oxide synthase. *Bioorg Med Chem* **20**, 2435-2443, doi:10.1016/j.bmc.2012.01.037 (2012).
- 237 Carey, L. M. *et al.* Small molecule inhibitors of PSD95-nNOS protein-protein interactions suppress formalin-evoked Fos protein expression and nociceptive behavior in rats. *Neuroscience* **349**, 303-317, doi:10.1016/j.neuroscience.2017.02.055 (2017).

- 238 Zhou, L. *et al.* Treatment of cerebral ischemia by disrupting ischemia-induced interaction of nNOS with PSD-95. *Nat Med* **16**, 1439-1443, doi:10.1038/nm.2245 (2010).
- 239 Lee, W. H. *et al.* Small molecule inhibitors of PSD95-nNOS protein-protein interactions as novel analgesics. *Neuropharmacology* **97**, 464-475, doi:10.1016/j.neuropharm.2015.05.038 (2015).
- 240 Aziz, W. *et al.* Multi-input Synapses, but Not LTP-Strengthened Synapses, Correlate with Hippocampal Memory Storage in Aged Mice. *Curr Biol* **29**, 3600-3610 e3604, doi:10.1016/j.cub.2019.08.064 (2019).
- 241 Iribarren, J., Prolo, P., Neagos, N. & Chiappelli, F. Post-traumatic stress disorder: evidence-based research for the third millennium. *Evid Based Complement Alternat Med* **2**, 503-512, doi:10.1093/ecam/neh127 (2005).
- 242 Grillon C, S. S., Charney DS. The psychobiological basis of posttraumatic stress disorder. *Mol Psychiatry* **1**, 278– 297 (1996).
- 243 LeDoux, J. Fear and the brain: where have we been, and where are we going? *Biological Psychiatry* **44**, 1229-1238, doi:10.1016/s0006-3223(98)00282-0 (1998).
- 244 Schafe, G., Nadel NV, Sullivan, GM, Harris, A, LeDoux, JE. Memory Consolidation for Contextual and Auditory Fear Conditioning Is Dependent on Protein Synthesis, PKA, and MAP Kinase. *Cold Spring Harbor Laboratory Press* **6**, 97-110, doi:10.1101/lm.6.2.97 (1999).
- 245 Kim, J. *et al.* Reactivation of fear memory renders consolidated amygdala synapses labile. *J Neurosci* **30**, 9631-9640, doi:10.1523/JNEUROSCI.0940-10.2010 (2010).
- 246 Nader, K., Schafe, G. E. & LeDoux, J. E. The labile nature of consolidation theory. *Nat Rev Neurosci* **1**, 216-219, doi:10.1038/35044580 (2000).
- 247 Pitman, R. K. *et al.* Biological studies of post-traumatic stress disorder. *Nat Rev Neurosci* **13**, 769-787, doi:10.1038/nrn3339 (2012).
- 248 Sattler, R. *et al.* Specific coupling of NMDA receptor activation to nitric oxide neurotoxicity by PSD-95 protein. *Science* **284**, 1845-1848, doi:10.1126/science.284.5421.1845 (1999).
- 249 Niethammer, M., Kim, E. & Sheng, M. Interaction between the C terminus of NMDA receptor subunits and multiple members of the PSD-95 family of membrane-associated guanylate kinases. *The Journal of Neuroscience* **16**, 2157-2163, doi:10.1523/jneurosci.16-07-02157.1996 (1996).
- 250 Andrew, P. Enzymatic function of nitric oxide synthases. *Cardiovascular Research* **43**, 521-531, doi:10.1016/s0008-6363(99)00115-7 (1999).
- 251 Qin, C. *et al.* Uncoupling nNOS-PSD-95 in the ACC can inhibit contextual fear generalization. *Biochem Biophys Res Commun* **513**, 248-254, doi:10.1016/j.bbrc.2019.03.184 (2019).
- 252 Li, J. *et al.* Disrupting nNOS-PSD-95 coupling in the hippocampal dentate gyrus promotes extinction memory retrieval. *Biochem Biophys Res Commun* **493**, 862-868, doi:10.1016/j.bbrc.2017.09.003 (2017).
- 253 Robinson, M. D., McCarthy, D. J. & Smyth, G. K. edgeR: a Bioconductor package for differential expression analysis of digital gene expression data. *Bioinformatics* **26**, 139-140, doi:10.1093/bioinformatics/btp616 (2010).

- 254 Tanaka, M. *et al.* Region- and time-dependent gene regulation in the amygdala and anterior cingulate cortex of a PTSD-like mouse model. *Mol Brain* **12**, 25, doi:10.1186/s13041-019-0449-0 (2019).
- 255 Lori, A. *et al.* Dynamic Patterns of Threat-Associated Gene Expression in the Amygdala and Blood. *Front Psychiatry* **9**, 778, doi:10.3389/fpsy.2018.00778 (2018).
- 256 Sullivan, S. E., Jones, M. E., Jamieson, S., Rumbaugh, G. & Miller, C. A. Bioinformatic analysis of long-lasting transcriptional and translational changes in the basolateral amygdala following acute stress. *PLoS One* **14**, e0209846, doi:10.1371/journal.pone.0209846 (2019).
- 257 McNamara, G. I., John, R. M. & Isles, A. R. Territorial Behavior and Social Stability in the Mouse Require Correct Expression of Imprinted *Cdkn1c*. *Front Behav Neurosci* **12**, 28, doi:10.3389/fnbeh.2018.00028 (2018).
- 258 Agis-Balboa, R. C. *et al.* A hippocampal insulin-growth factor 2 pathway regulates the extinction of fear memories. *EMBO J* **30**, 4071-4083, doi:10.1038/emboj.2011.293 (2011).
- 259 Burgdorf, J. *et al.* IGF2BP2 Produces Rapid-Acting and Long-Lasting Effects in Rat Models of Posttraumatic Stress Disorder via a Novel Mechanism Associated with Structural Plasticity. *Int J Neuropsychopharmacol* **20**, 476-484, doi:10.1093/ijnp/pyx007 (2017).
- 260 Johnston, J., Forsythe, I. D. & Kopp-Scheinflug, C. Going native: voltage-gated potassium channels controlling neuronal excitability. *J Physiol* **588**, 3187-3200, doi:10.1113/jphysiol.2010.191973 (2010).
- 261 Laszczyk, A. M. *et al.* Klotho regulates postnatal neurogenesis and protects against age-related spatial memory loss. *Neurobiol Aging* **59**, 41-54, doi:10.1016/j.neurobiolaging.2017.07.008 (2017).
- 262 Nakamura, E. *et al.* Disruption of the midkine gene (*Mdk*) resulted in altered expression of a calcium binding protein in the hippocampus of infant mice and their abnormal behaviour. *Genes Cells* **3**, 811-822, doi:10.1046/j.1365-2443.1998.00231.x (1998).
- 263 Brouillette, J. & Quirion, R. Transthyretin: a key gene involved in the maintenance of memory capacities during aging. *Neurobiol Aging* **29**, 1721-1732, doi:10.1016/j.neurobiolaging.2007.04.007 (2008).
- 264 Kiser, D. P. *et al.* Early-life stress impairs developmental programming in Cadherin 13 (*CDH13*)-deficient mice. *Prog Neuropsychopharmacol Biol Psychiatry* **89**, 158-168, doi:10.1016/j.pnpbp.2018.08.010 (2019).
- 265 Schmeisser, M. J. *et al.* I $\kappa$ B kinase/nuclear factor  $\kappa$ B-dependent insulin-like growth factor 2 (*Igf2*) expression regulates synapse formation and spine maturation via *Igf2* receptor signaling. *J Neurosci* **32**, 5688-5703, doi:10.1523/JNEUROSCI.0111-12.2012 (2012).
- 266 Cazals, V., Nabeyrat, E., Corroyer, S., de Keyzer, Y. & Clement, A. Role for NF- $\kappa$ B in mediating the effects of hyperoxia on IGF-binding protein 2 promoter activity in lung alveolar epithelial cells. *Biochimica et Biophysica Acta (BBA) - Molecular Cell Research* **1448**, 349-362, doi:10.1016/s0167-4889(98)00095-0 (1999).



- 267 Feldser, D. *et al.* Reciprocal Positive Regulation of Hypoxia-inducible Factor 1 $\alpha$  and Insulin-like Growth Factor 2. *Cancer Research* **59**, 3915-3918 (1999).
- 268 Togashi, H. *et al.* Neuronal (type I) nitric oxide synthase regulates nuclear factor kappaB activity and immunologic (type II) nitric oxide synthase expression. *Proc Natl Acad Sci U S A* **94**, 2676-2680, doi:10.1073/pnas.94.6.2676 (1997).
- 269 Studer, R. K. *et al.* Nitric oxide inhibits chondrocyte response to IGF-I: inhibition of IGF-IRbeta tyrosine phosphorylation. *Am J Physiol Cell Physiol* **279**, C961-969, doi:10.1152/ajpcell.2000.279.4.C961 (2000).
- 270 Ridnour, L. A. *et al.* Molecular mechanisms for discrete nitric oxide levels in cancer. *Nitric Oxide* **19**, 73-76, doi:10.1016/j.niox.2008.04.006 (2008).
- 271 Gariboldi, M. B., Ravizza, R. & Monti, E. The IGFR1 inhibitor NVP-AEW541 disrupts a pro-survival and pro-angiogenic IGF-STAT3-HIF1 pathway in human glioblastoma cells. *Biochem Pharmacol* **80**, 455-462, doi:10.1016/j.bcp.2010.05.011 (2010).
- 272 Sun, J. *et al.* Up-regulation of INSR/IGF1R by C-myc promotes TSCC tumorigenesis and metastasis through the NF-kappaB pathway. *Biochim Biophys Acta Mol Basis Dis* **1864**, 1873-1882, doi:10.1016/j.bbadis.2018.03.004 (2018).
- 273 Li, T. *et al.* Insulin-like growth factor 2 axis supports the serum-independent growth of malignant rhabdoid tumor and is activated by microenvironment stress. *Oncotarget* **8**, 47269-47283, doi:10.18632/oncotarget.17617 (2017).
- 274 Dupont, J. & LeRoith, D. Insulin and insulin-like growth factor I receptors: similarities and differences in signal transduction. *Horm Res* **55 Suppl 2**, 22-26, doi:10.1159/000063469 (2001).
- 275 Ogundele, O. M., Pardo, J., Francis, J., Goya, R. G. & Lee, C. C. A Putative Mechanism of Age-Related Synaptic Dysfunction Based on the Impact of IGF-1 Receptor Signaling on Synaptic CaMKIIalpha Phosphorylation. *Front Neuroanat* **12**, 35, doi:10.3389/fnana.2018.00035 (2018).
- 276 Oka, Y. R., L. M. Czech, M. P. . Direct demonstration of rapid insulin-like growth factor II Receptor internalization and recycling in rat adipocytes. *J Biol Chem* **260**, 9435-9442 (1985).
- 277 Poulos, A. M. *et al.* Persistence of fear memory across time requires the basolateral amygdala complex. *Proc Natl Acad Sci U S A* **106**, 11737-11741, doi:10.1073/pnas.0905257106 (2009).
- 278 Gale, G. D. *et al.* Role of the basolateral amygdala in the storage of fear memories across the adult lifetime of rats. *J Neurosci* **24**, 3810-3815, doi:10.1523/JNEUROSCI.4100-03.2004 (2004).
- 279 van der Staay, F. J., Rutten, K., Erb, C. & Blokland, A. Effects of the cognition impairer MK-801 on learning and memory in mice and rats. *Behav Brain Res* **220**, 215-229, doi:10.1016/j.bbr.2011.01.052 (2011).
- 280 Radford, K. D. *et al.* Dose-response characteristics of intravenous ketamine on dissociative stereotypy, locomotion, sensorimotor gating, and nociception in male Sprague-Dawley rats. *Pharmacol Biochem Behav* **153**, 130-140, doi:10.1016/j.pbb.2016.12.014 (2017).
- 281 Wang, J. *et al.* Impact of ketamine on learning and memory function, neuronal apoptosis and its potential association with miR-214 and PTEN in adolescent rats. *PLoS One* **9**, e99855, doi:10.1371/journal.pone.0099855 (2014).

- 282 Roozendaal, B. *et al.* Basolateral amygdala noradrenergic activity mediates corticosterone-induced enhancement of auditory fear conditioning. *Neurobiol Learn Mem* **86**, 249-255, doi:10.1016/j.nlm.2006.03.003 (2006).
- 283 Ogden, K. K., Khatri, A., Traynelis, S. F. & Heldt, S. A. Potentiation of GluN2C/D NMDA receptor subtypes in the amygdala facilitates the retention of fear and extinction learning in mice. *Neuropsychopharmacology* **39**, 625-637, doi:10.1038/npp.2013.241 (2014).
- 284 Stuehr, D., Pou, S. & Rosen, G. M. Oxygen reduction by nitric-oxide synthases. *J Biol Chem* **276**, 14533-14536, doi:10.1074/jbc.R100011200 (2001).
- 285 Fedele, E., Marchi, M. & Raiteri, M. In vivo NO/cGMP signalling in the hippocampus. *Neurochem Res* **26**, 1069-1078, doi:10.1023/a:1012309223236 (2001).
- 286 Arnold, W. P., Mittal, C. K., Katsuki, S. & Murad, F. Nitric oxide activates guanylate cyclase and increases guanosine 3':5'-cyclic monophosphate levels in various tissue preparations. *Proc Natl Acad Sci U S A* **74**, 3203-3207, doi:10.1073/pnas.74.8.3203 (1977).
- 287 Miki, N., Kawabe, Y. & Kuriyama, K. Activation of cerebral guanylate cyclase by nitric oxide. *Biochemical and Biophysical Research Communications* **75**, 851-856, doi:10.1016/0006-291x(77)91460-7 (1977).
- 288 Radulovic, J., Kammermeier, J. & Spiess, J. Relationship between Fos Production and Classical Fear Conditioning: Effects of Novelty, Latent Inhibition, and Unconditioned Stimulus Preexposure. *The Journal of Neuroscience* **18**, 7452-7461, doi:10.1523/jneurosci.18-18-07452.1998 (1998).
- 289 Cho, J. H., Rendall, S. D. & Gray, J. M. Brain-wide maps of Fos expression during fear learning and recall. *Learn Mem* **24**, 169-181, doi:10.1101/lm.044446.116 (2017).
- 290 Song, D. *et al.* Role of dopamine D3 receptor in alleviating behavioural deficits in animal models of post-traumatic stress disorder. *Prog Neuropsychopharmacol Biol Psychiatry* **84**, 190-200, doi:10.1016/j.pnpbp.2018.03.001 (2018).
- 291 Diaz, M. R., Chappell, A. M., Christian, D. T., Anderson, N. J. & McCool, B. A. Dopamine D3-like receptors modulate anxiety-like behavior and regulate GABAergic transmission in the rat lateral/basolateral amygdala. *Neuropsychopharmacology* **36**, 1090-1103, doi:10.1038/npp.2010.246 (2011).
- 292 Kwon, O.-B. *et al.* Dopamine Regulation of Amygdala Inhibitory Circuits for Expression of Learned Fear. *Neuron* **88**, 378-389, doi:10.1016/j.neuron.2015.09.001 (2015).
- 293 Shin, M. S. & Helmstetter, F. J. Antinociception following application of DAMGO to the basolateral amygdala results from a direct interaction of DAMGO with Mu opioid receptors in the amygdala. *Brain Res* **1064**, 56-65, doi:10.1016/j.brainres.2005.09.065 (2005).
- 294 Lichtenberg, N. T. & Wassum, K. M. Amygdala mu-opioid receptors mediate the motivating influence of cue-triggered reward expectations. *Eur J Neurosci* **45**, 381-387, doi:10.1111/ejn.13477 (2017).
- 295 Blaesse, P. *et al.* mu-Opioid Receptor-Mediated Inhibition of Intercalated Neurons and Effect on Synaptic Transmission to the Central Amygdala. *J Neurosci* **35**, 7317-7325, doi:10.1523/JNEUROSCI.0204-15.2015 (2015).

- 296 Ciocchi, S. *et al.* Encoding of conditioned fear in central amygdala inhibitory  
circuits. *Nature* **468**, 277-282, doi:10.1038/nature09559 (2010).
- 297 Grillon C, S. S., Charney DS. . The psychobiological basis of posttraumatic stress  
disorder. *Mol Psychiatry* **1**, 278-297.
- 298 Shimizu, E., Tang, Y. P., Rampon, C. & Tsien, J. Z. NMDA receptor-dependent  
synaptic reinforcement as a crucial process for memory consolidation. *Science*  
**290**, 1170-1174, doi:10.1126/science.290.5494.1170 (2000).
- 299 Hong, I. *et al.* AMPA receptor exchange underlies transient memory  
destabilization on retrieval. *Proc Natl Acad Sci U S A* **110**, 8218-8223,  
doi:10.1073/pnas.1305235110 (2013).
- 300 Matsuo, N., Reijmers, L. & Mayford, M. Spine-type-specific recruitment of  
newly synthesized AMPA receptors with learning. *Science* **319**, 1104-1107,  
doi:10.1126/science.1149967 (2008).
- 301 Seeburg, P. H., Burnashev, N., Kohr, G., Kuner, T., Sprengel, R., Monyer, H. .  
The NMDA receptor channel: molecular design of a coincidence detector. *Recent  
Progress in Hormone Research* **50**, 19-34 (1995).
- 302 Christopherson, K. S., Hillier, B. J., Lim, W. A. & Brecht, D. S. PSD-95  
Assembles a Ternary Complex with the N-Methyl-D-aspartic Acid Receptor and a  
Bivalent Neuronal NO Synthase PDZ Domain. *Journal of Biological Chemistry*  
**274**, 27467-27473 (1999).
- 303 Feyder, M., Wiedholz, L., Sprengel, R. & Holmes, A. Impaired associative fear  
learning in mice with complete loss or haploinsufficiency of AMPA GluR1  
receptors. *Front Behav Neurosci* **1**, 4, doi:10.3389/neuro.08.004.2007 (2007).
- 304 Sun, Y. Y. *et al.* Surface expression of hippocampal NMDA GluN2B receptors  
regulated by fear conditioning determines its contribution to memory  
consolidation in adult rats. *Sci Rep* **6**, 30743, doi:10.1038/srep30743 (2016).
- 305 Morris, R. G., Anderson, E., Lynch, G. S. & Baudry, M. Selective impairment of  
learning and blockade of long-term potentiation by an N-methyl-D-aspartate  
receptor antagonist, AP5. *Nature* **319**, 774-776, doi:10.1038/319774a0 (1986).
- 306 Dejanovic, B. & Schwarz, G. Neuronal nitric oxide synthase-dependent S-  
nitrosylation of gephyrin regulates gephyrin clustering at GABAergic synapses. *J  
Neurosci* **34**, 7763-7768, doi:10.1523/JNEUROSCI.0531-14.2014 (2014).
- 307 Nedelescu, H. *et al.* Endogenous GluR1-containing AMPA receptors translocate  
to asymmetric synapses in the lateral amygdala during the early phase of fear  
memory formation: an electron microscopic immunocytochemical study. *J Comp  
Neurol* **518**, 4723-4739, doi:10.1002/cne.22472 (2010).
- 308 Hu, H. *et al.* Emotion enhances learning via norepinephrine regulation of AMPA-  
receptor trafficking. *Cell* **131**, 160-173, doi:10.1016/j.cell.2007.09.017 (2007).
- 309 Yeh, S. H., Mao, S. C., Lin, H. C. & Gean, P. W. Synaptic expression of  
glutamate receptor after encoding of fear memory in the rat amygdala. *Mol  
Pharmacol* **69**, 299-308, doi:10.1124/mol.105.017194 (2006).
- 310 Rumpel, S., LeDoux, J., Zador, A. & Malinow, R. Postsynaptic receptor  
trafficking underlying a form of associative learning. *Science* **308**, 83-88,  
doi:10.1126/science.1103944 (2005).
- 311 Thoeringer, C. K. *et al.* Consolidation of remote fear memories involves  
Corticotropin-Releasing Hormone (CRH) receptor type 1-mediated enhancement

- of AMPA receptor GluR1 signaling in the dentate gyrus. *Neuropsychopharmacology* **37**, 787-796, doi:10.1038/npp.2011.256 (2012).
- 312 Zinebi, F. *et al.* NMDA Currents and Receptor Protein Are Downregulated in the Amygdala during Maintenance of Fear Memory. *The Journal of Neuroscience* **23**, 10283-10291, doi:10.1523/jneurosci.23-32-10283.2003 (2003).
- 313 Lee, S. *et al.* GluA1 phosphorylation at serine 831 in the lateral amygdala is required for fear renewal. *Nat Neurosci* **16**, 1436-1444, doi:10.1038/nn.3491 (2013).
- 314 Tu, W. *et al.* DAPK1 interaction with NMDA receptor NR2B subunits mediates brain damage in stroke. *Cell* **140**, 222-234, doi:10.1016/j.cell.2009.12.055 (2010).
- 315 Qiu, S. *et al.* An increase in synaptic NMDA receptors in the insular cortex contributes to neuropathic pain. *Sci Signal* **6**, ra34, doi:10.1126/scisignal.2003778 (2013).
- 316 Sanz-Clemente, A., Matta, J. A., Isaac, J. T. & Roche, K. W. Casein kinase 2 regulates the NR2 subunit composition of synaptic NMDA receptors. *Neuron* **67**, 984-996, doi:10.1016/j.neuron.2010.08.011 (2010).
- 317 Ahern, G., Klyachko, V. A. & Jackson, M. B. cGMP and S-nitrosylation: two routes for modulation of neuronal excitability by NO. *Trends in Neurosciences* **25**, 510-517, doi:10.1016/s0166-2236(02)02254-3 (2002).
- 318 Johnston, H. M. & Morris, B. J. N-Methyl-d-aspartate and nitric oxide regulate the expression of calcium/calmodulin-dependent kinase II in the hippocampal dentate gyrus. *Molecular Brain Research* **31**, 141-150, doi:10.1016/0169-328x(95)00046-u (1995).
- 319 Derbyshire, E. R. & Marletta, M. A. Structure and regulation of soluble guanylate cyclase. *Annu Rev Biochem* **81**, 533-559, doi:10.1146/annurev-biochem-050410-100030 (2012).
- 320 Pavesi, E., Heldt, S. A. & Fletcher, M. L. Neuronal nitric-oxide synthase deficiency impairs the long-term memory of olfactory fear learning and increases odor generalization. *Learn Mem* **20**, 482-490, doi:10.1101/lm.031450.113 (2013).
- 321 Setten, R. L., Rossi, J. J. & Han, S. P. The current state and future directions of RNAi-based therapeutics. *Nat Rev Drug Discov* **18**, 421-446, doi:10.1038/s41573-019-0017-4 (2019).
- 322 Zhang, M. M., Bahal, R., Rasmussen, T. P., Manautou, J. E. & Zhong, X. B. The growth of siRNA-based therapeutics: Updated clinical studies. *Biochem Pharmacol*, 114432, doi:10.1016/j.bcp.2021.114432 (2021).
- 323 Resende, F. F. B., Titze-de-Almeida, S. S. & Titze-de-Almeida, R. Function of neuronal nitric oxide synthase enzyme in temozolomide-induced damage of astrocytic tumor cells. *Oncol Lett* **15**, 4891-4899, doi:10.3892/ol.2018.7917 (2018).
- 324 Titze-de-Almeida, R. *et al.* Suppressing nNOS Enzyme by Small-Interfering RNAs Protects SH-SY5Y Cells and Nigral Dopaminergic Neurons from 6-OHDA Injury. *Neurotox Res* **36**, 117-131, doi:10.1007/s12640-019-00043-9 (2019).
- 325 Olson, N. & van der Vliet, A. Interactions between nitric oxide and hypoxia-inducible factor signaling pathways in inflammatory disease. *Nitric Oxide* **25**, 125-137, doi:10.1016/j.niox.2010.12.010 (2011).

- 326 Zhang, D. *et al.* nNOS Translocates into the Nucleus and Interacts with Sox2 to Protect Neurons Against Early Excitotoxicity via Promotion of Shh Transcription. *Mol Neurobiol* **53**, 6444-6458, doi:10.1007/s12035-015-9545-z (2016).
- 327 Baldelli, S., Lettieri Barbato, D., Tatulli, G., Aquilano, K. & Ciriolo, M. R. The role of nNOS and PGC-1alpha in skeletal muscle cells. *J Cell Sci* **127**, 4813-4820, doi:10.1242/jcs.154229 (2014).
- 328 Chen, D. Y. *et al.* A critical role for IGF-II in memory consolidation and enhancement. *Nature* **469**, 491-497, doi:10.1038/nature09667 (2011).
- 329 Shahmoradi, A., Radyushkin, K. & Rossner, M. J. Enhanced memory consolidation in mice lacking the circadian modulators Sharp1 and -2 caused by elevated Igf2 signaling in the cortex. *Proc Natl Acad Sci U S A* **112**, E3582-3589, doi:10.1073/pnas.1423989112 (2015).
- 330 Stein, T. D. *et al.* Neutralization of transthyretin reverses the neuroprotective effects of secreted amyloid precursor protein (APP) in APPSW mice resulting in tau phosphorylation and loss of hippocampal neurons: support for the amyloid hypothesis. *J Neurosci* **24**, 7707-7717, doi:10.1523/JNEUROSCI.2211-04.2004 (2004).
- 331 Khan, S. *et al.* IGFBP2 Plays an Essential Role in Cognitive Development during Early Life. *Adv Sci (Weinh)* **6**, 1901152, doi:10.1002/advs.201901152 (2019).
- 332 Jeong, E. Y. *et al.* Enhancement of IGF-2-induced neurite outgrowth by IGF-binding protein-2 and osteoglycin in SH-SY5Y human neuroblastoma cells. *Neurosci Lett* **548**, 249-254, doi:10.1016/j.neulet.2013.05.038 (2013).
- 333 Yu, S. Y., Wu, D. C., Liu, L., Ge, Y. & Wang, Y. T. Role of AMPA receptor trafficking in NMDA receptor-dependent synaptic plasticity in the rat lateral amygdala. *J Neurochem* **106**, 889-899, doi:10.1111/j.1471-4159.2008.05461.x (2008).
- 334 Beique, J. C. *et al.* Synapse-specific regulation of AMPA receptor function by PSD-95. *Proc Natl Acad Sci U S A* **103**, 19535-19540, doi:10.1073/pnas.0608492103 (2006).
- 335 Coley, A. A. & Gao, W. J. PSD-95 deficiency disrupts PFC-associated function and behavior during neurodevelopment. *Sci Rep* **9**, 9486, doi:10.1038/s41598-019-45971-w (2019).
- 336 Selvakumar, B. *et al.* AMPA receptor upregulation in the nucleus accumbens shell of cocaine-sensitized rats depends upon S-nitrosylation of stargazin. *Neuropharmacology* **77**, 28-38, doi:10.1016/j.neuropharm.2013.08.036 (2014).
- 337 Dachtler, J. *et al.* Experience-dependent plasticity acts via GluR1 and a novel neuronal nitric oxide synthase-dependent synaptic mechanism in adult cortex. *J Neurosci* **31**, 11220-11230, doi:10.1523/JNEUROSCI.1590-11.2011 (2011).
- 338 Hopper, R., Lancaster, B. & Garthwaite, J. On the regulation of NMDA receptors by nitric oxide. *Eur J Neurosci* **19**, 1675-1682, doi:10.1111/j.1460-9568.2004.03306.x (2004).
- 339 Wang, X. *et al.* Neuronal Nitric Oxide Synthase Knockdown Within Basolateral Amygdala Induces Autistic-Related Phenotypes and Decreases Excitatory Synaptic Transmission in Mice. *Front Neurosci* **14**, 886, doi:10.3389/fnins.2020.00886 (2020).

- 340 Vaiva, G. *et al.* Immediate treatment with propranolol decreases posttraumatic stress disorder two months after trauma. *Biological Psychiatry* **54**, 947-949, doi:10.1016/s0006-3223(03)00412-8 (2003).
- 341 Stein, M. B., Kerridge, C., Dimsdale, J. E. & Hoyt, D. B. Pharmacotherapy to prevent PTSD: Results from a randomized controlled proof-of-concept trial in physically injured patients. *J Trauma Stress* **20**, 923-932, doi:10.1002/jts.20270 (2007).
- 342 Bowers, M. E. & Ressler, K. J. An Overview of Translationally Informed Treatments for Posttraumatic Stress Disorder: Animal Models of Pavlovian Fear Conditioning to Human Clinical Trials. *Biol Psychiatry* **78**, E15-27, doi:10.1016/j.biopsych.2015.06.008 (2015).
- 343 Dachtler, J., Hardingham, N. R. & Fox, K. The role of nitric oxide synthase in cortical plasticity is sex specific. *J Neurosci* **32**, 14994-14999, doi:10.1523/JNEUROSCI.3189-12.2012 (2012).
- 344 Gill, J. M., Szanton, S. L. & Page, G. G. Biological underpinnings of health alterations in women with PTSD: a sex disparity. *Biol Res Nurs* **7**, 44-54, doi:10.1177/1099800405276709 (2005).
- 345 Christiansen, D. M. & Berke, E. T. Gender- and Sex-Based Contributors to Sex Differences in PTSD. *Curr Psychiatry Rep* **22**, 19, doi:10.1007/s11920-020-1140-y (2020).
- 346 Monsey, M. S., Ota, K. T., Akingbade, I. F., Hong, E. S. & Schafe, G. E. Epigenetic alterations are critical for fear memory consolidation and synaptic plasticity in the lateral amygdala. *PLoS One* **6**, e19958, doi:10.1371/journal.pone.0019958 (2011).
- 347 Koshibu, K., Graff, J. & Mansuy, I. M. Nuclear protein phosphatase-1: an epigenetic regulator of fear memory and amygdala long-term potentiation. *Neuroscience* **173**, 30-36, doi:10.1016/j.neuroscience.2010.11.023 (2011).
- 348 Valiati, F. E. *et al.* Administration of a Histone Deacetylase Inhibitor into the Basolateral Amygdala Enhances Memory Consolidation, Delays Extinction, and Increases Hippocampal BDNF Levels. *Front Pharmacol* **8**, 415, doi:10.3389/fphar.2017.00415 (2017).
- 349 Resstel, L. B., Correa, F. M. & Guimaraes, F. S. The expression of contextual fear conditioning involves activation of an NMDA receptor-nitric oxide pathway in the medial prefrontal cortex. *Cereb Cortex* **18**, 2027-2035, doi:10.1093/cercor/bhm232 (2008).
- 350 Schuman, E. M. & Madison, D. V. A requirement for the intercellular messenger nitric oxide in long-term potentiation. *Science* **254**, 1503-1506, doi:10.1126/science.1720572 (1991).

## **CURRICULUM VITAE**

**Jheel Patel**

### **Education**

- 2021 Ph.D., Major: Medical Neuroscience; Minor: Business of Biomedical Sciences, Indiana University, Indianapolis, IN
- 2014 B.S., Major: Biochemistry; Minor: Anthropology, Biology, Purdue University, IN

### **Awards and Fellowships**

- 2021 Larry Kays Fellowship, Stark Neurosciences Research Institute, IUSM
- 2020 Kroenke Poster Award, Indiana Clinical and Translational Sciences Institute, IUSM
- 2019-2021 Pre-Doctoral Training Award (TL1), Indiana Clinical and Translational Sciences Institute, IUSM
- 2019 Society for Neuroscience Trainee Professional Development Award, Society for Neuroscience
- 2019 Elite 50 & Premier 10 Graduate Student Award, Indiana University-Purdue University Indianapolis
- 2017-2018 Paul & Carole Stark Fellowship, Stark Neurosciences Research Institute, IUSM
- 2014 IUPUI Top 10 Female Student, Indiana University-Purdue University Indianapolis

- 2013 Special Mention, Annual Research Competition, Indiana University Health
- 2013 Amazing Jaguar, Indiana University-Purdue University Indianapolis
- 2012 Ralph L. Collins Living-Learning Center Leadership Award, Indiana University Bloomington

### **Publications**

1. Overview of genetic models of autism spectrum disorders. **Patel J**, Lukkes J, Shekhar A. Genetic Models and Molecular Pathways Underlying Autism Spectrum Disorders, 1st ed. Progress in Brain Research. *2018 Nov; 241.*
2. Long-term intermittent high-amplitude subcutaneous nerve stimulation reduces sympathetic tone in ambulatory dogs. Yuan Y, Jiang Z, Zhao Y, Tsai WC, **Patel J**, Chen LS, Shen C, Lin SF, Chen HV, Everett TH 4th, Fishbein M, Chen Z, Chen PS. Heart Rhythm. *2018 Mar; 15(3):451-459.*
3. Small-Conductance Calcium-Activated Potassium Current in Normal Rabbit Cardiac Purkinje Cells. Reher TA, Wang Z, Hsueh CH, Chang PC, Pan Z, Kumar M, **Patel J**, Tan J, Shen C, Chen Z, Fishbein M, Rubart M, Boyden P, Chen PS. Journal of the American Heart Association. *2017 Mar; 6(6):1-9.*
4. Effects of renal sympathetic denervation on the stellate ganglion and brain stem in dogs. Tsai WC, Chan YH, Chinda K, Chen Z, **Patel J**, Shen C, Zhao Y, Jiang Z, Yuan Y, Ye M, Chen L, Riley A, Persohn SA, Territo PR, Everett TH, Lin SF,



Vinters HV, Fishbein MC, Chen PS. *Heart Rhythm Journal*. 2017 Feb;14(2):255-262.

5. Intermittent Left Cervical Vagal Nerve Stimulation Damages the Stellate Ganglia and Reduces Ventricular Rate During Sustained Atrial Fibrillation in Ambulatory Dogs. Chinda K, Tsai WC, Chan YH, Lin AYT, **Patel J**, Zhao Y, Tan AY, Shen MJ, Lin H, Shen C, Chattipakorn N, Rubart M, Chen LS, Fishbein MC, Everett T, Lin SF, Chen Z, Chen PS. *Heart Rhythm Journal*. 2016 Mar; 13(3):771-780.
6. Cervical Vagal Nerve Stimulation Activates the Stellate Ganglion in Ambulatory Dogs. Rhee KS, Hsueh CH, Hellyer J, Park HW, Lee YS, Garlie J, Onkka P, Doytchinova A, Garner J, **Patel J**, Chen LS, Fishbein MC, Everett T, Lin SF, Chen PS. *Korean Circulation Journal*. 2015 Mar;45(2):149-57.
7. Subcutaneous nerve activity and spontaneous ventricular arrhythmias in ambulatory dogs. Doytchinova A, **Patel J**, Zhou S, Chen LS, Lin H, Shen C, Everett TH, Lin SF, Chen PS. *Heart Rhythm Journal*. 2015 Mar; 12(3):612-20.
8. Autonomic Nerve Activity and Blood Pressure Fluctuation in Ambulatory Dogs. Hellyer J, Akingba G, Rhee KS, Tan A, Lane K, Shen C, **Patel J**, Fishbein M, Lin SF, Chen PS. *Heart Rhythm Journal*. 2014 Feb;11(2):307-313.
9. Sympathetic nerve fibers and ganglia in canine cervical vagus nerves: localization and quantitation. Onkka P, Maskoun W, Rhee KS, Hellyer J, **Patel J**, Tan J, Chen LS, Vinters HV, Fishbein MC, Chen PS. *Heart Rhythm Journal*. 2013 Apr; 10(4):585-91.

## **Manuscripts in preparation/under review**

1. Transcriptomic Study of Molecular Mechanisms Underlying NMDAR-PSD95-nNOS-NO Axis Mediated Fear Consolidation in the Amygdala: Key Role of IGF2 and IGFBP2. **Patel J**, Haulcomb MM, Li L, Jiang G, Lukkes J, Liu Y, Molosh AI, Shekhar A. *Translational Psychiatry*. 2021. *Under Review*.
2. Fear consolidation requires neuronal nitric oxide synthase mediated, sequentially orchestrated changes in AMPA and NMDA mediated glutamatergic neurotransmission in the basolateral amygdala. **Patel J**, Dustrude ET, Haulcomb MM, Molosh AI, Shekhar A. 2021. *In Submission*.
3. Behavioral phenotypic profile of the Nf1<sup>+/-</sup> mouse model. Lukkes J, **Patel J**, Fitz SD, Eng C, Molosh AI, Shekhar A. 2021. *In Preparation*.

## **Abstracts and Poster Presentations**

PSD95-nNOS interaction alters the basolateral amygdala transcriptome following fear conditioning: implications for molecular mechanisms underlying PTSD. **Patel J**, Haulcomb MM, Li L, Jiang G, Dustrude ET, Liu Y, Lai YY, Molosh AI, Shekhar A.

- Abstract Accepted for Association for Clinical and Translational Science Annual Meeting, April 2021.

Pharmacological and genetic regulation of nNOS in the basolateral amygdala impairs cued fear memory consolidation and reveals novel molecular mechanism. **Patel J**, Haulcomb MM, Li L, Jiang G, Dustrude ET, Liu Y, Lai YY, Molosh AI, Shekhar A.

- Oral Presentation at Stark Neurosciences Research Institute Post-Doctoral Association Annual Symposium, September 2020.

Role of PSD95 and nNOS interaction in gene regulation in the basolateral amygdala following cued fear conditioning and implications for molecular mechanisms underlying PTSD. **Patel J**, Dustrude ET, Haulcomb MM, Li L, Jiang G, Liu Y, Lai YY, Molosh AI, Shekhar A.

- Oral presentation at Indiana Clinical and Translational Sciences Institute Annual Meeting, September 2020.
- Abstract Accepted for Society of Biological Psychiatry Annual Meeting, May 2020.
- Abstract Accepted for Association for Clinical and Translational Science Annual Meeting, April 2020.
- Abstract Submitted to Greater Indiana Society for Neuroscience Annual Meeting, April 2020.
- Poster Presented at National Society for Neuroscience Annual Meeting, October 2019.

The effects of PSD95 and nNOS interaction in consolidation of conditioned fear and fear dependent gene expression in the basolateral amygdala. **Patel J**, Dustrude ET, Haulcomb MM, Li L, Molosh AI, Shekhar A.

- Poster Presented at Gill Neuroscience Annual Symposium, September 2019.
- Poster Presented at Indiana Clinical Translational Sciences Institute Annual Meeting, September 2019.
- Poster Presented at Greater Indiana Society for Neuroscience Annual Meeting, March 2019.

Limbic system-associated membrane protein may contribute to neurocognitive deficits in Neurofibromatosis type 1. **Patel J**, Lukkes J, Spence J, Clapp WD, Molosh A, Shekhar A.

- Poster Presented at Gill Neuroscience Annual Symposium, September 2018.
- Poster Presented at Greater Indiana Society for Neuroscience Annual Meeting, March 2018.

Stellate Ganglion Damage Induced by Vagal Nerve Stimulation and Renal Sympathetic Nerve Ablation. **Patel J**, Lin A, Tsai WC, Chinda K, Shen MJ, Fishbein MC, Chen Z, Chen PS.

- Poster Presented at Gordon Research Seminar and Conference, March 2015.

Small Conductance Calcium-Activated Potassium Channels Specifically Co-localizes with Sympathetic Nerve Fibers in the Stellate Ganglion. **Patel J**, Tan J, Fishbein MC, Chen PS.

- Poster Presented at Heart Rhythm Society Annual Session, May 2014.

### **Service Activities**

- Plan and lead daVinci Pursuit biannual fundraisers, 2018 - ongoing
- Host of Women in STEM video series featuring local women in STEM and their stories, in collaboration with daVinci Pursuit, 2019 - ongoing
- Taste of Science event coordinator, 2019 - ongoing
- Scientist pen-pal as part of Letters to a Pre-Scientist program, 2019 - 2020.
- Guest on He Says Science, She Says Art radio show on WICR, Aug & Nov 2020

- Invited to discuss program pivoting during a pandemic at Indiana Arts Homecoming Conference, Oct 2020
- Facilitated Indiana Sciences event, theme: 'Science Policy, Society, and You', Oct 2020
- Facilitated Indiana Sciences event, theme: 'Science: Communication and Advocacy', Dec 2019
- Co-led International Anatomy Nights heart and brain dissection at Centerpoint Brewery, Feb & Oct 2019
- Discussion leader at daVinci Pursuit's Science x Art Roundtables (topic: importance of fine arts education in medical and scientific training), Apr 2019 - Jun 2019
- Facilitate graduate student mental health roundtables with IUSM Neuroscience department, 2019
- Discussed graduate student mental health education at local NAMIWalks 5K, Oct 2018
- Led interactive Neuroscience table at safe trick-or-treating at Riley Children's Hospital, Oct 2018
- Women in STEM Meet-a-Scientist (elementary/middle schools), Oct 2016 & Apr 2017

## **Leadership**

2019-Present	Central Indiana Science Outreach, Board of Directors
2018-Present	daVinci Pursuit, Board of Directors
2018-Present	Science Outreach Community at IUSM, Vice President
2020-2021	Diversity, Inclusion, and Wellness Committee at Stark Neurosciences Research Institute
2018-2020	Biomedical Graduate Student Advocacy Association at IUSM, Medical Neuroscience Representative, Treasurer
2017-2020	Student Mental Health Initiative at IUSM, President
2018-2019	Medical Neurosciences Graduate Organization at IUSM, Student Development

## **Professional Affiliations**

2019-Present	Society for Neuroscience
2020-Present	International Behavioral Neuroscience Society

## **Certificates**

2020	Bioinformatics for Biologists, IUSM
2019	Ingenuity Pathway Analysis Intro Workshop, IUSM
2017	Making Medicines: The Process of Drug Development, Eli Lilly